CIVIL ENGINEERING

JOINT HIGHWAY RESEARCH PROJECT

JHRP-77-4

DEVELOPMENT OF AN INSTRUMENTATION PROGRAM FOR STUDYING BEHAVIOR OF A SEGMENTAL CONCRETE BOX GIRDER BRIDGE

R. J. Holman

PURDUE UNIVERSITY
INDIANA HIGHWAY COMMISSION

Final Report

DEVELOPMENT OF AN INSTRUMENTATION PROGRAM FOR STUDYING BEHAVIOR OF A SEGMENTAL CONCRETE BOX GIRDER BRIDGE

TO: J. F. McLaughlin, Director
Joint Highway Research Project

March 2, 1977

Project: C-36-56T

FROM: H. L. Michael, Associate Director
Joint Highway Research Project

File: 7-4-20

The attached Final Report titled "Development of an Instrumentation Program for Studying Behavior of a Segmental Concrete Box Girder Bridge" is submitted on a JHRP Study of similar title. Mr. R. J. Holman was the principal investigator on this study under the direction of Professors Gutzwiller and Lee.

The purpose of this study was to develop an instrumentation scheme for monitoring structural response of the Turkey Run segmental box girder bridge. Such a scheme is reported. It includes strain gages on reinforcement bars and in concrete to monitor transverse moment tractions, thermistors to determine thermal gradients, and implants to monitor long-term deformations. A second phase is planned during which these measurements would be made.

The approved study has been completed and the attached report is submitted as fulfillment of the objectives of the Study.

Respectfully submitted,

Harold L. Michael
Associate Director

HLM:ms

cc:
W. L. Dolch
R. L. Eskew
G. D. Gibson
W. H. Goetz
M. J. Gutzwiller
G. K. Hallock
D. E. Hancher
M. L. Hayes
K. R. Hoover
G. A. Leonards
R. D. Miles
P. L. Owens
G. T. Satterly
C. F. Scholer
M. B. Scott
K. C. Sinha
L. E. Wood
E. J. Yoder
S. R. Yoder

Final Report

DEVELOPMENT OF AN INSTRUMENTATION PROGRAM FOR STUDYING BEHAVIOR OF A SEGMENTAL CONCRETE BOX GIRDER BRIDGE

by

R. J. Holman
Graduate Instructor in Research

Joint Highway Research Project

Project No.: C-36-56T

File No.: 7-4-20

Prepared as Part of an Investigation
Conducted by
Joint Highway Research Project
Engineering Experiment Station
Purdue University
in cooperation with the
Indiana State Highway Commission

Purdue University
West Lafayette, Indiana
March 2, 1977

ACKNOWLEDGEMENTS

The author wishes to express his appreciation to Professors M. J. Gutzwiller, C. D. Sutton, and R. H. Lee for their assistance throughout the course of this project.

Financial assistance which made this study possible was provided by the Joint Highway Research Project of Purdue University.

Special thanks are extended to F. A. Batla and the bridge design section of the Indiana State Highway Commission for their technical assistance and consultation.

The author is extremely grateful to Jim Rodgers and the staff of Construction Products Corporation for their assistance during installation of strain gages. Their cooperation and technical assistance greatly aided in the completion of this phase of the investigation.

TABLE OF CONTENTS

TABLE OF CONTENTS (Continued)

LIST OF TABLES

LIST OF FIGURES

LIST OF FIGURES (Continued)

LIST OF FIGURES (Continued)

ABSTRACT

Holman, R. J., MSCE, Purdue University, May 1977. Development of an Instrumentation Program for Studying Behavior of a Segmental Concrete Box Girder Bridge. Major Professors: M. J. Gutzwiller and R. H. Lee.

An instrumentation scheme is developed for monitoring structural response of the Turkey Run segmental box girder bridge. Instrumentation is specified and analytic models are described which will be correlated with behavior of the actual structure in the second phase of the project.

Strain gages are placed on reinforcement bars and concrete at selected segment sections to monitor transverse moment tractions. Tractions will be monitored under pre-specified truck loads. The same truck loads are used in a finite element analysis and an influence surface analysis of transverse bending. Empirical results will be compared with those of the finite element analysis in order to check the accuracy of the computer program used by the Indiana State Highway Commission and to check assumptions of the analytic models.

Thermal response of box girders is an important design consideration, yet little information is available. Thermistors are placed in the Turkey Run bridge to determine the magnitudes of thermal gradients and to determine the daily and seasonal variation of thermal gradients.

Finally, long-term deformations are important in any concrete structure. Implants are attached near the pier segment in order to monitor long-term creep rotations with mechanical strain gages. This will help determine the significance of moment re-distribution resulting

from creep rotations in this precast structure.

The instrumentation scheme is designed to minimize errors during testing and to provide a systematic organization of testing procedures and data evaluation.

CHAPTER I

INTRODUCTION

1.1 General

Segmental bridge construction began with the construction of a small county road bridge in New York State in 1952. Ten years later the first major segmental structure was built in France over the Seine River south of Paris. Since 1962 the precast segmental construction process has grown steadily in Europe and continues to gain popularity. The construction of segmental bridges in the United States has only gained impetus in the last few years but promises to be an effective and economic alternative for medium and long-span bridges in the future. The first precast prestressed segmental box girder bridge in the United States was completed at Corpus Christi, Texas in 1973. Since then five other bridges have been constructed nationwide and others are now in the planning phase.

The reason for the increasing popularity of segmental bridges is the advantage of precast segmental construction over cast-in-place construction. Precasting under factory conditions allows for better quality control and mass production economies. The construction techniques applicable to segmental bridges, the cantilever method for example, allow speedier construction and more efficient use of labor and materials. These reasons along with the structural efficiency of segmental box girders make the method an attractive alternative to

Figure 1. Segments for Turkey Run Bridge

Figure 2. Completed Parke County Segmental Bridge

cast-in-place structures.

Precast segmental box girder bridges will continue to gain popularity as a design alternate among State and Federal highway agencies. Indiana has been at the forefront in the development and application of segmental construction. With the increasing use of this structural system it is desirable and necessary to be able to better predict the behavior of segmental box girders on both a short-term and long-term basis. The gathering and evaluation of research data will allow a more accurate and efficient design. The purpose of this phase of the project was to devise and implement an instrumentation scheme for the Turkey Run segmental bridge in Parke County. The instrumentation program will permit acquisition of data which can be used to check existing design and analysis methods and the gathering of short-term and long-term data which can be used to better predict behavior.

1.2 Construction Procedure

The Turkey Run bridge segments are cast by the short-line method. This method involves casting each segment in an adjustable metal form. The segment is match-cast against the preceding segment to insure a perfect fit of joints. Figures 3 and 4 show the formwork and the reinforcement cage for a segment. The cages are assembled prior to being placed in the form. Post-tensioning ducts are positioned during cage assembly. Once the cage is secured in the form the matching segment is placed next to the form as shown in Figure 5. A bulkhead is used to close the opposing side of the form. This procedure is then repeated while cast segments are stockpiled (see Figure 6) until time of erection.

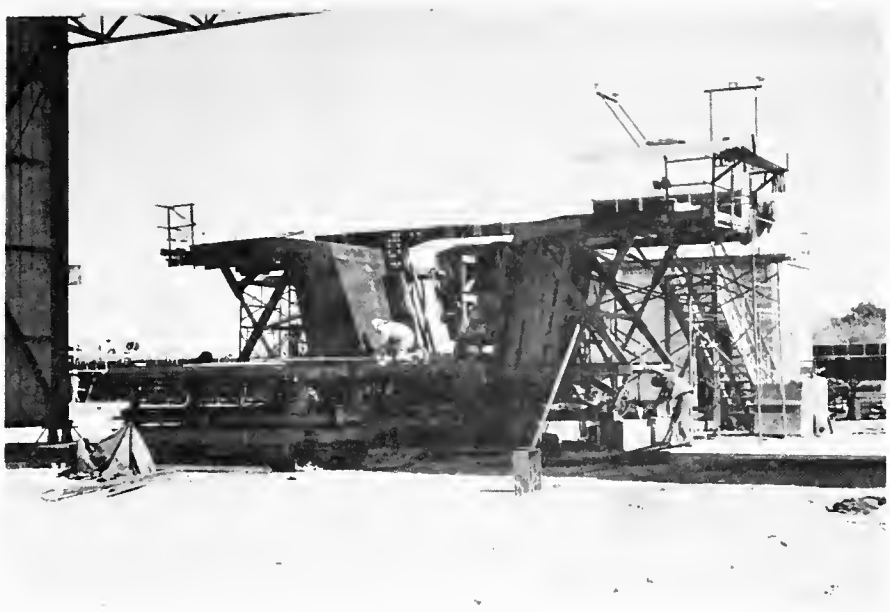

Figure 3. Segment Formwork

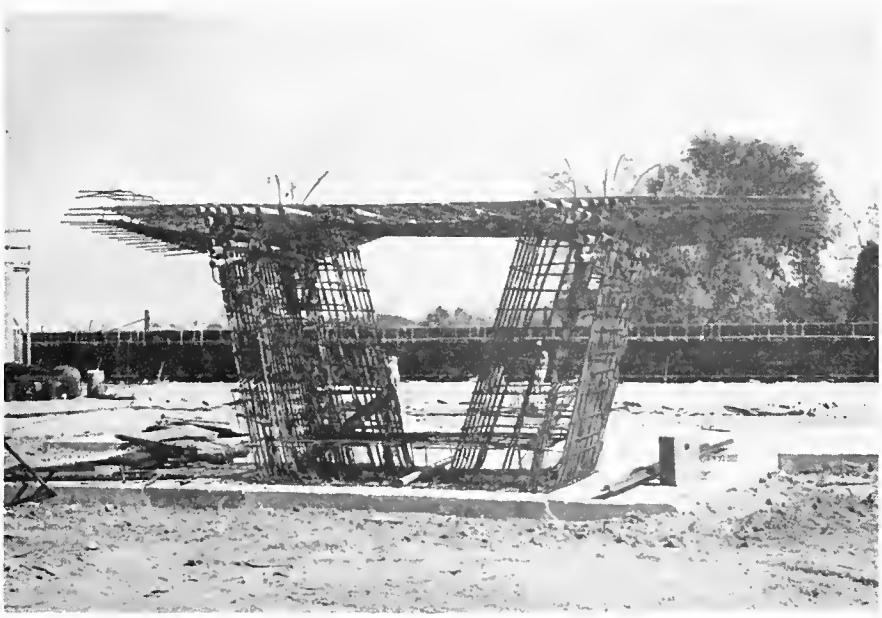

Figure 4. Reinforcement Cage

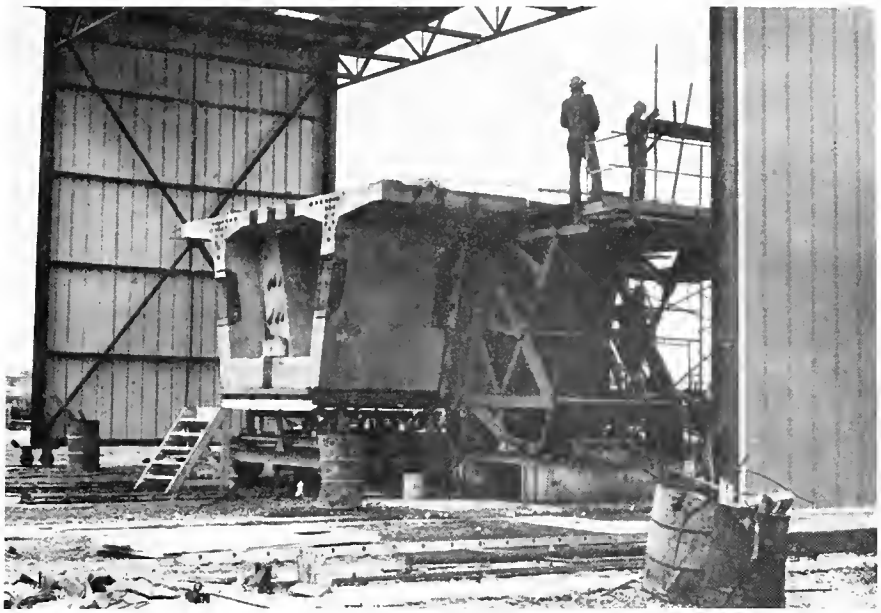

Figure 5. Match Casting

Figure 6. Stockpiled Segments

After a span is cast the segments are trucked to the construction site for erection. The Turkey Run bridge will be erected by the cantilever method. Figures 7 and 8 are photographs taken of the recently completed Parke County bridge. Figure 7 shows segments cantilevered from the central pier. Segments are lifted into place and then temporarily post-tensioned against the preceding segment. This holds the segment in place while the epoxy joint filler cures. The epoxy is placed on joint faces to lubricate the joint during placement and to make the joint moisture resistant. Segments are cantilevered from both sides of the pier simultaneously to insure stability of the balanced cantilever. While two opposing segments are temporarily secured tendons are threaded through the post-tensioning ducts. The tendons are anchored in steps as the span progresses. After cantilever spans are completed from two adjacent piers the spans are connected by a cast-in-place segment as shown in Figure 8. References listed at the end of the report contain more detailed descriptions of the cantilever construction procedure.

1.3 Review of Previous Research

Previous research on segmental bridges can generally be divided into two categories: (1) short-term investigations, (2) long-term investigations.

Short-term investigations have been concerned with verifying structural response as predicted by available analytic methods. The University of Texas in cooperation with the Texas Highway Department carried out extensive tests on a 1/6th scale model of the Corpus Christi bridge prior to construction. The main purpose of this research was to compare

Figure 7. Cantilevered Erection

Figure 8. Cast-in-Place Segment

observed stresses with those predicted by analysis and to verify the validity of the assumptions used in design by observing behavior at ultimate load. Similar projects have been conducted in Europe and Japan. Limited research has been conducted on the effects of thermal loading on segmental bridges. It has been found that in continuous bridges the alteration of dead load moment distribution by temperature gradients is significant and should be accounted for, especially in determining prestress levels. Also, researchers in France have found that the temperature gradient effect must be considered when evaluating long-term behavior data in order to obtain valid results.

Investigations of long-term behavior have mainly been conducted in Europe. Since segmental box girder bridges have only been completed in the United States within the past three years, limited data has been collected on long-term behavior. European research has been concerned with the redistribution of moments in continuous structures caused by the combined effects of creep, shrinkage and loss of prestress. Instrumentation of the Champigny-Sur-Yonne bridge in France has shown that the final stresses in the completed structure are significantly different from the initial stresses immediately following construction. This phenomenon is of course produced by the time dependent deformations caused by creep, shrinkage, and prestress loss.

Most information used for the analysis and design of segmental box girder bridges has previously been obtained from theory or model test. In order to refine the methodology of segmental bridge design and construction, it is desirable to obtain short-term and long-term data on the behavior of actual structures. This data may be used to improve

the design as well as to better predict behavior during and subsequent to construction. Future research should be aimed at correlating design assumptions with actual structural behavior as determined from instrumentation of actual structures.

1.4 Scope of Project

The instrumentation of the Turkey Run segmental bridge will provide information on transverse bending tractions in the box beam cross-section, thermal gradients within the girder, and long-term creep deformations after erection. Transverse moments will be monitored by strain gage installations on transverse reinforcement. The moment data obtained for pre-specified load positions will be compared to data from two types of elastic analyses. Thermal gradients have a significant effect on structural response. It is desirable for the designer to know the magnitudes of thermal gradients and the variation of gradients with time. The Turkey Run bridge will be instrumented with thermistors which will allow thermal gradients to be monitored at any time during the life of the structure. Creep rotations at continuous supports can cause significant re-distribution of longitudinal moments. Mechanical strain gages will be used to measure creep rotations at the pier support section of the Turkey Run bridge. This instrumentation will help determine if creep deformations are significant in this precast structure.

Due to scheduling of construction of the Turkey Run bridge it is necessary that the instrumentation program be carried out in two phases. This report describes work done in phase one of the project. The objectives of phase one are as follows: (1) devise an instrumentation scheme for objectives mentioned above, (2) acquire necessary materials and

install as much of the instrumentation as time allows, (3) develop an analytic base by gathering analysis data for the pre-specified loadings with analytic techniques used by the Indiana State Highway Commission and industry. Phase two of the project will involve consummation of item two above and the actual gathering of data as outlined in this report.

CHAPTER II

TRANSVERSE BENDING

2.1 Introduction

In conventional concrete bridges such as concrete deck girders the effect of transverse distortions of the deck and girder unit is of little importance except in designing the deck for transverse moments. Wheel loads in conventional deck girder bridges are delivered to multiple girders directly and by slab action. Each girder behaves independently in the transverse direction with the only carry-over distortions resulting from continuous slab action. In contrast segmental box girders behave as tubular members with high torsional and transverse stiffness. Box girders may have as few as two webs with a large slab span between webs. As a result torsional resistance and transverse stiffness are required for load transfer into the webs and supports. Significant transverse stresses may occur in the webs as well as the top and bottom slabs of the segment. Examples of distorted cross-sections are shown below. An accurate prediction of the magnitude of transverse stresses is necessary for proportioning of members and determining the necessary transverse reinforcement.

Box girder bridges with single box cross-sections have fillets at the slab web connections and reinforcement through the connection, providing moment continuity around the section. The Turkey Run bridge has a twin box cross-section and thus behaves quite differently from

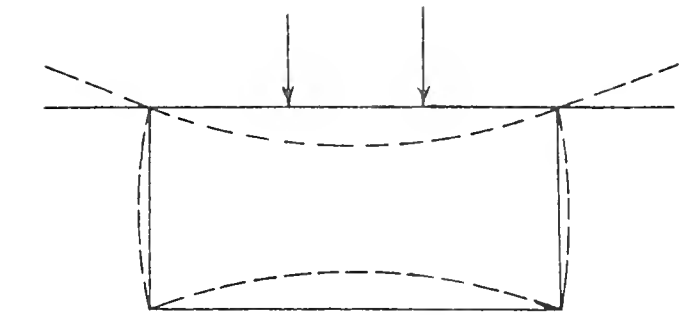

Symmetric Loading

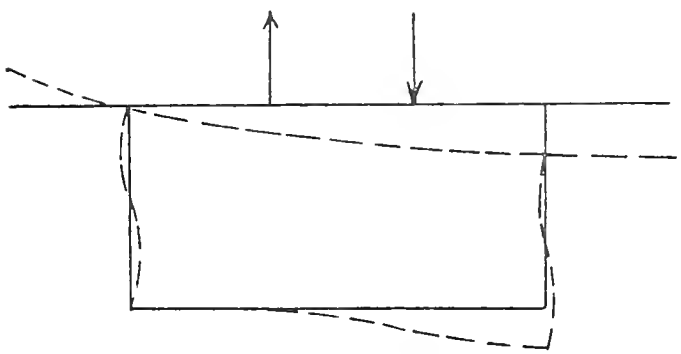

Torsional Loading

Figure 9. Cross-section Distortion Under Different Loadings

a single section bridge. The twin boxes are cantilevered independently. After making the continuity splice in both spans a cast-in-place longitudinal joint connects the two boxes. (See Figure 10.) Assuming the joint provides total moment continuity the structural response of one section is significantly affected by the loading condition on the adjacent box section. A truck loading over one box will produce a significantly larger deflection in the loaded span than in the parallel girder, thus causing a relative vertical displacement of the twin boxes.

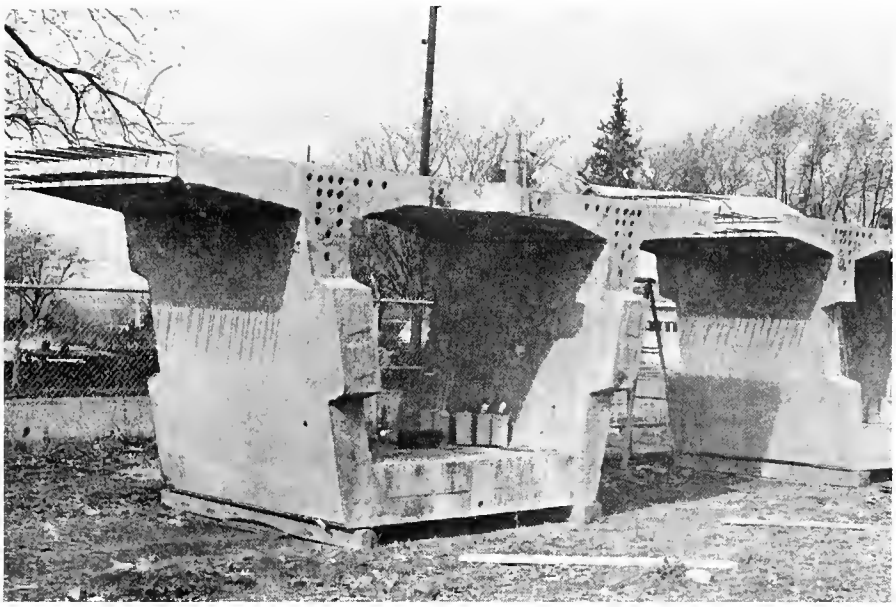

Figure 10. Twin Box Cross-section

This action causes a transverse moment transfer between the boxes due to the lateral stiffness of the connecting slab and cast-in-place joint. Also, as a result of asymmetry of loading the two boxes will rotate relative to one another, again causing transverse moment interaction. (See Figure 11.) Both factors rely on the continuity of the cast-in-place longitudinal joint for transfer of moment. As seen in detail in Figure 12, the bar lap splice provides continuity of bond between connecting reinforcement of the twin boxes. The question remains as to whether the cold joint and lap splice provide full moment continuity.

It is generally assumed that continuity exists in multiple box girder cross-sections. As a result a conventional elastic analysis technique can be utilized to determine design tractions in the transverse as well as longitudinal directions, treating the twin boxes as a single system. However, due to the complexity of the box girder system and variable boundary conditions induced by internal diaphragms and support conditions, the analysis usually involves approximations. The analytic approximation may be based on behavioral assumptions or numerical solutions of exact elastic equations. The more popular methods of analysis include the finite element method, the finite strip method, folded plate theory, and others. These methods model three dimensional plate action as well as in-plane membrane response. The distinct advantage of the above analysis techniques is that they simultaneously model overall structural response and localized effects such as transverse bending. Analysis methods using a modified frame analysis in conjunction with influence surfaces can be used to determine transverse moments but must be augmented by beam theory to determine

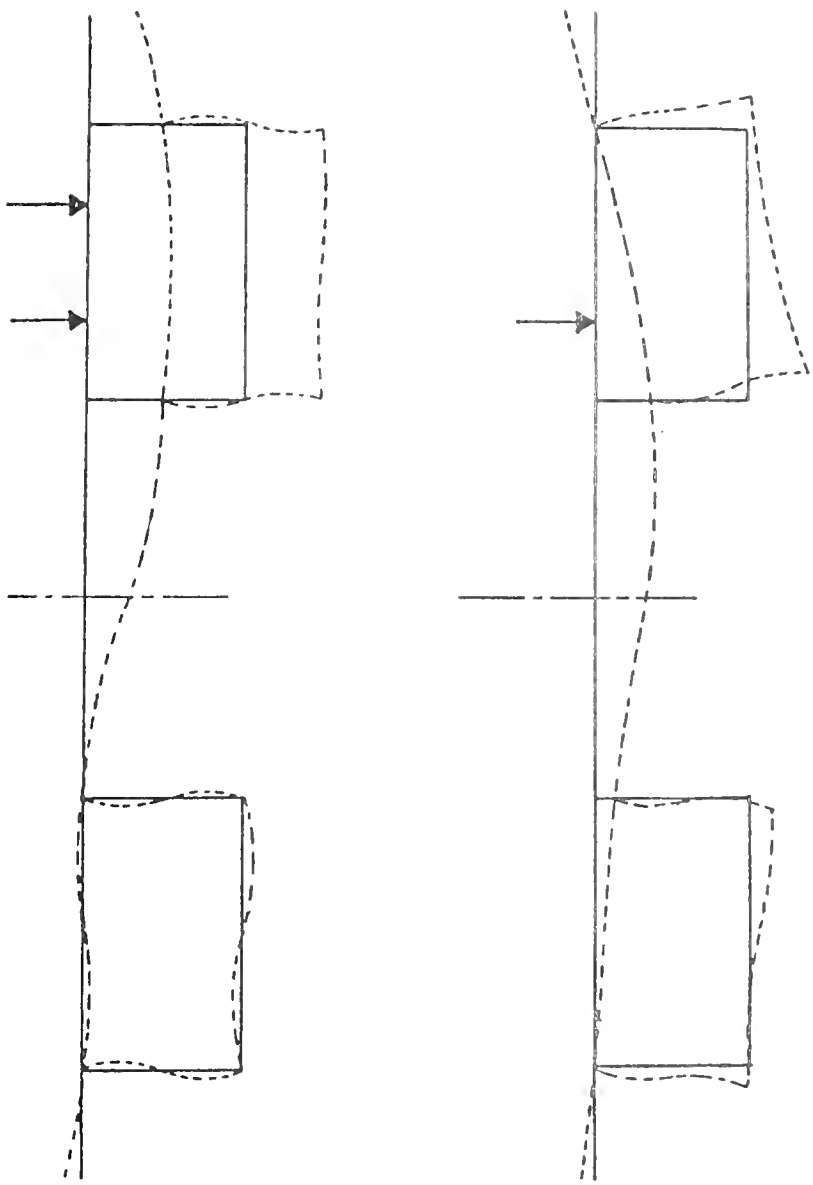

Figure 11. Transverse Moment Carry-Over Due to Relative Vertical and Rotational Displacements

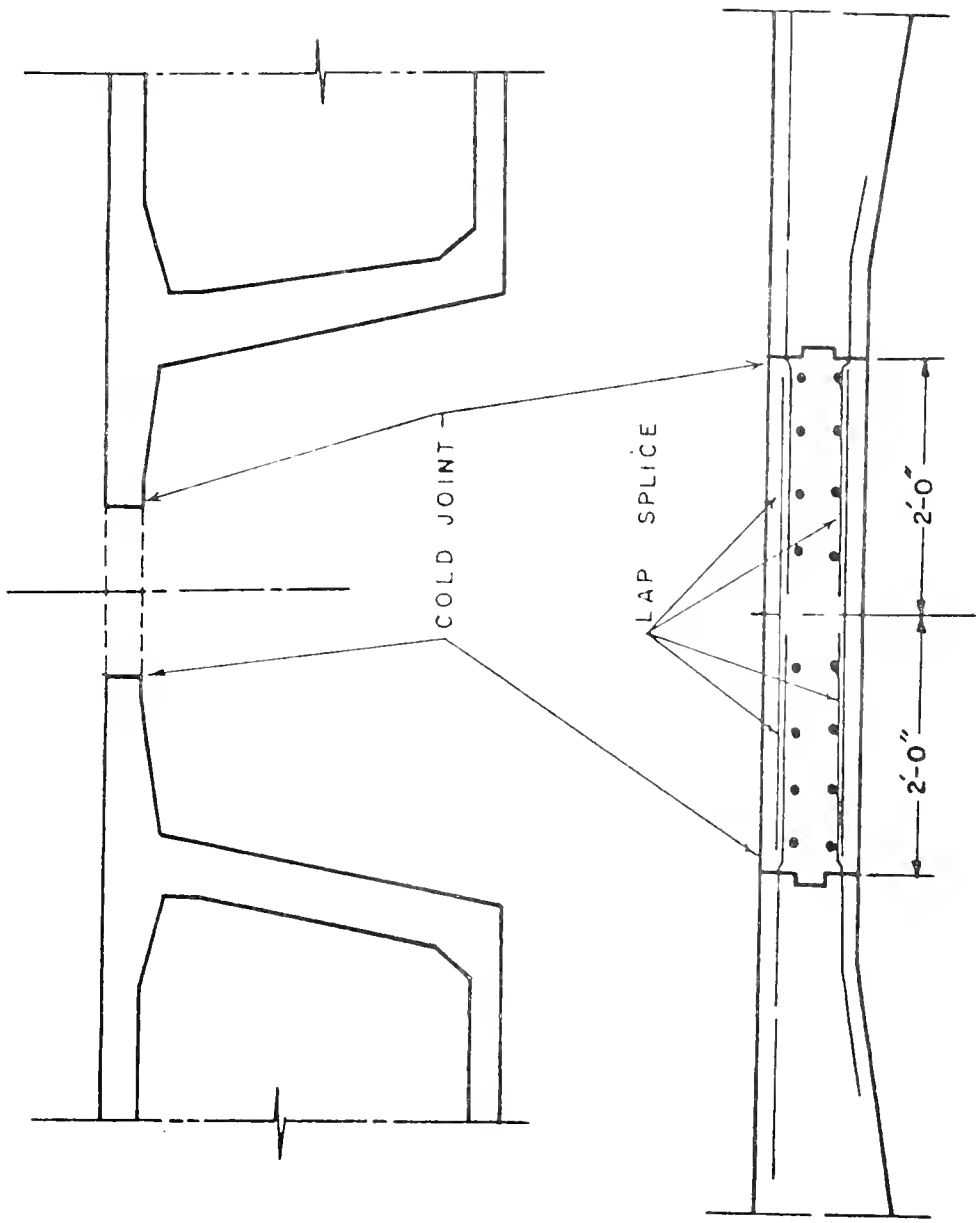

Figure 12. Cast-in-Place Longitudinal Joint

longitudinal effects. The finite element analysis similar to that used on the Turkey Run bridge and the modified frame method will be discussed in detail later.

As noted earlier the above elastic analysis methods are approximate from a mathematical viewpoint, but they are also approximate from a physical viewpoint. The methods do not account for the presence of reinforcement but rather assume the structure to be homogeneous. Effects such as localized cracking and non-linear material properties are also neglected. Nevertheless, past engineering experience has shown elastic analysis methods to be acceptable approximations to actual behavior. The purpose of the transverse bending instrumentation of the Turkey Run bridge is to provide a physical check of tractions in the prototype structure. Once data is collected, the measured tractions will be compared with those determined from the finite element analysis and the modified frame analysis detailed in this report. This should provide valuable data to design engineers involved with segmental bridge analysis and design.

2.2 Proposed Testing Scheme

One of the main objectives of this report is to provide detailed analytic stress data which will later be compared to observed stresses obtained during the testing program. Of course it is necessary to know structural loadings, load positions, and load distributions before such an analysis can be made. The detailed drawings of Figures 13 through 18 present proposed test truck loadings, longitudinal positions, transverse positions, and axle spacings. These hypothetical loading schemes were used in the finite element analysis described later in the

report. Although the analysis provides concise detailed data the problem of reproducing the exact hypothetical loading in the field is quite difficult. If one wishes to correlate theoretical and actual behavior, variations in the analytic model and prototype structure must be minimized. Proposed test loads and positions were chosen in a fashion to require minimal corrections to analytic data.

Figure 13 details the axle loads and spacings of the tandem test truck. These axle spacings are standardized and should cause no conflicts since the same spacings were used in the finite element analysis. The reference positioning points are located on the left and right midway between the front and rear tandem axles. The axle loads shown in Figure 13 are hypothetical and therefore would be difficult if not impossible to exactly reproduce in the field. The given axle loads are based on truck weight data from a previous JHRP project. The front and rear axle loads represent an approximate lower range of actual truck weights from a bridge deck testing project conducted by the Purdue staff. The ratio of front to rear axle loads is exactly 0.40. (See Reference 18.) This is the mean ratio determined from data of the above mentioned project. Once the instrumentation is installed and testing begins, the test truck should approximate the above specifications as closely as possible. For example, if sand is used to load the test truck the front and rear axle load distribution can be manually altered by hand shoveling until the ratio is near 0.40. Also, the magnitudes of axle loads should be within an acceptable range of the hypothetical loads. It is not critical that the magnitudes be exact. Since the structure is assumed to be linearly elastic for

analysis purposes, the tractions predicted by the finite element analysis can be proportioned linearly according to the variation of actual truck weights to theoretical truck weights. This correction should be adequate as long as the front to rear axle weight ratio is near 0.40.

Figure 14 illustrates the longitudinal test truck positions proposed for the testing program. Positioning points will be located longitudinally over segments 24, 12, 3, 2, and 25 respectively. The segment numbering scheme corresponds to that shown on the plan sheets of Appendix D. Test sections near segments 24 and 25 represent points of maximum relative vertical displacement of the twin boxes. This condition should produce maximum cross-sectional distortion and thus will cause a more pronounced transverse bending interaction between the two boxes. Test sections are located at segments 2 and 3 due to their proximity to the central pier. Near the pier there is negligible relative movement between boxes. As a result, frame action predominates and transverse moments are more easily transferred from one box to the other. The stiffness of the thickened bottom slab and the support provided by the pier will cause transverse moments to be more significant at these sections. The test position over segment 12 produces about three-fourths of the maximum moment and shear near the pier sections. This position provides a stress field amenable to longitudinal stress and shear lag instrumentation. It should be noted that the longitudinal positioning points do not exactly concur with the location of the instrumented sections. The reason for the deviation is that the ideal location of load application on a finite element does

not always agree with the ideal location of stress calculations on the element. This situation is described in detail in the section on the finite element analysis of the Turkey Run bridge. Basically, it is desirable for concentrated loads to be applied at the nodes of an element and for stresses to be calculated at the center of an element side, which should correspond to strain gage locations.

Figures 15 through 18 show the exact transverse positions of the test truck measured from the left curb line. There are eight transverse positions for each longitudinal test section. Transverse positions no. 1 and no. 8 place the outer wheel at the outermost extremity of the bridge cross-section. These positions should maximize relative rotational distortions of the two boxes. Positions no. 2 through no. 7 correspond to rational geometric divisions of the box cross-section. As mentioned earlier, it is desirable for loads to be applied at analytic model nodes. The transverse positions used in the analysis may vary slightly in order to fulfill this requirement. Each of the eight transverse positions shown have a symmetrical counterpart on the opposite side of the bridge center line. As a result, a finite element analysis is only required for the first four positions. Tractions for the last four positions are found by symmetry. It is recommended that all eight positions be used in the testing program. This will provide additional data which may be used as a double check for correlation of instrumentation results at symmetric strain gage locations.

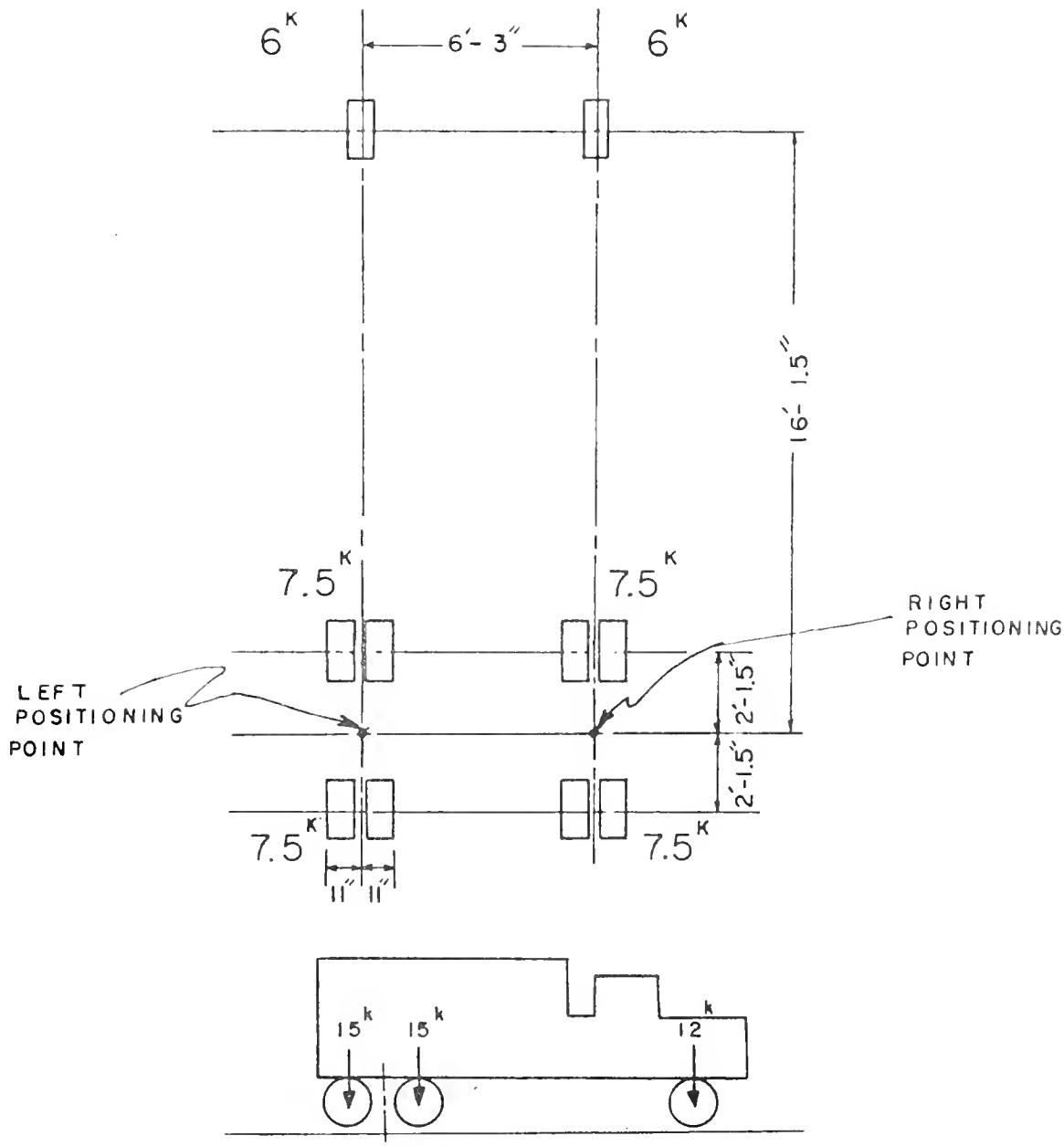

Figure 13. Typical Test Truck Axle Spacings and Loads

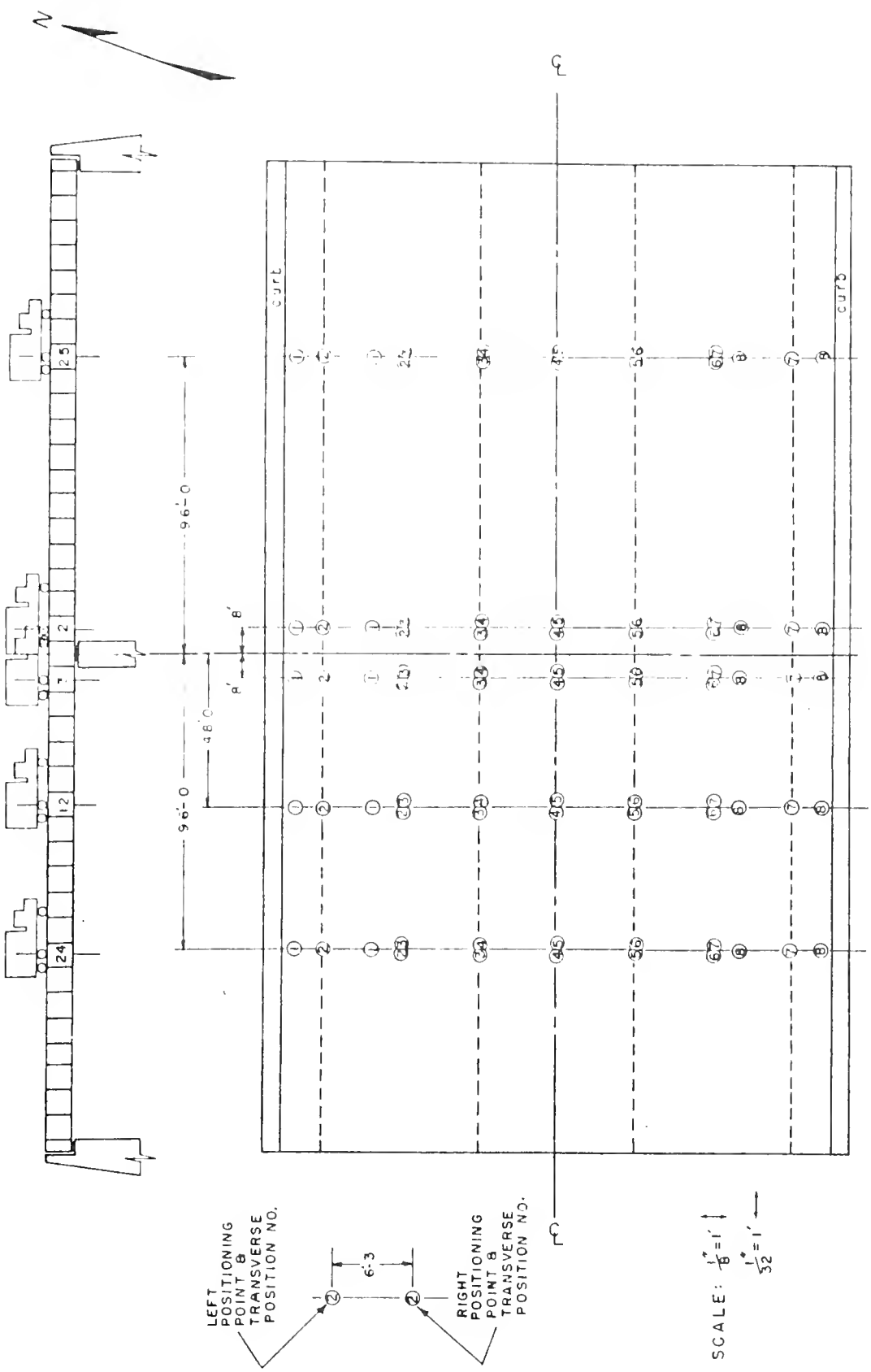

Figure 14. Longitudinal Test Truck Positions

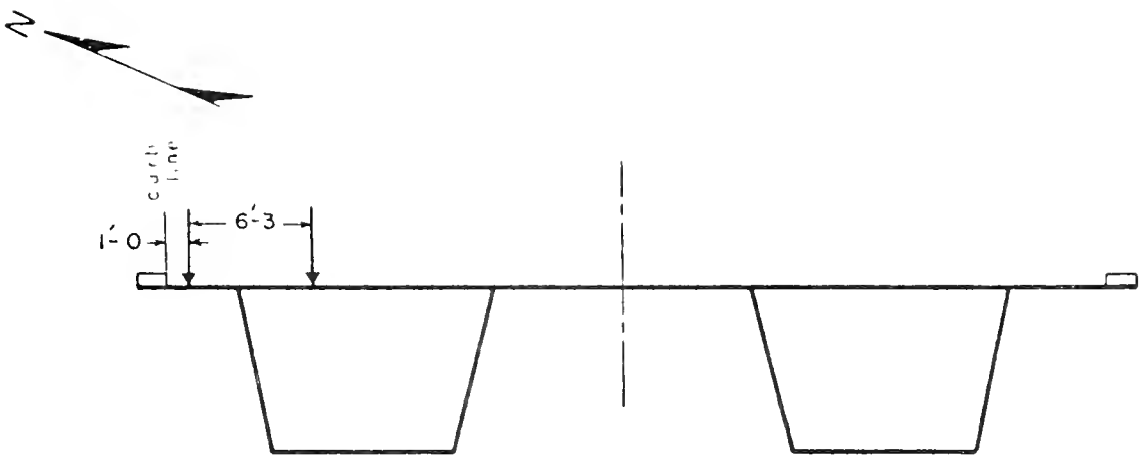

TRANSVERSE POSITION NO. 1

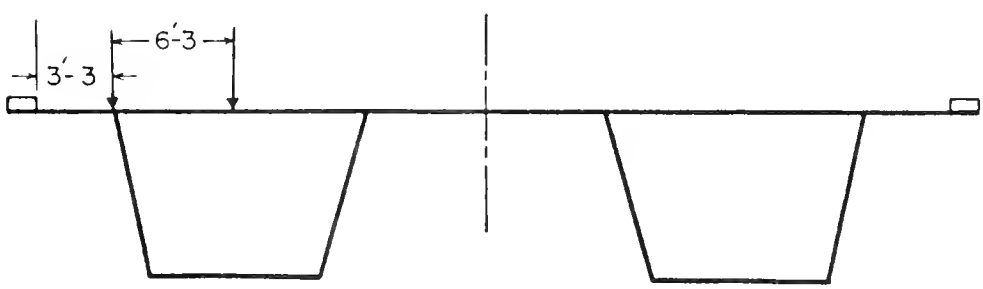

TRANSVERSE POSITION NO. 2

Figure 15. Position Nos. 1 and 2

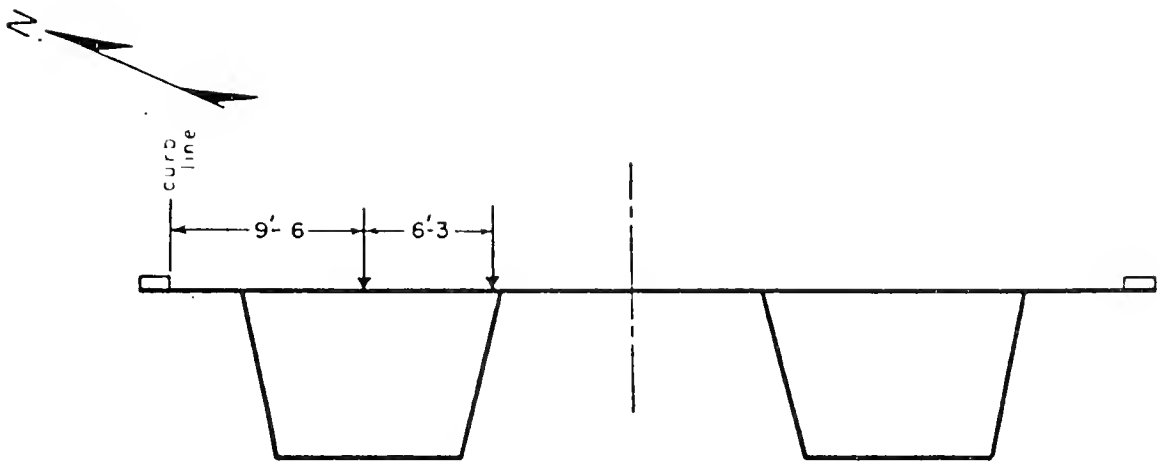

TRANSVERSE POSITION NO. 3

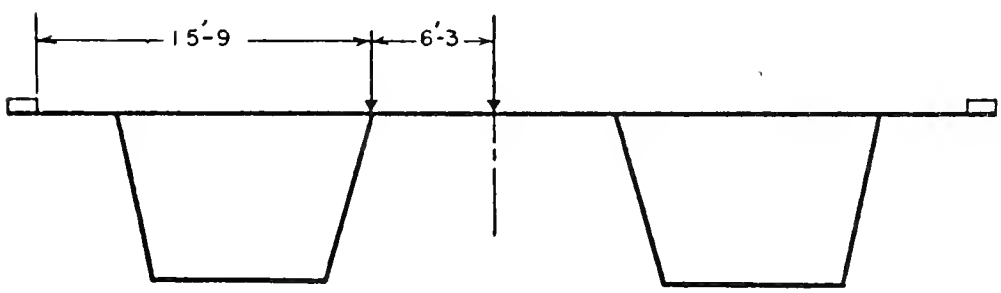

TRANSVERSE POSITION NO. 4

Figure 16. Position Nos. 3 and 4

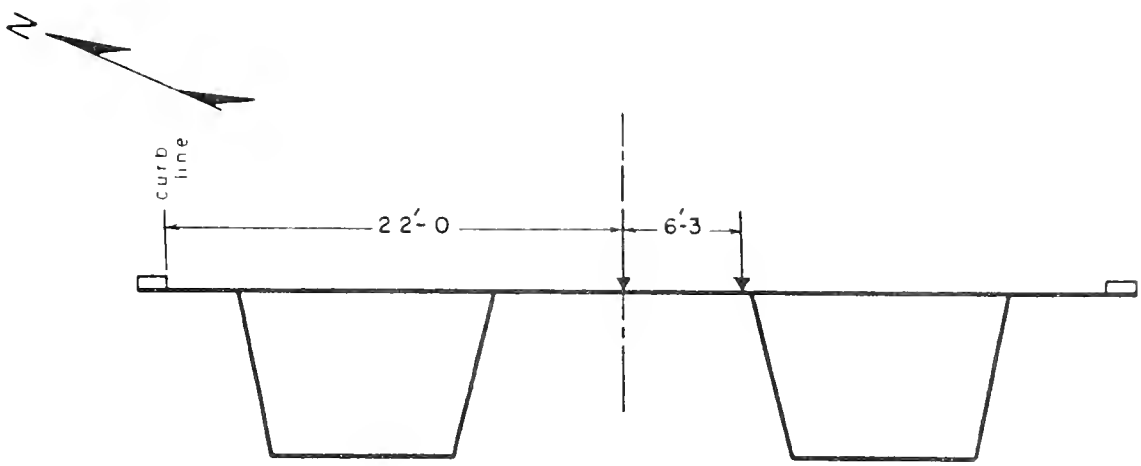

TRANSVERSE POSITION NO. 5

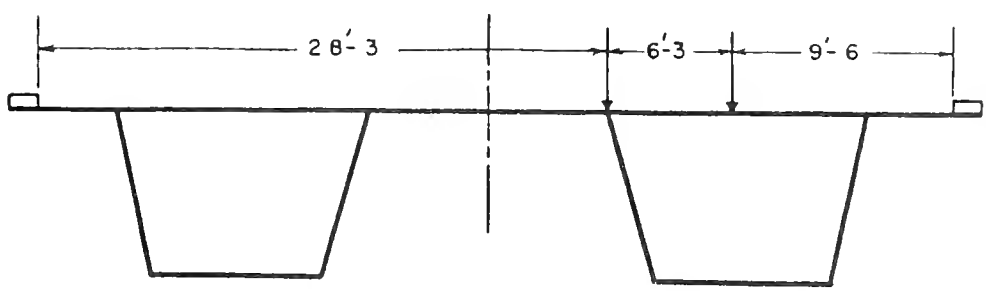

TRANSVERSE POSITION NO. 6

Figure 17. Position Nos. 5 and 6

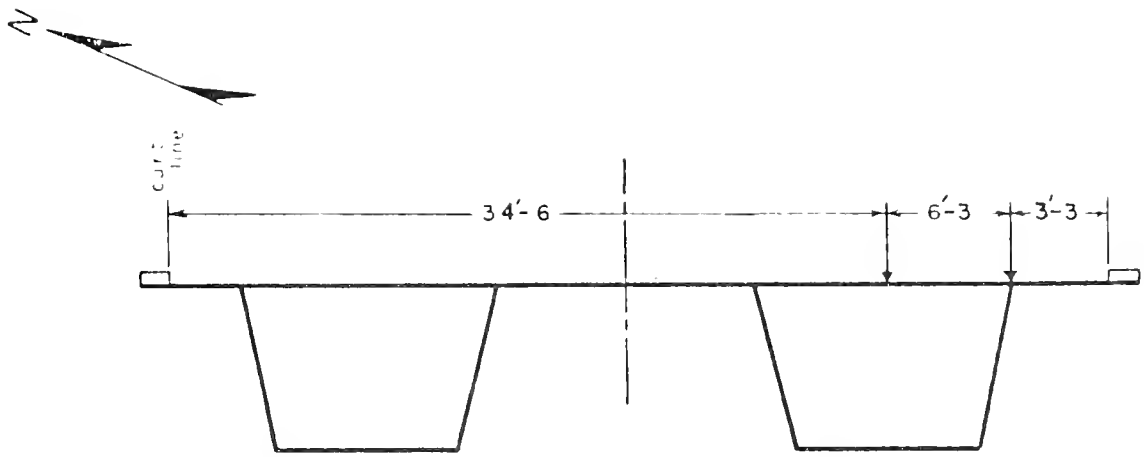

TRANSVERSE POSITION NO. 7

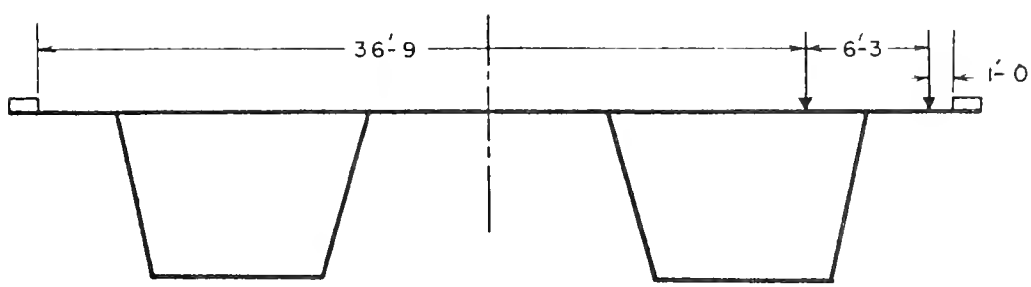

TRANSVERSE POSITION NO. 8

Figure 18. Position Nos. 7 and 8

CHAPTER III

TRANSVERSE BENDING ANALYSIS

3.1 Introduction

The analysis data presented in this section are meant to provide an analytical base to which the empirical test results can be compared. A structural analysis can provide information on structural response under actual loading conditions, or under design loads which are pre-specified. The first case should yield stresses which closely correlate with behavior, if the analytic model is valid. A design load analysis generally has inherent safety factors and cannot be expected to compare favorably with behavior. In most cases the computed design load stresses would be higher than those measured due to the conservative nature of the design process. The analysis of transverse bending tractions in the Turkey Run bridge was done using two independent methods. The first method represents an accepted design analysis technique based on the use of influence surfaces. The second analysis attempts to model actual behavior mathematically using the finite element method. The finite element analysis should compare with actual stresses within reasonable limits. The design analysis procedure is included to show the inherent conservatism of the method and to provide a comparison of design data and data representing actual behavior.

The influence surface technique was suggested by a state-of-the-art paper on segmentally constructed box girder bridges[1]. The method

is based on the use of influence surfaces developed for plates with variable depths. The philosophy behind this method is to provide a hand technique which can conveniently be used in design, thus eliminating the need for a computer. If simple beam theory is used for longitudinal moments, the entire analysis of a segmental bridge can be done by conventional methods without a computer. It will be shown that this technique is quite conservative when compared to the finite element analysis. It follows that the influence surface tractions will probably be conservative in reference to the measured tractions found in the second phase of this project.

The finite element analysis of transverse bending tractions was done by the Indiana State Highway Commission using a finite element program developed specifically for segmental box girder bridges[2]. This program was used in the actual design of the Turkey Run bridge. For the purposes of this project, the suggested axle loads and spacings mentioned earlier were used in the analysis. This was done in an attempt to model actual behavior under the pre-specified loadings with the finite element analysis. This should provide a direct check on the finite element program as well as the behavioral assumptions made in the analysis.

A detailed description of the two analysis techniques follows. The results of both analyses are tabulated with the tractions listed corresponding to the positions of strain gage installations. The results are then compared in light of the analysis assumptions.

3.2 Influence Surface Analysis

This method is based on the use of the Homberg influence surfaces for plates with variable depth[3]. The method of analysis as outlined in the state-of-the-art paper cited earlier reduces the three dimensional plate bending problem to a two dimensional frame analysis of the segment cross-section. The influence surfaces are used to find fixed-end moment tractions of the top slabs. Influence surfaces for plates are analogous to influence lines for beam elements. Figures 19 through 23 are influence surfaces taken from the Homberg book. The three-dimensional nature of these charts allows the effect of a series of wheel loads to be included in the fixed-end tractions. Once the fixed-end tractions are determined for a particular loading position, a frame analysis is done to determine tractions in the segment section. The fixed-end tractions at a cross-section are found from plate theory, but the frame analysis is based on a unit length of the box girder. The frame analysis is done with the webs of the cross-section supported. Three different support conditions were analyzed. The results of the three analyses are tabulated. The frame analysis can be accomplished by conventional moment-distribution or by matrix methods. In this case the STRUDL program was used which is available on Purdue's IBM 360 computer.

In order to determine the fixed-end moment tractions the top roadway slabs and side cantilevers are assumed fixed at the slab-web juncture. Each plate between fixations behaves independently. The cross-section is analyzed for eight transverse loading positions as detailed in Chapter II. Each position will place wheel loads in some

of the plate panels and not in the others. Those panels containing wheel loads will have fixed-end tractions. The wheel loads are actually three dimensional with a tandem axle and front axle. Also, the wheel loads do not represent point loads but are actually distributed over a tire contact area. The test truck contact areas and axle spacings are scaled according to the influence surfaces. If this arrangement is overlaid on the influence surface as shown in Figure 19, the volume of the frustrum created by the intersection of the contact area cylinder and the influence surface can be found. The total volume represents the fixed-end moment traction per unit load at the section under consideration for that particular loading position.

The Homberg influence surfaces were developed in Europe and are thus based on the metric system. The lateral and longitudinal dimensions of the surfaces are based on the ratio of length to slab span length and are thus dimensionless. The vertical ordinate of the surfaces is metric. Thus the volume of the frustum yields moments in kg-m per unit kg. A proper conversion to ft-kips per kip must be made.

In pavement design the tire contact area is usually assumed to be elliptical in shape. The contact area is found by dividing the wheel load (lb) by the tire pressure (psi). For the purposes of this analysis, the tire pressure was assumed to be 70 psi. The wheel loads are as specified in Chapter II. The contact area was assumed to be rectangular rather than elliptical in order to simplify the analysis. The contact pressure area enlarges as the depth into the slab increases. The imprint area used in the analysis was found by extending the rectangular contact area at 45° to the mid-depth of the slab. The result

is an expanded imprint area as shown in Figure 19. The contact rectangle intersects the influence surface forming a parallelepiped truncated by a curved surface. The volume and thus the influence value must be found by a numerical technique. For this analysis each contact area was divided into a rectangular grid. The influence ordinate was found at each grid point. By using Simpson's rule of numerical integration the frustrum volume was determined. Considering the errors introduced by simplifying assumptions made in the analysis, the above technique is probably too rigorous. An alternative would be to use an average influence ordinate multiplied by the imprint area as an acceptable influence value. As seen in Figures 19 through 23, the influence surfaces are developed for specific slab depth ratios (d_r). Tractions for the actual depth ratios were found by interpolating between values determined from the influence surfaces. The above procedure was used to determine fixed-end moment tractions for the eight transverse loading conditions. In all cases the imprint area made by the front tires was beyond the zone of influence for the test sections analyzed. The resulting fixed-end moment tractions are tabulated in Table 1.

Once the fixed-end moments are found, a frame analysis is done to determine the moment distribution in the box section. The analysis is accomplished in the conventional manner by superimposing the fixed-end case with the case in which joints are free to move under joint loads equal and opposite in sense to the fixed end member forces. The analysis is based on the assumption that a unit length of the box section behaves as a frame. As previously mentioned, the fixed-end moments

Table 1. Fixed-End Moment Tractions

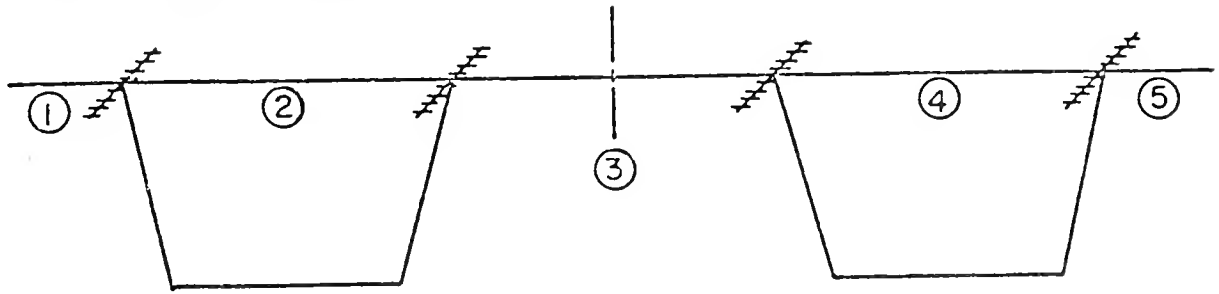

(ft-k/ft)

Position	Station							
	M_c^1	$M_{left}^{F\ 2}$	$M_{right}^{F\ 2}$	$M_{left}^{F\ 3}$	$M_{right}^{F\ 3}$	$M_{left}^{F\ 4}$	$M_{right}^{F\ 4}$	M_c^5
1	2.82	4.94	2.02	0	0	0	0	0
2	0	3.75	3.75	0	0	0	0	0
3	0	3.75	3.75	0	0	0	0	0
4	0	0	0	3.50	3.50	0	0	0
5	0	0	0	3.50	3.50	0	0	0
6	0	0	0	0	0	3.75	3.75	0
7	0	0	0	0	0	3.75	3.75	0
8	0	0	0	0	0	2.02	4.94	2.82

are based on plate theory. Although the analysis is based on a unit width, the actual tandem axle arrangement distributes the load over a larger area depending on the stiffness of the slab. This is overcome by dividing the total wheel load by an assumed distribution length which reduces it to a load per unit width. For the Turkey Run analysis the distribution length was assumed to be 6 ft. This is based on the test truck axle spacing and on the expanded contact area found by distributing the load area at 45° to the mid-depth of the slab. Another factor which should be considered in the analysis is the corner fillets in the box section. The fillets in effect make the "frame" members have a variable moment of inertia. This should be considered in an analysis. This was done in the present analysis by breaking each member into several segments, each with different section properties.

For analysis a frame must be supported in a stable manner. For the transverse bending analysis the box section webs are assumed to be supported at their bases. As shown on the schematics of Tables 2 through 4, three different boundary conditions were considered in the analysis. First, the supports were assumed to be pinned on rollers with no lateral restraint. Secondly, the supports were pinned with full restraint against lateral displacement. Finally, the supports were completely fixed against rotation or lateral displacement. These three conditions should bound the actual web base support conditions. Near the pier, the web diaphragm and the thickened bottom slab tends to restrain the web base, while at midspan the lateral and rotational stiffnesses diminish. One drawback of the present approach is the neglect of the relative vertical displacements of the web supports.

This factor could be accounted for by using spring supports, although this would complicate the analysis beyond practicality. The results of the three analyses are tabulated in Tables 2 through 4. Moment tractions are tabulated only at strain gage test section locations.

For this analysis technique it is seen that moment tractions are much larger in the vicinity of the wheel loads. In fact, the moment tractions in members twice removed from loaded members are several orders of magnitude smaller than the primary tractions. Due to the variability of support conditions these tractions are probably unreliable. Note that the primary moments for all three cases vary by only a small percentage. This is partially due to the transverse web stiffness being larger relative to the top slab stiffness. One could conclude that the fixed base case would be adequate for predicting primary transverse moment tractions.

3.3 Finite Element Analysis of Transverse Bending

The finite element method is a technique of analysis which models a continuous structure by subdividing it into discrete elements. Each element is actually a mathematical unit which determines the displacement field within the element through the use of interpolating polynomials. The displacement field is represented in terms of displacements at the element corners or nodes. Through the use of the principle of minimization of total potential energy a stiffness matrix is formulated for each element. Equilibrium is enforced at the nodes resulting in a set of simultaneous equations. The solution of the equations and backsubstitution of results yields the stress distribution within the continuous structure.

Table 2. No Lateral Restraint of Supports

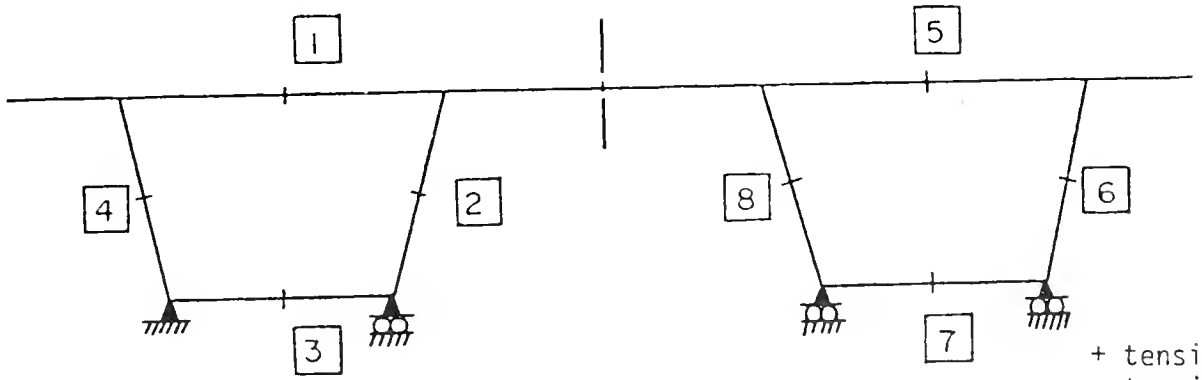

+ tension on inside
- tension on outside

(ft-kip/ft)

		Station							
		1	2	3	4	5	6	7	8
Position	1	+1.67	-0.81	+0.29	-0.27	+0.03	+0.02	+0.07	-0.26
	2	+4.36	-1.25	+0.58	-1.05	+0.03	+0.02	+0.06	-0.25
	3	+4.42	-1.00	+0.67	-1.70	-0.00	-0.00	-0.00	+0.02
	4	-0.12	+1.38	-0.18	-0.52	-0.18	-0.13	-0.41	+1.55
	5	-0.18	+1.55	-0.41	-0.13	-0.12	-0.52	-0.18	+1.38
	6	-0.00	+0.02	-0.00	-0.00	+4.42	-1.70	+0.67	-1.00
	7	+0.03	-0.25	+0.06	+0.02	+4.36	-1.05	+0.58	-1.25
	8	+0.03	-0.26	+0.07	+0.02	+1.67	-0.27	+0.29	-0.81

Table 3. Supports Restrained Laterally

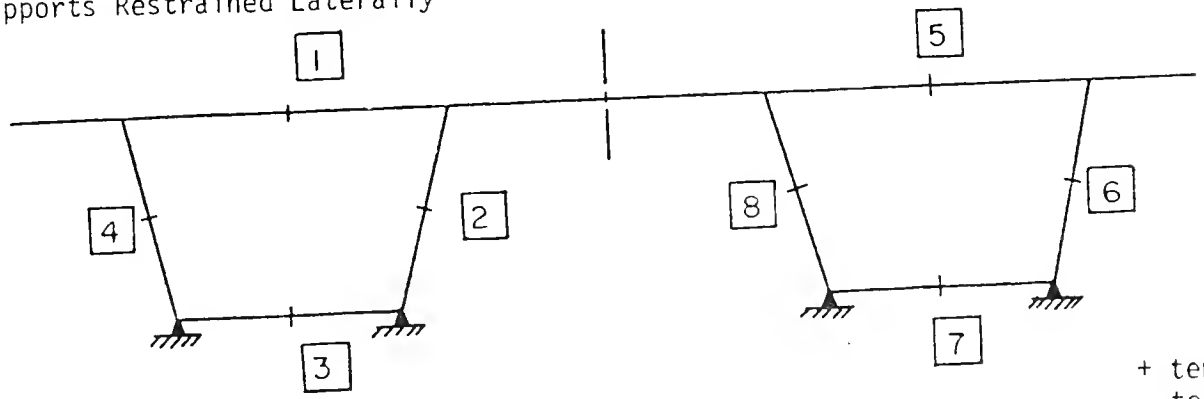

+ tension on inside
- tension on outside

(ft-kip/ft)

Position	Station 1	2	3	4	5	6	7	8
1	+1.68	-0.64	+0.30	-0.50	+0.04	-0.21	+0.07	-0.07
2	+4.37	-1.14	+0.59	-1.19	+0.03	-0.12	+0.06	-0.13
3	+4.41	-1.13	+0.66	-1.53	-0.01	+0.17	-0.02	-0.11
4	-0.14	+0.97	-0.24	+0.04	-0.18	+0.35	-0.32	+0.98
5	-0.18	+0.98	-0.32	+0.35	-0.14	+0.04	-0.24	+0.97
6	-0.01	-0.11	-0.02	+0.17	+4.41	-1.53	+0.66	-1.13
7	+0.03	-0.13	+0.06	-0.12	+4.37	-1.19	+0.59	-1.14
8	+0.04	-0.07	-0.07	-0.21	+1.68	-0.50	+0.30	-0.64

Table 4. Supports Fixed

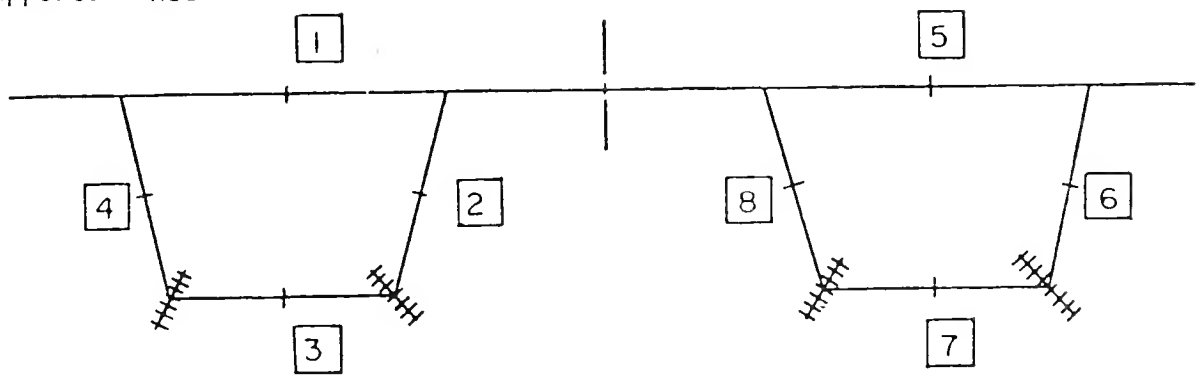

(ft-kip/ft)

+ tension on inside
- tension on outside

Position	Station 1	2	3	4	5	6	7	8
1	+1.65	-0.53	0	-0.13	+0.02	-0.24	0	+0.12
2	+4.31	-0.75	0	-0.62	+0.02	-0.13	0	+0.01
3	+4.34	-0.50	0	-1.04	-0.00	+0.23	0	-0.21
4	-0.11	+0.77	0	-0.14	-0.14	+0.23	0	+0.53
5	-0.14	+0.53	0	+0.23	-0.11	-0.14	0	+0.77
6	-0.00	-0.21	0	+0.23	+4.34	-1.04	0	-0.50
7	+0.02	+0.01	0	-0.13	+4.31	-0.62	0	-0.75
8	+0.02	+0.12	0	-0.24	+1.65	-0.13	0	-0.53

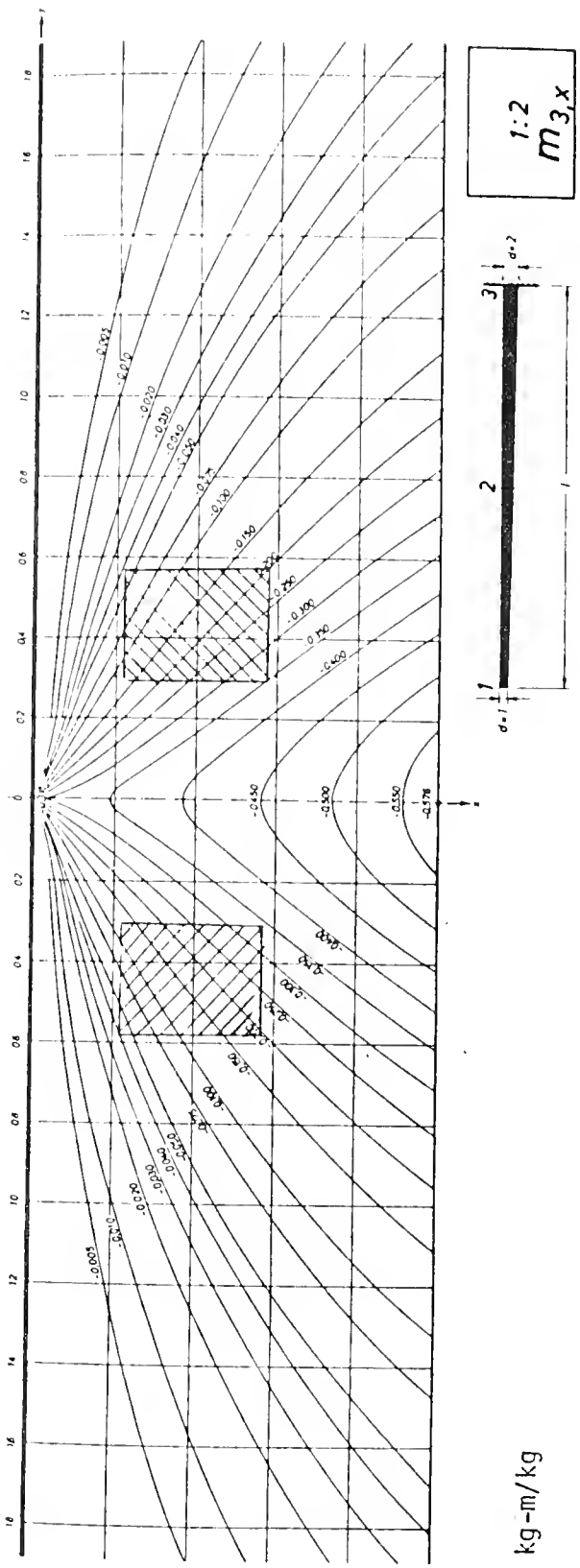

Figure 19. Cantilever Plate Influence Surface With Contact Area (d_r 1:2)

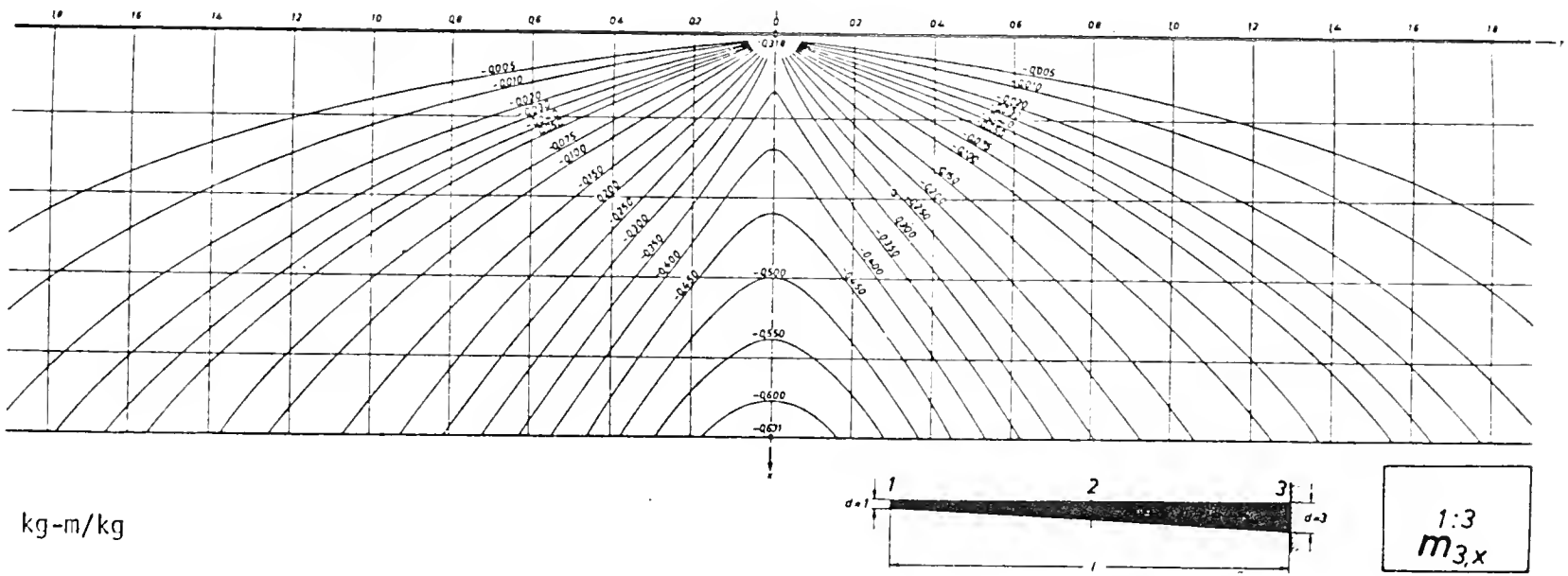

kg-m/kg

Figure 20. d_r 1:3

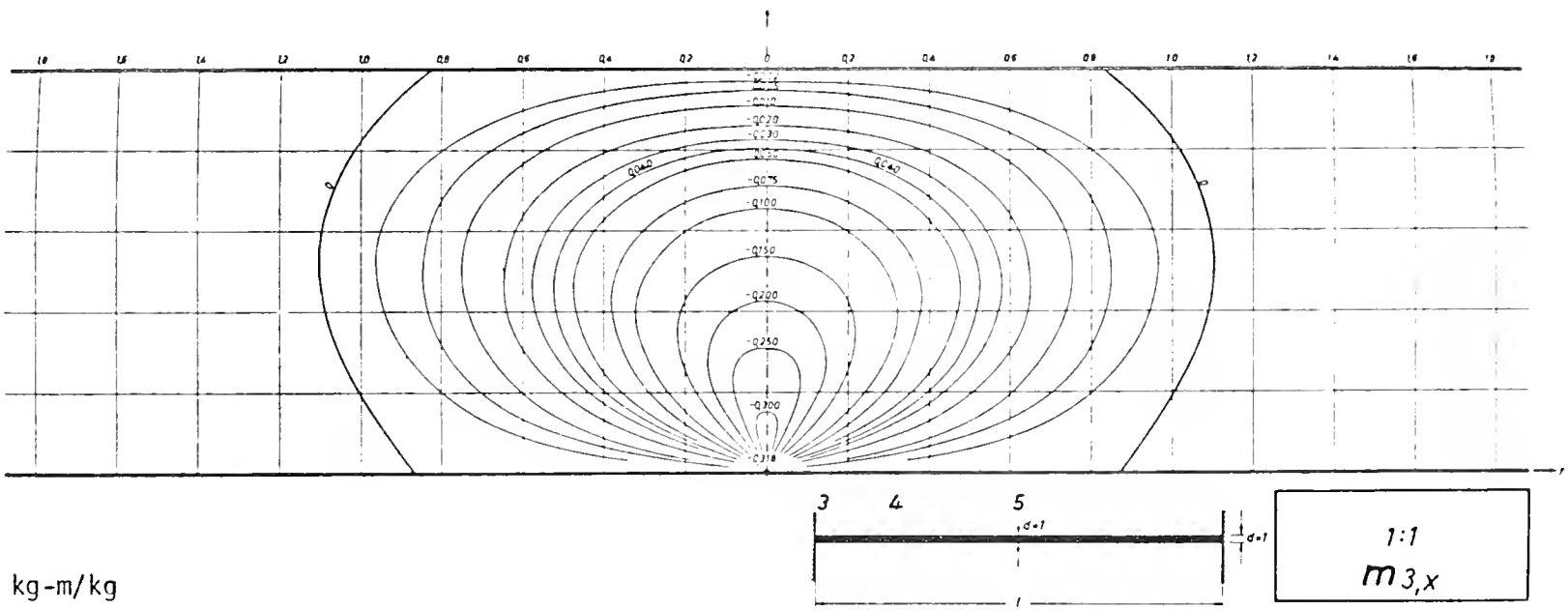

kg-m/kg

Figure 21. Fixed-Fixed Plate Influence Surface (d_r 1:1)

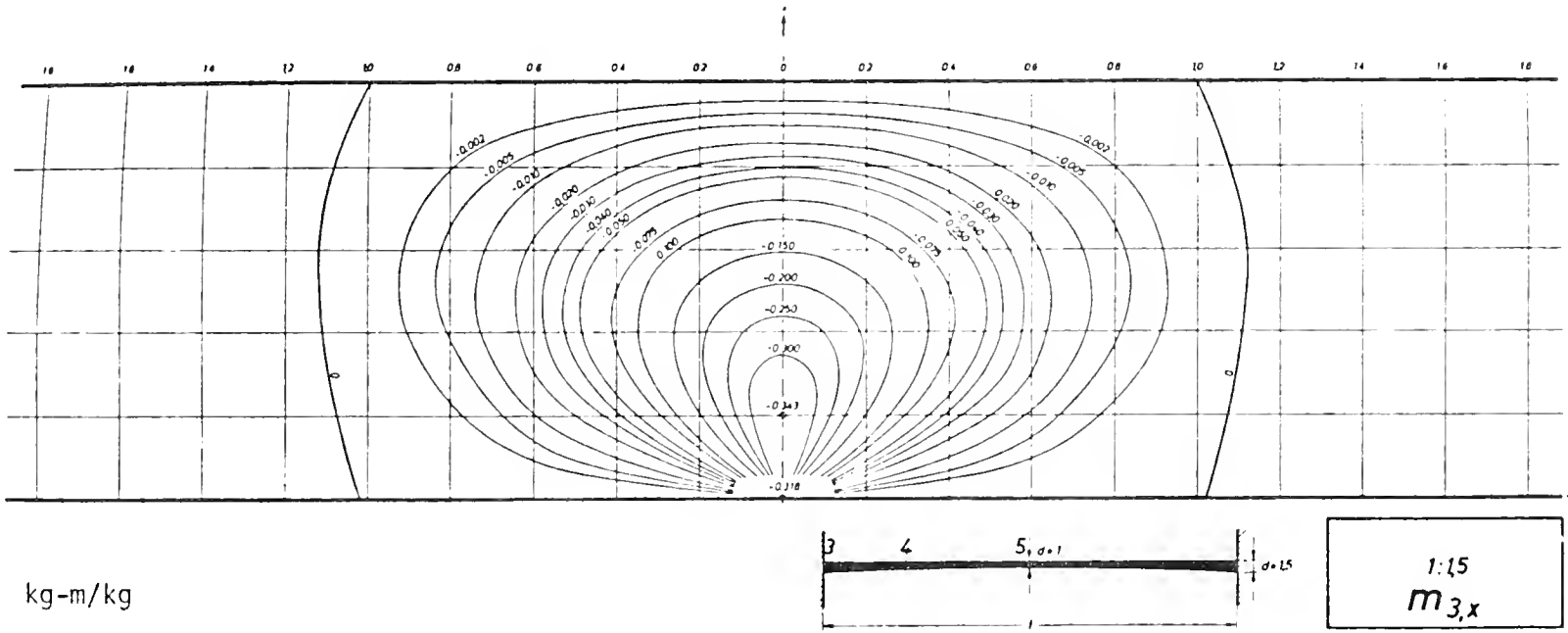

kg-m/kg

Figure 22. d_r 1:1.5

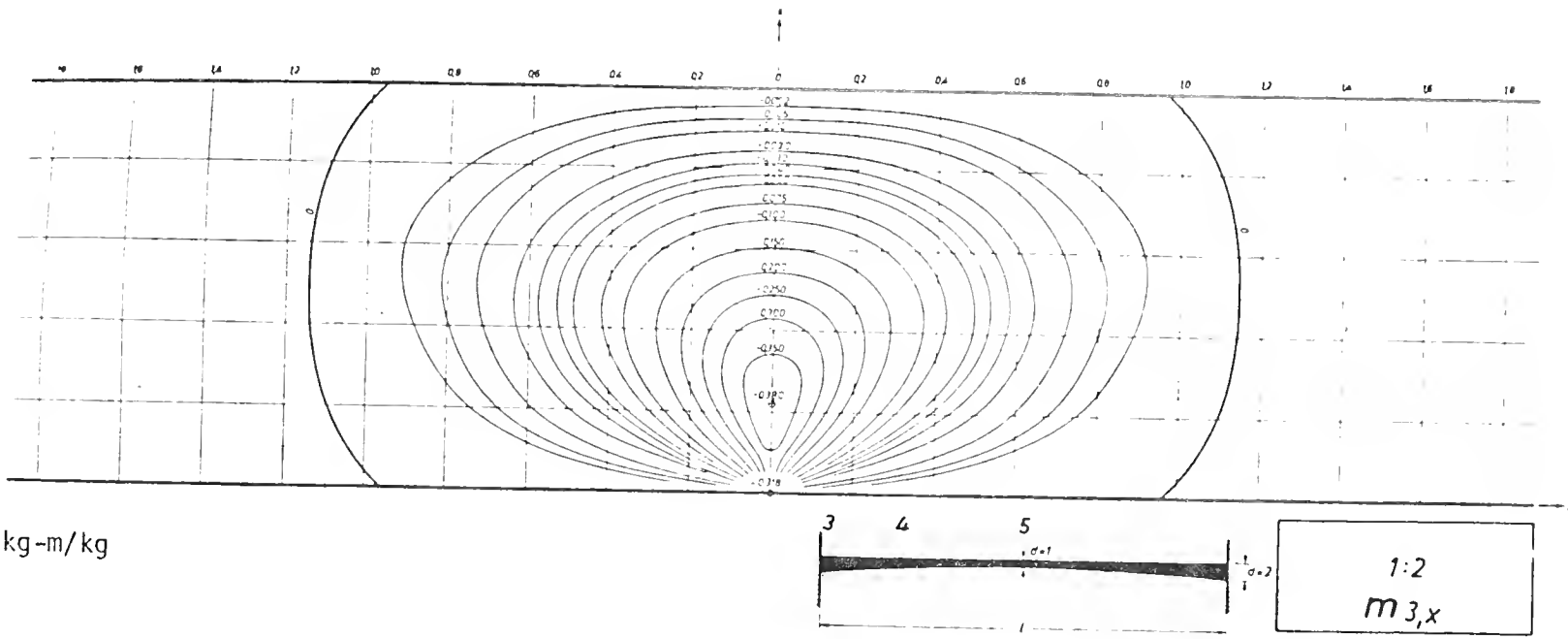

Figure 23. d_r 1:2

The discrete element used in the present analysis is actually the superposition of a rectangular plane stress element and plate bending element as shown in Figure 24. Altogether there are six degrees of freedom per node with four nodes per element. A detailed description of the element stiffness matrix formulation can be found in Reference 15. It should be noted that this element is formulated with a constant depth (t). For the analysis of variable depth box girder decks an average slab thickness must be used in each element.

The entire structure is divided into discrete elements as shown in Figure 25. The elements composing the mesh are mathematically connected at the nodes by enforcing equilibrium of element forces and external nodal forces at each node point. Each top slab panel is laterally divided into two elements. The longitudinal element dimension depends on the degree of mesh refinement. A finer mesh theoretically produces more accurate results. The bottom slab and webs are modeled by single elements having the same longitudinal dimension as the top slab elements. Figure 25 shows two mathematical segments. It should be noted that the mathematical segment divisions do not necessarily correspond to the physical bridge segments. A more detailed description of the mesh chosen for the analysis of the Turkey Run segmental bridge can be found in Reference 15..

The results of the finite element analysis of the Turkey Run bridge are tabulated in Tables 5 through 8. Transverse moment tractions are listed at locations corresponding to the strain gage installations. There are eight transverse truck positions at each of four test sections. Details of positioning points are found in Chapter II.

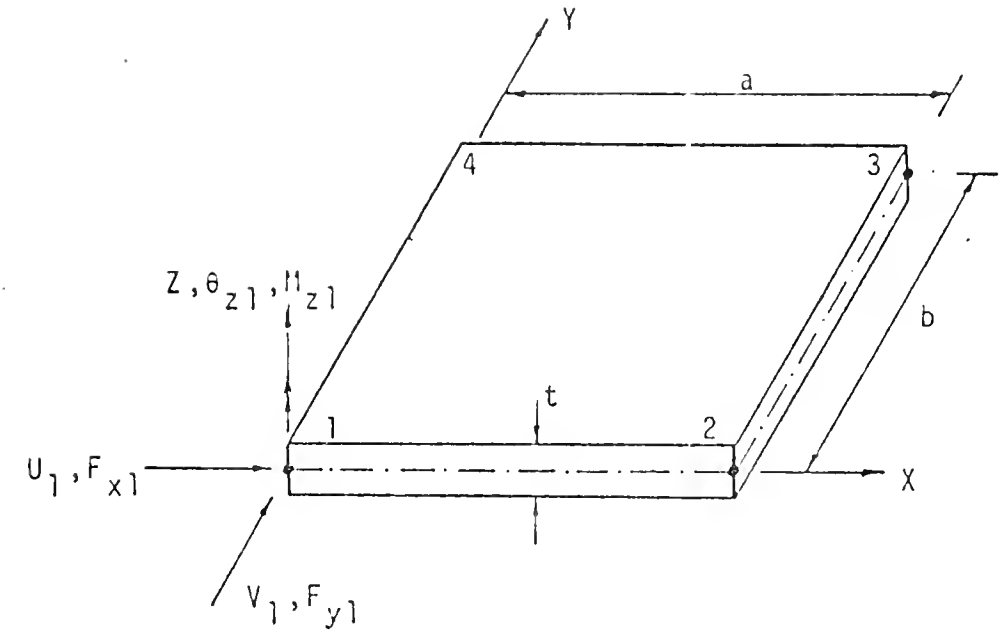

(a) Plane stress element

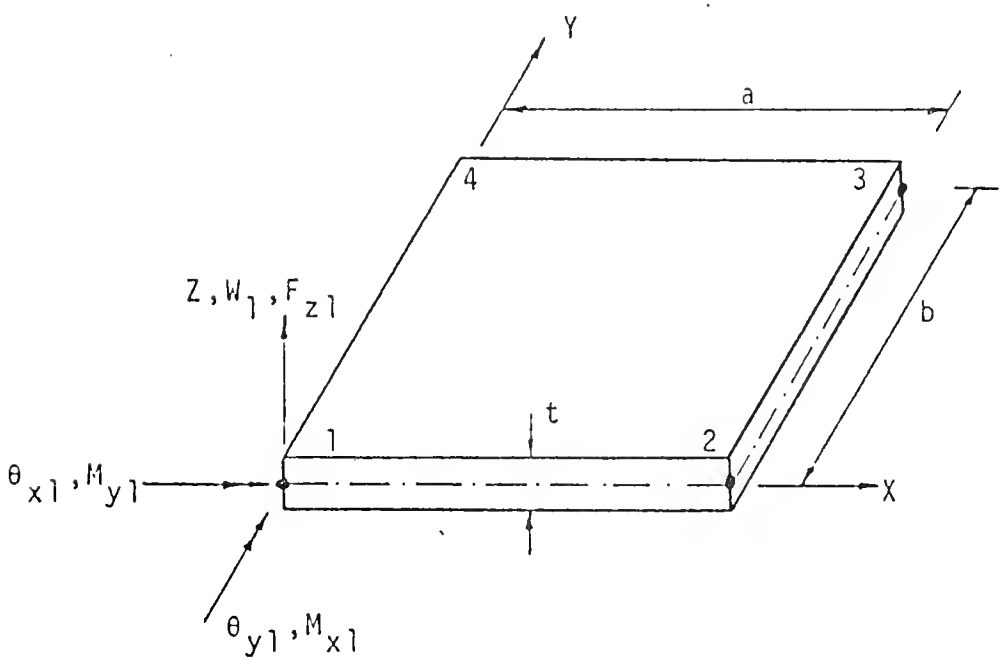

(b) Plate bending element

Figure 24. Finite Element Used in Analysis[1]

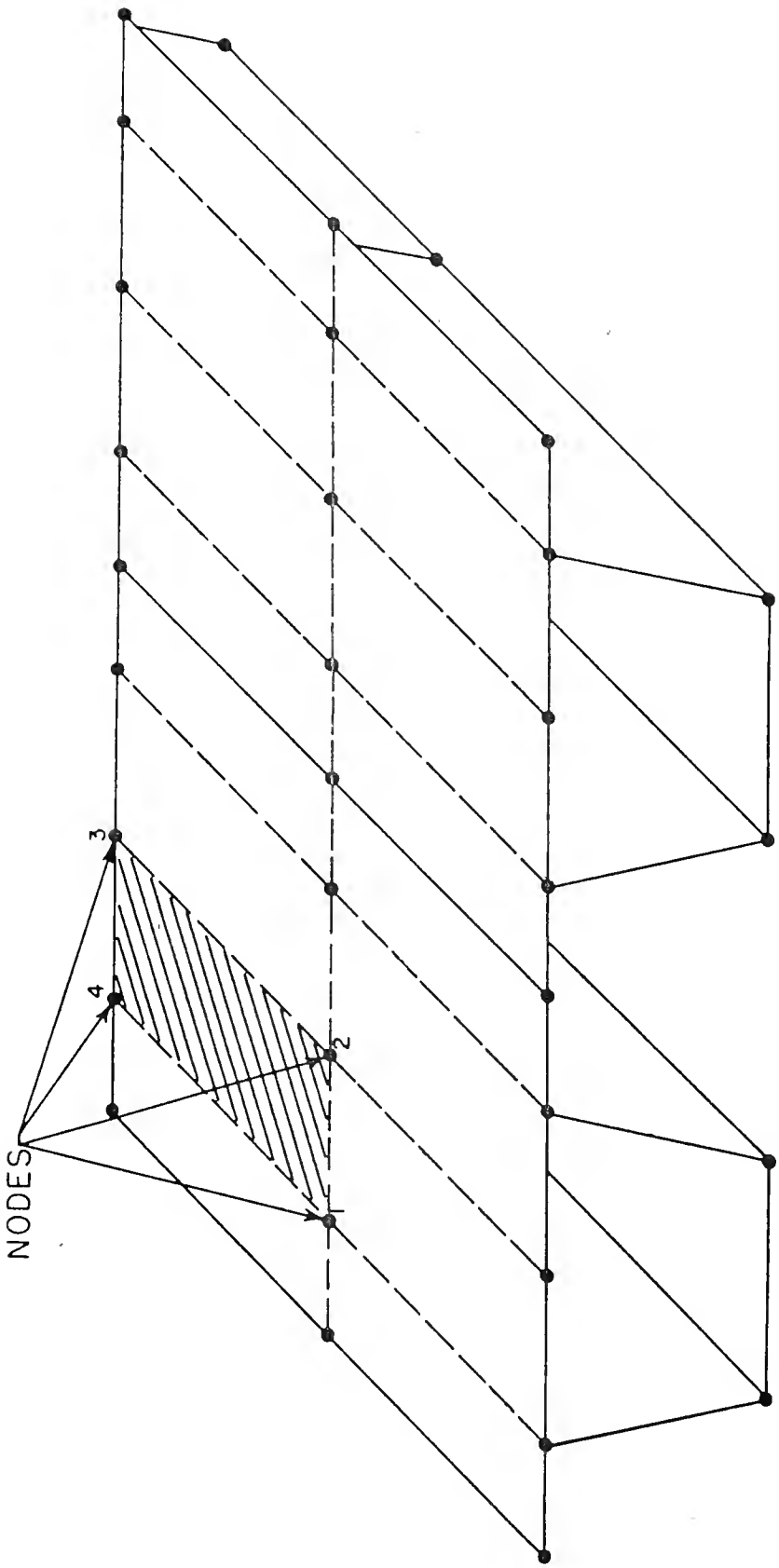

Figure 25. Finite Element Mesh

Table 5. Longitudinal Position No. 1

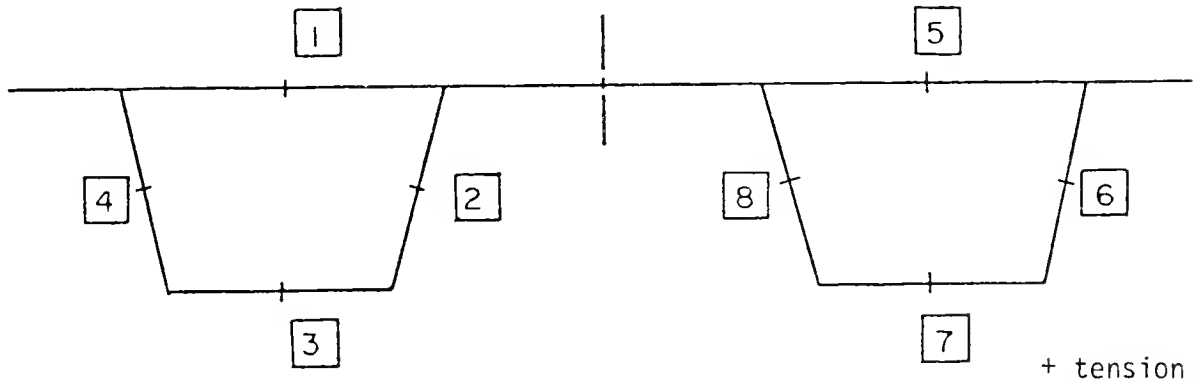

(ft-lb/ft)

+ tension on inside face
- tension on outside face

		Station							
		1	2	3	4	5	6	7	8
Position	1	-134	-193	-42	+1398	-70	+51	-17	+366
	2	+2202	-950	+57	-615	-72	+47	-17	+372
	3	+2220	-989	+62	-682	-80	+56	-19	+419
	4	-15	+253	-8	-22	-102	+67	-29	+717
	5	-102	+717	-29	+67	-15	-22	-8	+253
	6	-80	+419	-19	+56	+2220	-682	+62	-989
	7	-72	+372	-17	+47	+2202	-615	+57	-950
	8	-70	+366	-17	+51	-134	+1398	-42	-193

Table 6. Longitudinal Position No. 2

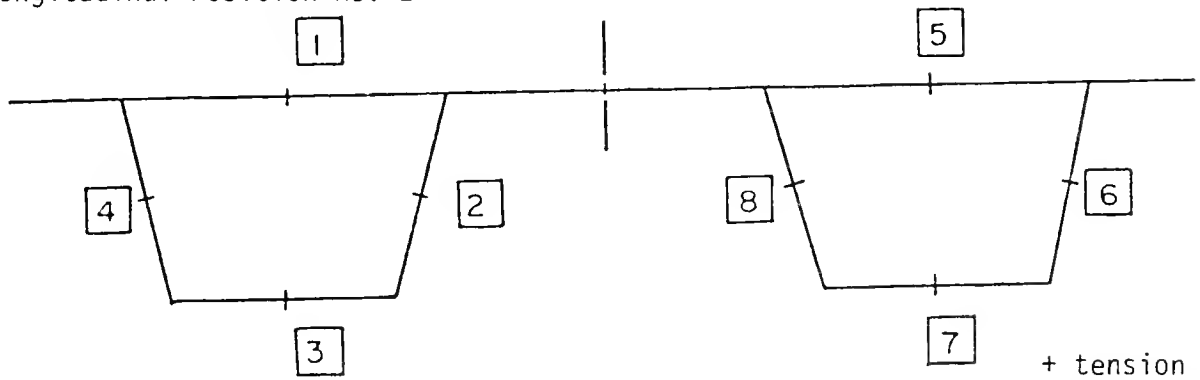

(ft-lb/ft)

+ tension on inside face
- tension on outside face

Position	Station 1	2	3	4	5	6	7	8
1	-117	+159	-241	+1109	-2	+1	-2	+12
2	+2090	-403	+172	-493	-1	-	+2	-9
3	+2094	-478	+174	-433	-2	+3	-2	+2
4	-47	+365	-86	+84	-40	+60	-95	+403
5	-40	+403	-95	+60	-47	+84	-86	
6	-2	+2	-2	+3	+2094	-433	+174	
7	-1	-9	+2	-	+2090	-493	+172	
8	-2	+12	-2	+1	-117	+1109	-241	

Table 7. Longitudinal Position No. 3

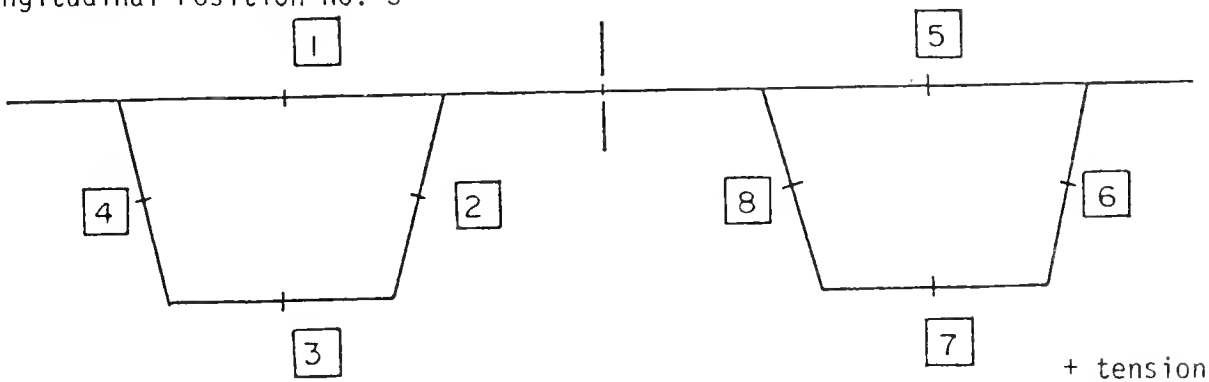

(ft-lb/ft)

+ tension on inside face
- tension on outside face

		Station							
		1	2	3	4	5	6	7	8
Position	1	-135	+190	-245	+1086	-6	+6	-6	+28
	2	+2104	-411	+186	-535	-4	+6	-3	+9
	3	+2108	-533	+190	-433	-7	+10	-9	+24
	4	-51	+323	-85	+113	-50	+76	-101	+434
	5	-50	+434	-101	+76	-51	+113	-85	+323
	6	-7	+24	-9	+10	+2108	-433	+190	-533
	7	-4	+9	-3	+6	+2104	-535	+186	-411
	8	-6	+28	-6	+6	-135	+1086	-245	+190

Table 8. Longitudinal Position No. 4

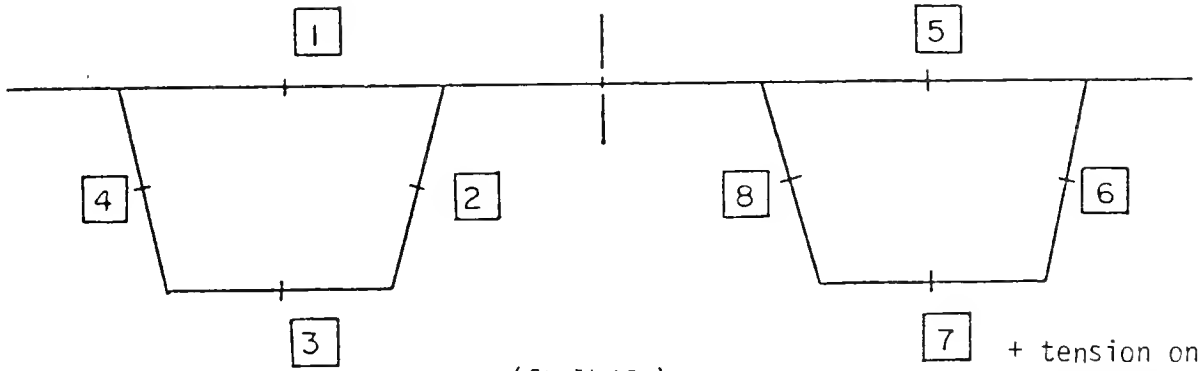

(ft-lb/ft)

+ tension on inside face
- tension on outside face

		Station							
		1	2	3	4	5	6	7	8
Position	1	-117	-282	-38	+1384	-87	+64	-21	+454
	2	+2218	-1029	+61	-627	-87	+63	-20	+451
	3	+2232	-1053	+64	-692	-93	+66	-22	+485
	4	-10	+225	-6	-25	-108	+78	-31	+747
	5	-108	+747	-31	+78	-10	-25	-6	+225
	6	-93	+485	-22	+66	+2232	-692	+64	-1053
	7	-87	+451	-20	+63	+2218	-627	+61	-1029
	8	-87	+454	-21	+64	-117	+1384	-38	-282

The finite element mesh was chosen in a fashion such that concentrated wheel loads fell on node points. Conveniently, most of the eight transverse positions placed the loads over the nodes. Exceptions were the outer positions, Nos. 1 and 8, which had to be altered in order to place the wheel loads over a node. This was done by decreasing the axle width. This invalidates data at these sections in reference to the actual loading positions. Primary bending moments cannot be expected to correlate at these particular positions. But, secondary moments at locations removed from the test truck location should not be affected significantly. Transverse bending tractions at sections other than the loaded test sections were not listed since they are several orders of magnitude smaller than the primary moment tractions. The reliability of these tractions might be questionable. Moments at locations between node points were found by linear interpolation between the node tractions.

As in the influence surface analysis, the primary tractions in the vicinity of the loads are significantly larger than those in members removed from the wheel loads. Again this might be attributed to the stiffness of the webs. This implies that the carry-over moments from one box to the adjacent box are very small even with full continuity of the cast-in-place longitudinal joint as assumed in the finite element analysis. It should be noted that for certain load positions the moments listed are not the maximum moments in that particular element. In some cases an inflection point might occur between nodes near a strain gage location, resulting in small tractions. Small tractions cannot be measured as accurately as larger tractions; therefore,

the reliability of the data at each test location should be considered when comparing the empirical results to the finite element results.

3.4 Finite Element Analysis vs. Influence Surface Analysis

As can be seen by comparing the tabulated results of the two analyses, the primary transverse moment tractions of the influence surface analysis are larger than those of the finite element analysis by a factor of two or greater. This reveals the inherent conservatism of the influence surface technique. The use of simple frame theory to model plate action and the assumption that the wheel load is distributed uniformly over an assumed longitudinal distribution length are the primary factors causing the conservative results. The secondary moments vary considerably in the two analyses. Due to the variation in support boundary conditions in the influence surface analysis, the location of inflection points will vary. This results in secondary moments of different sign than the finite element moments in some cases. Realistically, the secondary moments from the influence surface analysis are probably unreliable and of little significance for design. The results reveal that the simplified design approach and the more rigorous finite element technique do not compare favorably. The finite element results are more reliable and should correlate with actual behavior as determined by the testing program.

3.5 Transverse Moments Induced by Thermal Gradients

Transverse bending moments can be induced by conditions other than gravity loading. For example, if the top slab is post-tensioned transversely a shortening occurs in the top slab relative to the bottom

slab. The lateral stiffness of the webs causes transverse bending moments to be induced. The Turkey Run bridge does not have transverse post-tensioning, but relative shortening of the top and bottom slabs can occur due to thermal gradients through the superstructure. The transverse moments induced are similar to those caused by transverse post-tensioning, although they may be opposite in sign. This effect, although small, should be accounted for when correlating measured moments with moments found from an elastic live load analysis. A rigid frame analysis should provide a reasonable prediction of this phenomenon since the symmetric temperature loading causes primary curvature in the transverse direction only. If one considers the twin box beams as open tubular members, one-way plate action predominates. Curvature in the longitudinal direction is negligible except near the physical supports. The only variation from simple frame theory results from the Poisson effect as demonstrated below. Assuming Poisson's

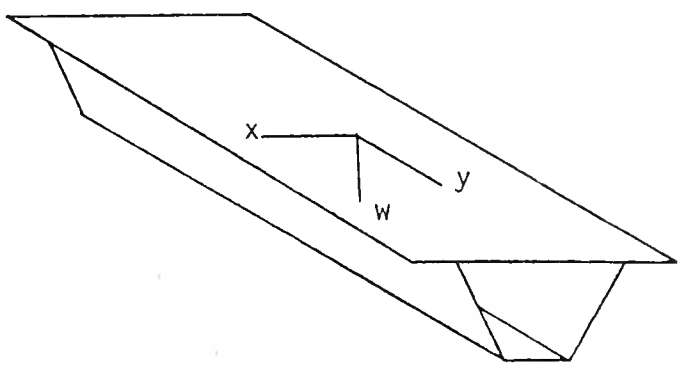

Figure 26. Tubular Box Beam

$$M_x = -D\left(\frac{\partial^2 w}{\partial x^2} + \nu \frac{\partial^2 w}{\partial y^2}\right) \quad (1)$$

$$M_y = -D\left(\frac{\partial^2 w}{\partial y^2} + \nu \frac{\partial^2 w}{\partial x^2}\right) \quad (2)$$

$$D = \frac{Eh^3}{12(1 - \nu^2)} \quad (3) \qquad D = \frac{Eh^3}{12} \quad (4)$$

Plate Theory Beam Theory

ratio as zero, a common practice in concrete design, and assuming longitudinal curvature is negligible at the section in question, then frame theory applies.

The frame analysis used considers fillets of the slabs and webs by subdividing each "member" into an appropriate number of segments each with different cross-sectional properties. The analysis represents a 10°F temperature gradient through the structure; thus, the top slab members increase in length according to the coefficient of thermal expansion of concrete. The coefficient of thermal expansion varies markedly with aggregate type. Gravel will be used in the superstructure concrete of the Turkey Run bridge. Concrete with gravel aggregate has a coefficient of thermal expansion of approximately 6.5×10^{-6} ft/ft/°F. Although the analysis below was done for a 10°F temperature gradient, transverse moments for other gradients may be found by proportioning. Two frame analyses were done, corresponding to the mid-span instrumented sections and the instrumented sections near the pier. Near the pier sections fictitious supports under the webs were assumed to be fixed against translation but free to rotate. The translational restraint is provided by the stiffness of the thickened

bottom slab and transverse diaphragm juncture. Near midspan transverse translational stiffness of the fictitious web supports is smaller, thus the supports were allowed to translate horizontally. The frame analyses were done using the ICES-STUDL-II program available at Purdue University on the IBM 360 computer.

As seen on Figures 27 and 28, the transverse induced moments near the pier are much larger than those near midspan. The actual distribution at a particular section will be bounded by the above cases. Although a 10°F thermal gradient was assumed in the analysis, the actual gradient is the variation in gradient from the time of strain gage balancing to the time of load application for a specific test position. Thermal gradients can be monitored continuously during the testing operation. Although the above analysis does not model exact behavior, it should provide the basis for a thermal moment correction which will reduce the error between actual moments and predicted moments of the finite element analysis.

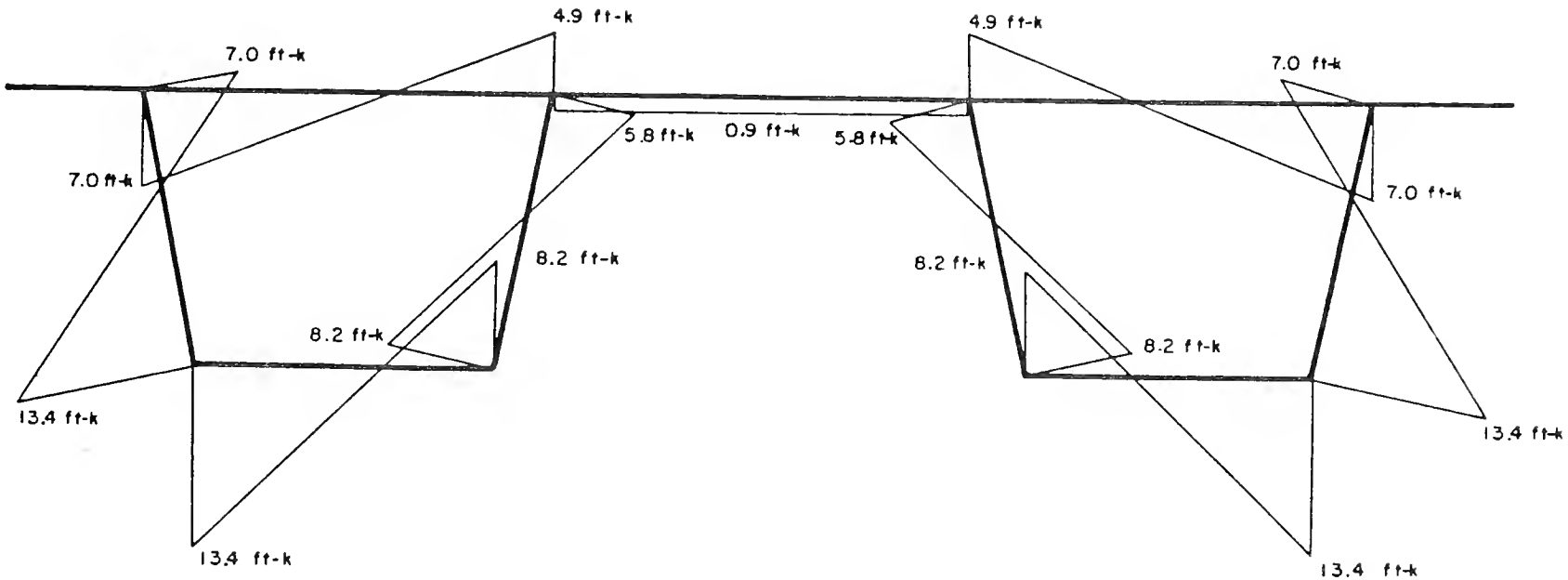

Figure 27. Transverse Moments Induced by a 10°F Thermal Gradient

Case I - Instrumented Segments 2 & 3

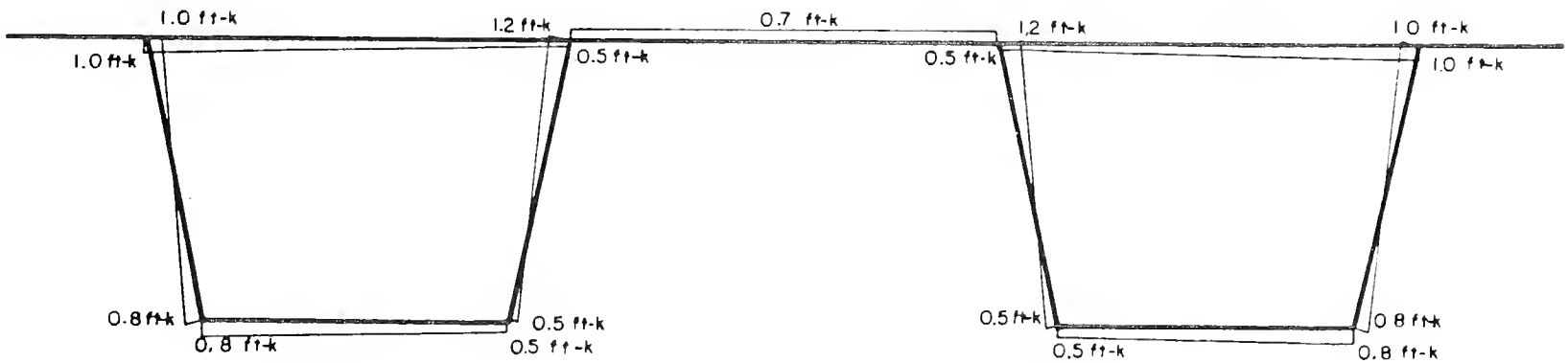

Figure 28. Transverse Moments Induced by a 10°F Thermal Gradient

Case II - Instrumented Segments 24 & 25

NOTES

1 Libby, James R., "Segmental Box Girder Bridge Superstructure Design", Journal of the American Concrete Institute, May 1976, No. 5, Proceedings V.73, pp. 279-291

2 Batla, F. A., "Finite Element Analysis of Prestressed Concrete Box Girders", Ph.D. Dissertation, Purdue University, Dec. 1976, pp. 23-41.

3 Homberg, Hellmut, "Decks with Variable Thickness (Fahrbahnplatten mit veraenderlicher Dicke), Springer-Verlag, New York, 1968, V. I and II.

4 Permission granted for reproduction on August 25, 1976 by Springer-Verlay, New York,.

5 Permission granted for reproduction on January 4, 1976 by F. A. Batla, Indiana State Highway Commission.

CHAPTER IV

TRANSVERSE BENDING INSTRUMENTATION DETAILS

4.1 General

The instrumented sections for transverse bending are located in a manner to maximize distortional effects for the prescribed loading situations. As mentioned earlier, the maximum relative displacements of the twin boxes will occur near the point of maximum vertical deflection; therefore, instrumented sections are located near the centerlines of segments 24 and 25, as illustrated in Figure 29. Also, the stiffness supplied by the thickened bottom slab and the interior diaphragm near the pier will produce more pronounced transverse moments in the vicinity of the pier. Instrumented sections are located near the pier at the centerline of segments 2 and 3 as shown in Figure 29. The instrumented sections are referred to as sections A through D. This coding is used to identify particular strain gages located at each section.

Figures 30 through 33 illustrate the relative positions of strain gage installations at each instrumented section. The section and gage number code should always be used to identify a particular gage. Installations consist of three types: surface installation type I, surface installation type II, and bar installation type III. Details of each installation type and installation procedures can be found in Appendix A. As can be seen, each section group of gages is located

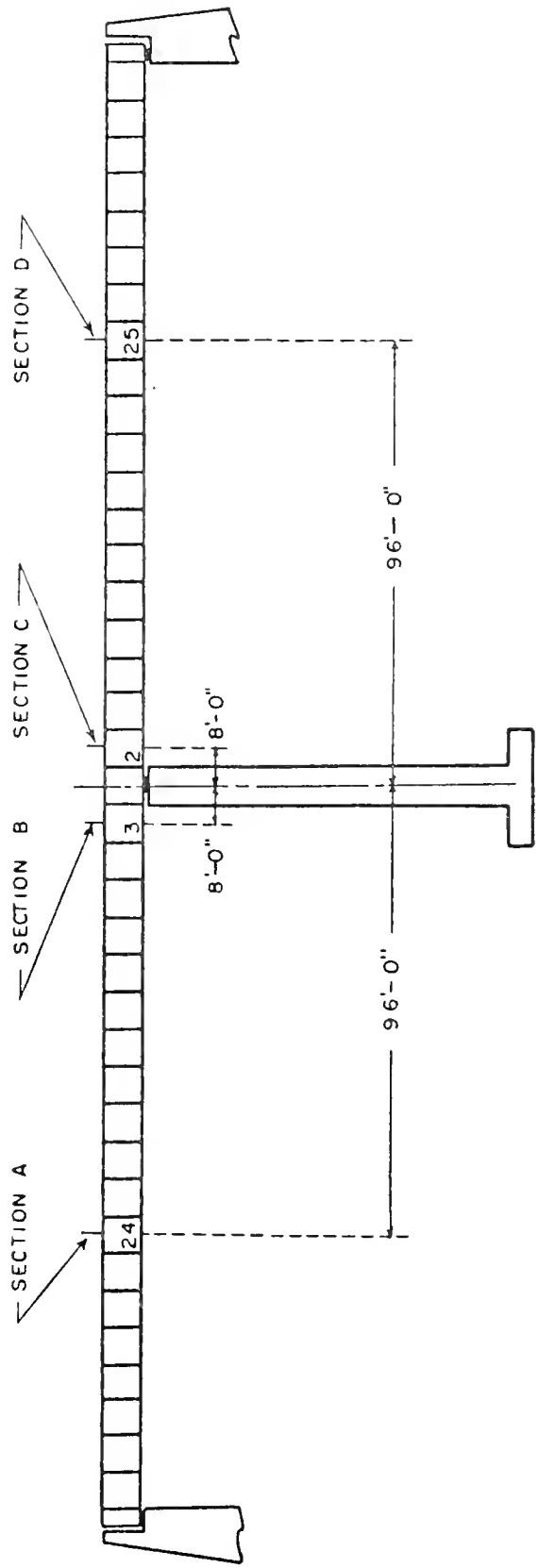

Figure 29. Instrumented Sections for Transverse Bending

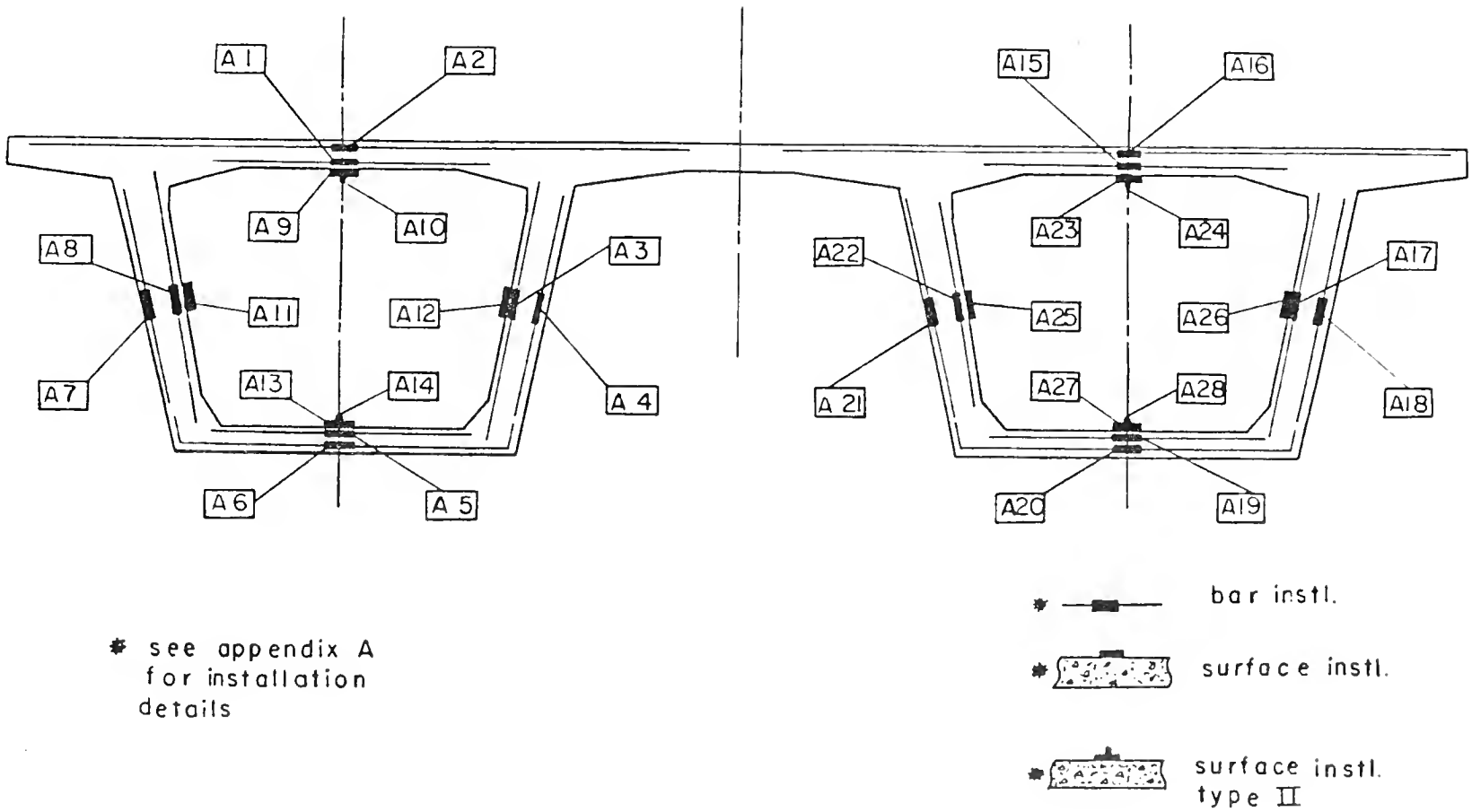

Figure 30. Section A

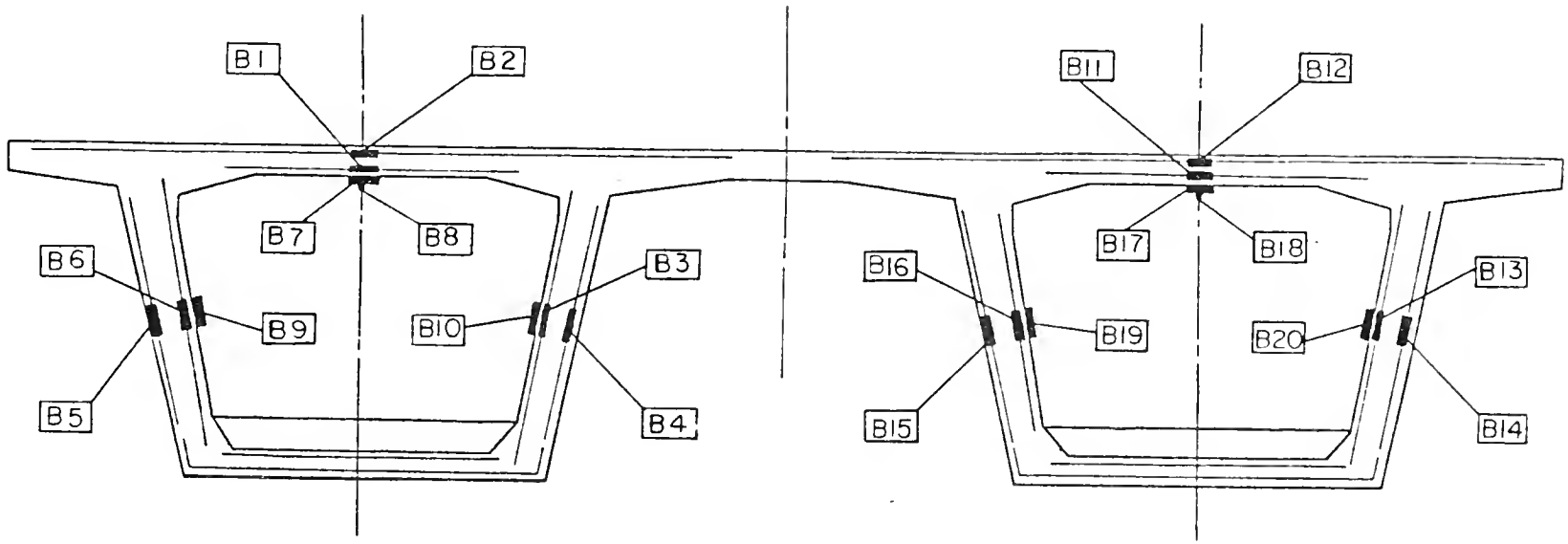

* see appendix A for installation details

* bar instl.

* surface instl.

* surface instl. type II

Figure 31. Section B

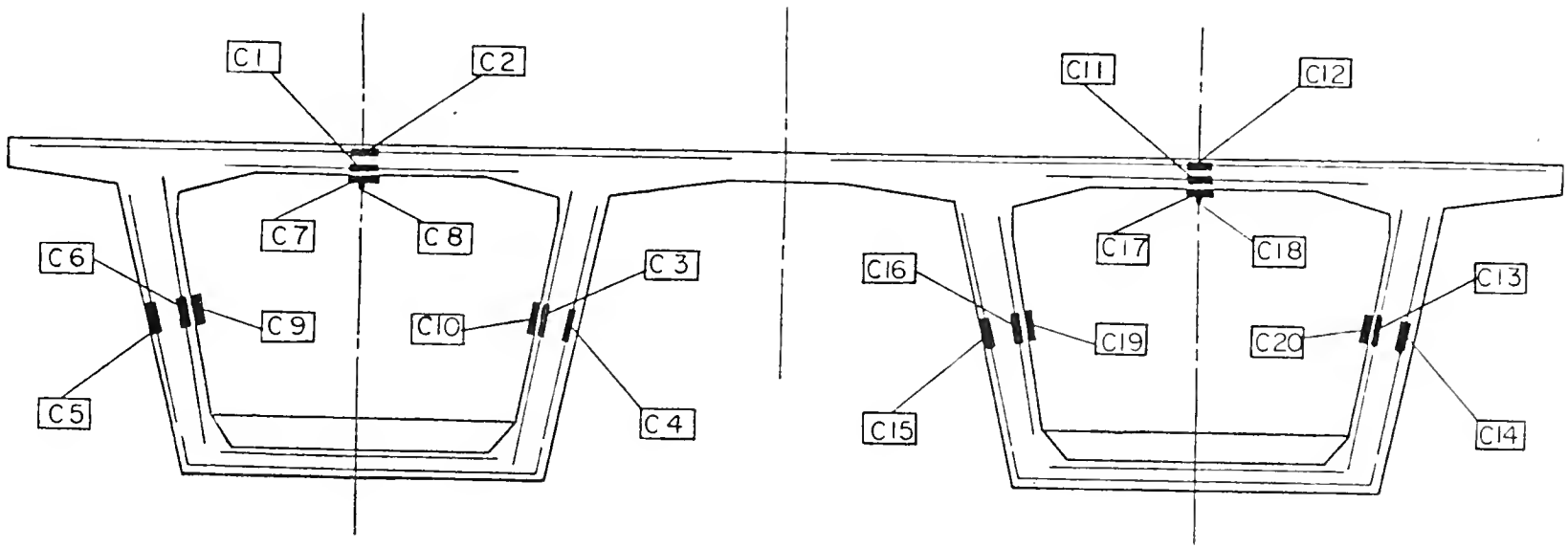

* see appendix A for installation details

* bar instl.

* surface instl.

* surface instl. type II

Figure 32. Section C

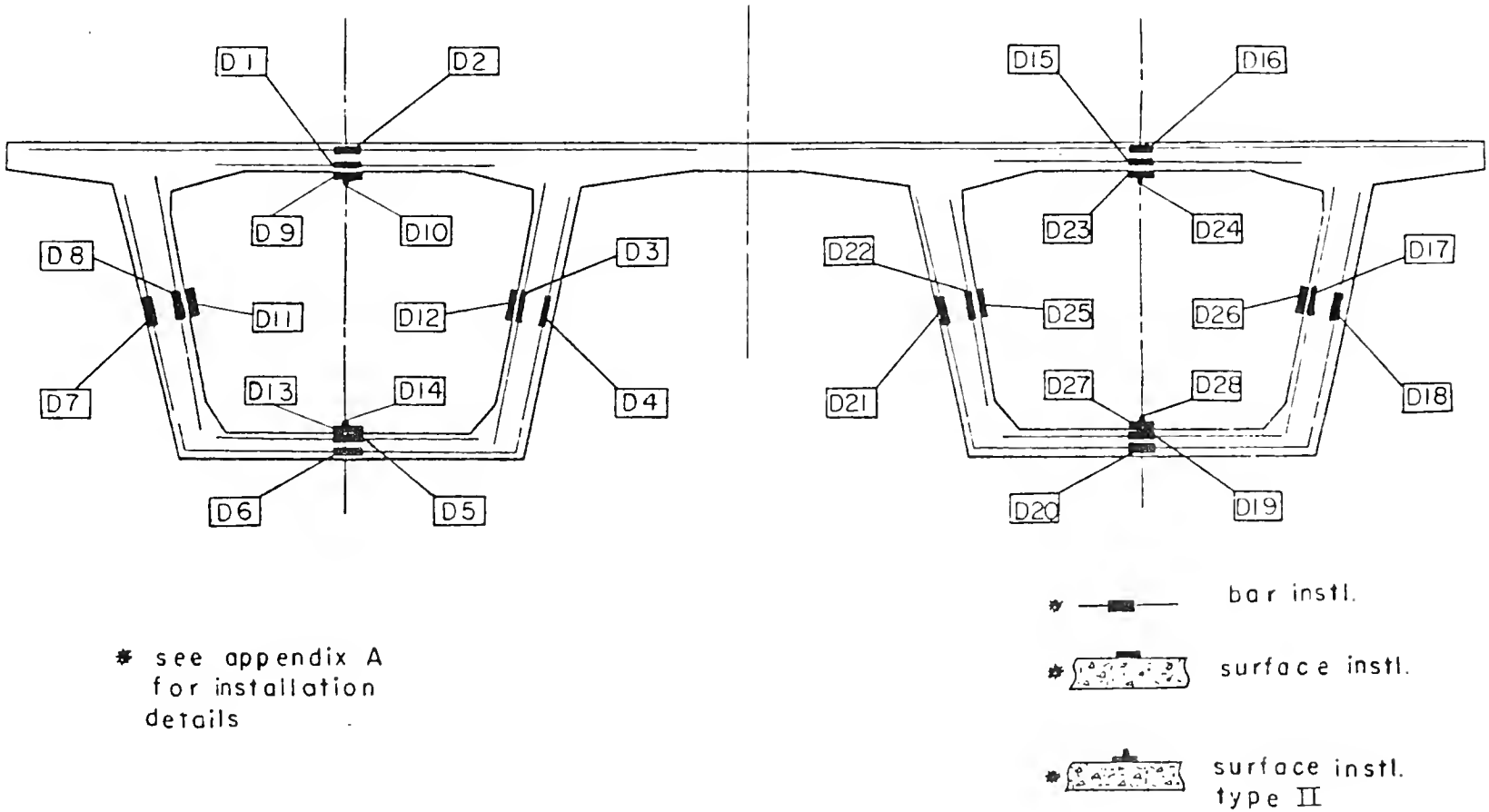

Figure 33. Section D

near the centerline of the top and bottom slabs, or near mid-depth of the webs. No gages are located in the bottom slab of segments 2 and 3 because the longitudinally tapered slab thickness would cause difficulties in traction interpretation. These locations are convenient but do not always correspond to locations of maximum transverse moment. In several loading cases maximum moments occur at the joints of the cross-section. Ideally, moments should be measured at the joints, but the conjestion and interference of post-tensioning cables makes this impractical. The exact locations of gage installations are detailed in Appendix A.

Each group of gage installations consists of bar installations (type III) on the interior and exterior bars of the slab or web and an interior surface installation. The bar installations for the webs and top slabs are illustrated respectively in Figures 34 and 35. The bar gages will supply strain distribution data at each section. With the strain distribution known, a working-stress section analysis can be used to calculate transverse moment tractions. The concrete surface installations (type I and II) provide a check on strain linearity through the section. On the web surfaces gages are located near the neutral axis of the section and are therefore in a low longitudinal stress field. As a result it is not necessary to make corrections for transverse sensitivity of the strain gages, and a single transverse surface gage (type I) is adequate. Essentially, transverse sensitivity is the error in gage output caused by strain transverse to the longitudinal gage axis. The surface gages on the top and bottom slabs are located in a high longitudinal stress field

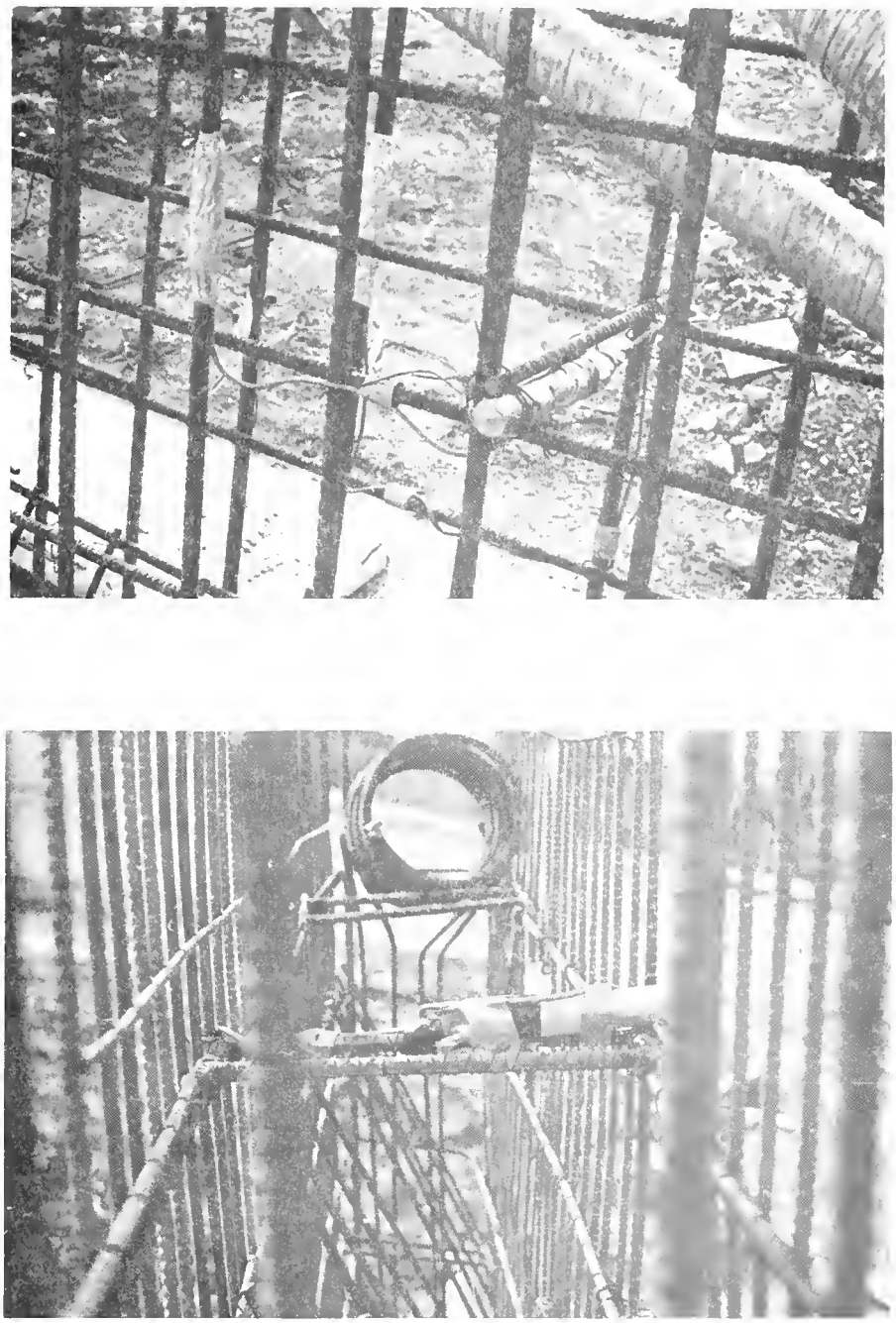

Figure 34. Web Installation

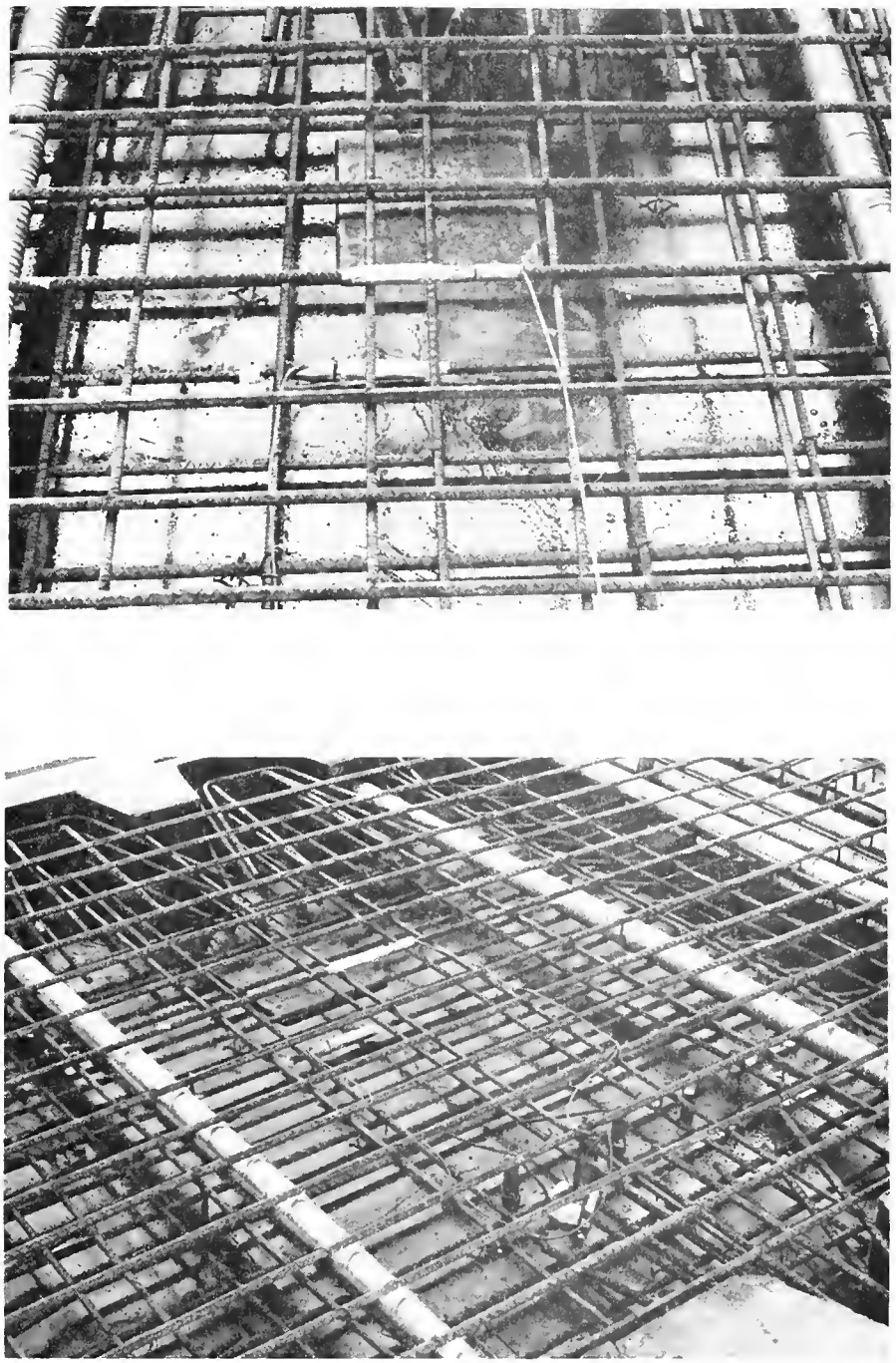

Figure 35. Slab Installation

and require corrections for transverse sensitivity. In order to make this correction a longitudinal gage is placed adjacent to the transverse gage to measure longitudinal strain intensity. This arrangement corresponds to the type II surface installation. Details of the transverse sensitivity correction are described later. Each instrumented bar (type III installation) has a weldable strain gage mounted in such a way as to minimize the effect of localized bending in the bar. This is accomplished by positioning the instrumented bar such that the longitudinal gage axis falls along the mid-depth of the bar. Appendix A contains typical strain gage specifications and engineering data for the gage types to be used. This information may vary slightly with a particular lot of gages.

All internal bar installations have lead wires running into the interior of the box section. This was accomplished by mounting outlet conduits on the rebar cage prior to casting. Once the forms were stripped the leads could be pulled out of the conduit. After the bridge is erected splices can be made and all gage leads can be run to a central junction box. Figures 36 and 37 show photographs of the top and bottom slabs and web installations in a completed segment. Outlets for the thermistor installations described in Chapter V are also shown. The junction box will contain outlets for all strain gages on both spans of the structure. An ideal location for the junction box is on the inside of the girder near the pier segment of one span. The data acquisition system could then be placed inside the girder during the testing operation. Figure 38 shows the interior of a similar box girder span. Note that a junction box need be placed

Figure 36. Web Installation Outlets

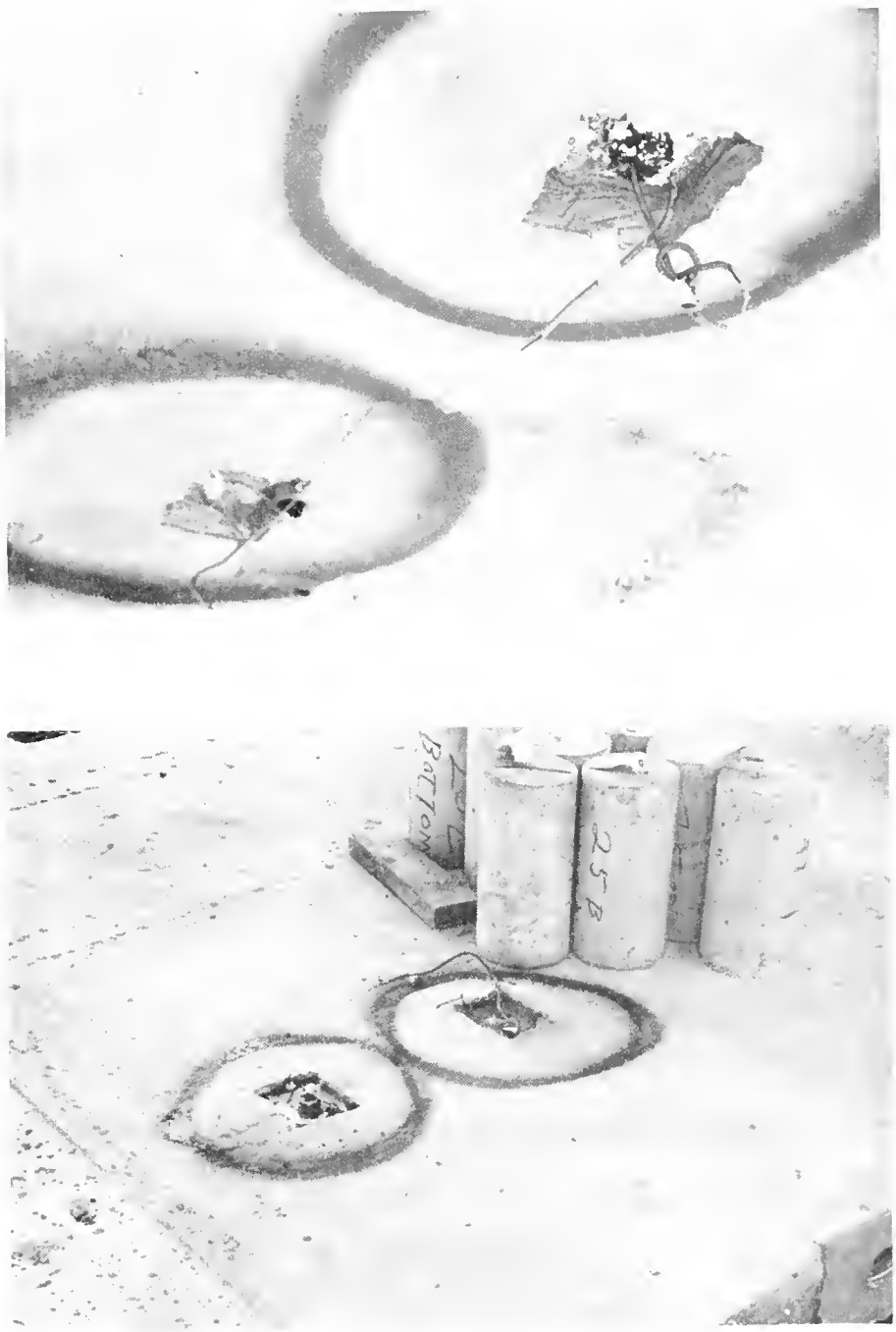

Figure 37. Top and Bottom Slab Installation Outlets

Figure 38. Interior of Box Girder Span

in only one span since a 2-1/2 diameter conduit will carry leads from one span to the other. Holes have been cast in segment 2B for placement of this conduit.

4.2 Transverse Sensitivity

All strain gages have a certain transverse sensitivity whose magnitude is governed by the grid geometry of the gage. For example, a gage with several loops will have a larger portion of the equivalent gage length in the transverse direction than a gage with few loops. Generally, strains in the direction of the longitudinal gage axis are largest with transverse strains being negligible. In such cases the effect of transverse sensitivity is negligible. But, when measuring low strains in a high transverse strain field, such as the case of measuring transverse moments in a high longitudinal stress field, transverse sensitivity error can be significant and should be taken into account.

The correction for transverse sensitivity effects can be made by adjusting the gage factor of the gage in question. The susceptibility to transverse sensitivity error depends on the magnitude of the cross-sensitivity factor (k) of the gage,

$$k = \frac{S_{transverse}}{S_{longitudinal}} = \frac{\Delta R/_{R/\varepsilon_y}}{\Delta R/_{R/\varepsilon_x}} \qquad (5)$$

$S_{transverse}$ = transverse sensitivity

$S_{longitudinal}$ = longitudinal sensitivity

ΔR = resistance change due to strain

R = initial gage resistance

ϵ_x = longitudinal strain

ϵ_y = transverse strain

The formula below is used to calculate the corrected gage factor for the primary gage.

$$G_{corrected} = G\left(\frac{1 + ck}{1 - vk}\right) \tag{6}$$

G = gage factor

$c = \epsilon_y/\epsilon_x$ (ratio of transverse to longitudinal strain)

k = cross-sensitivity factor

v = Poisson's ratio

The derivation of this formula can be found in any textbook on experimental stress analysis.

As an illustration suppose the longitudinal strain at an instrumented section of the Turkey Run bridge is 20 times the transverse strain. Since transverse bending strain is desired, the transverse gage of the type II installation is the primary gage. The transverse sensitivity of a 20 CBW gage is approximately -0.9%. A typical value of Poisson's ratio for concrete is 0.13. Therefore:

$$G_{corrected} = \frac{G(1 + ck)}{(1 - vk)} \qquad c = 20,\ k = -.009,\ v = .13$$

$$= \frac{G(1+20(-.009))}{(1-.13(-.009))}$$

$$G_{corrected} = 0.82G \tag{7}$$

If this correction were not made the observed strains would be in error by 18%.

4.3 Elimination of Signal Errors

All the gages shown in Figure 30 through 33 will be in the active leg of a quarter-bridge Wheatstone bridge circuit. The other three legs of the bridge circuit are located within the data acquisition system. If follows that the lead wires for the active gage will be very long in comparison with the other legs of the bridge located in the acquisition system. The long exposed lead wires are more susceptible to temperature variations during the testing procedure. This situation can cause errors in observed strains. This error can be minimized by using the three-wire lead system shown below.

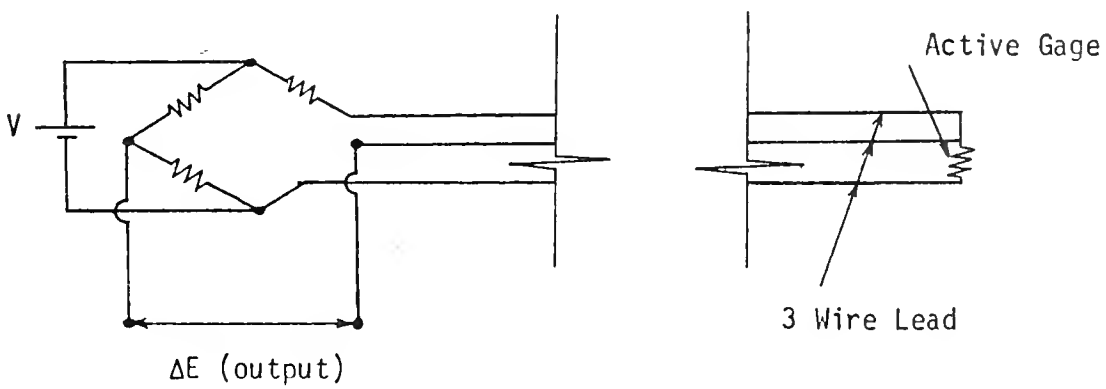

Figure 39. Three-wire Leads for Quarter Bridge

Another problem associated with the use of long lead wires is the error induced by the resistance of the lead wire itself. When the

lead length becomes excessive the resistance of the lead becomes significant relative to the resistance of the strain gage. Therefore, the resistance of the active quarter leg of the bridge is the sum of the gage resistance and the lead resistance. This is known as desensitization error. The resistance of the lead wire depends on the overall length and the AWG gage number. Standard instrumentation wire is AWG 22 with a resistance of approximately 16 ohms per thousand feet. Desensitization error is corrected by adjusting the gage factor by a desensitization factor (D), obtaining a new gage factor (k').

$$D = \frac{R_G}{R_G + R_L} \tag{8}$$

$$k' = Dk \tag{9}$$

R_G = gage resistance

R_L = lead wire resistance (resistance of one lead only for a three wire lead circuit)

k = initial gage factor

This correction must be made in addition to the transverse sensitivity error discussed earlier.

CHAPTER V

THERMAL RESPONSE

5.1 Introduction

In segmental box girders the top roadway slab is subjected to more extreme thermal conditions than the bottom slab. At some point the top and bottom slabs are at equal temperatures at which time thermal equilibrium exists. As the day progresses the angle of incidence of the sun's radiation decreases and the intensity of radiant energy absorption increases on the top slab while the bottom slab remains shaded. The magnitude of the temperature differential between the top and bottom slabs will depend on the thermal transfer conditions at the bridge site. For example, on a day with high wind intensity the heat energy absorbed by radiation is transferred from the slab by forced and natural convection resulting in a lower thermal gradient than on a similar day with negligible wind. Thermal gradients also vary with time due to the ever-changing angle of incidence of the sun. The result is a cyclic variation in thermal gradients similar to that shown in Figure 40.

Thermal gradients cause the top and bottom slabs to elongate by different amounts. The magnitude of the elongation depends on the coefficient of thermal expansion for the concrete. The structure must respond geometrically or the statical system must change, depending on the support boundary conditions. During the cantilevering phase of

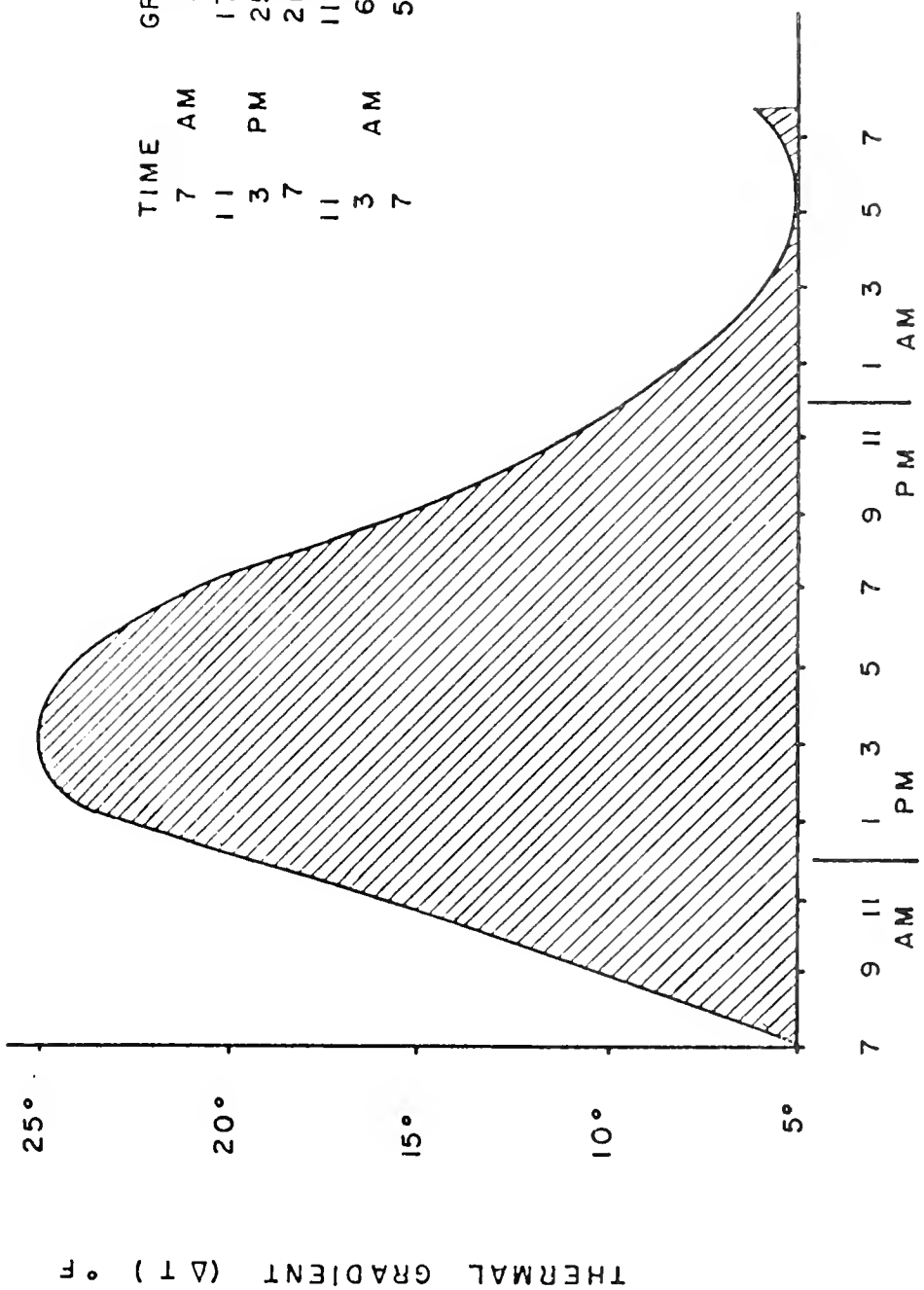

Figure 40. Typical Daily Variation in Thermal Gradients

construction the structure is statically determinate and the thermal gradient causes a constant curvature along the span, as long as gradient doesn't vary longitudinally, resulting in a cantilever tip deflection which varies with the magnitude of the gradient. This variation in deflection is erratic and causes problems in vertical alignment control during cantilevering. In the completed indeterminate structure the thermal curvature cannot occur freely, due to restraining boundary conditions. The statical system of the bridge must change in order to resist the induced thermal stresses. As a result the dead load reactions change and continue to fluctuate as long as the thermal gradient varies.

The main objective of instrumenting the Turkey Run bridge for thermal gradients is to obtain data which can be utilized to develop more accurate design parameters. At present most designers accept an arbitrary value for the design thermal gradient based on intuition and experience rather than experiment. By measuring actual gradients in an in-place structure the magnitude as well as the variation in thermal gradients can be accurately determined. French research has reported gradients significantly larger than those presently used in American design[1]. Of course it cannot be concluded that gradients in all bridges are higher than predicted since climate and site conditions may vary considerably in different locations. In addition to determining the yearly maximum gradient, the instrumentation scheme will provide data on the daily and seasonal variation of thermal gradients. This data should lead to a better understanding of the thermal response of box girders with respect to time. This becomes critical

when making alignment corrections during the cantilevering process. It would be desirable to make the alignment correction at a time of day when the thermal gradient is a minimum. This would minimize the alignment error caused by thermal induced deflections. By measuring thermal gradient variations on days with varying atmospheric conditions and in different seasons one might determine a relationship between these ambient parameters and the time of minimum gradient. From past construction experience it has been found that the vertical alignment correction is not uniform for every cantilevering sequence, and the magnitude of the correction is erratic. In order to determine the relative magnitude of gradient deflections and deflections caused by other sources, e.g. unbalanced construction loads, cantilever tip deflections and thermal gradients will be measured simultaneously for selected 24 hour periods during construction. This will provide a direct check on the correlation of daily gradient variations and predicted cantilever deflections. The following pages outline in detail the scheme for implementation of the instrumentation objectives.

5.2 Site Conditions

As stated previously, the site conditions at a particular bridge can affect thermal gradient magnitudes. Although the instrumentation of the Turkey Run bridge will provide basic information on the thermal response of box girders, the data must not be generalized to be representative of every box girder. The maximum thermal gradient at one bridge site may vary significantly from the gradient of an identical bridge at another site. For example, a bridge in a deep chasm shaded from sunlight will certainly have a different thermal response than

a bridge in open terrain with no shading.

Figure 41 shows photographs taken at the site of the proposed Turkey Run bridge. The proposed bridge will be similar in elevation to the existing spandrel arch structure. There are two dominant factors in the site topography. First, the bridge deck is not directly shaded and is exposed to the sun during most of the day. The surrounding woods might cause shading during the early morning and late afternoon. The shading angle, or angle from the bridge deck to the top of the tree line, is approximately 20°. The wind barrier produced by the surrounding trees might lessen convective transfer from the bridge deck, possibly causing higher gradients than would be expected at an open site with free wind flow. A second feature of the Turkey Run site is the shaded chasm under the bridge. On investigation of the site it was noticed that the atmospheric temperature in the chasm was significantly lower than that around the bridge deck. This is due to the extensive shading of the underside of the bridge and the cool spring water running through the chasm. These conditions might lead to lower temperatures in the bottom slab of the proposed structure. The topographic features mentioned above might tend to complement one another and cause thermal gradients of significant magnitude. Although there is no way to compare the gradients measured at Turkey Run with those of bridges with different site features, this parameter should be given consideration when evaluating the Turkey Run data.

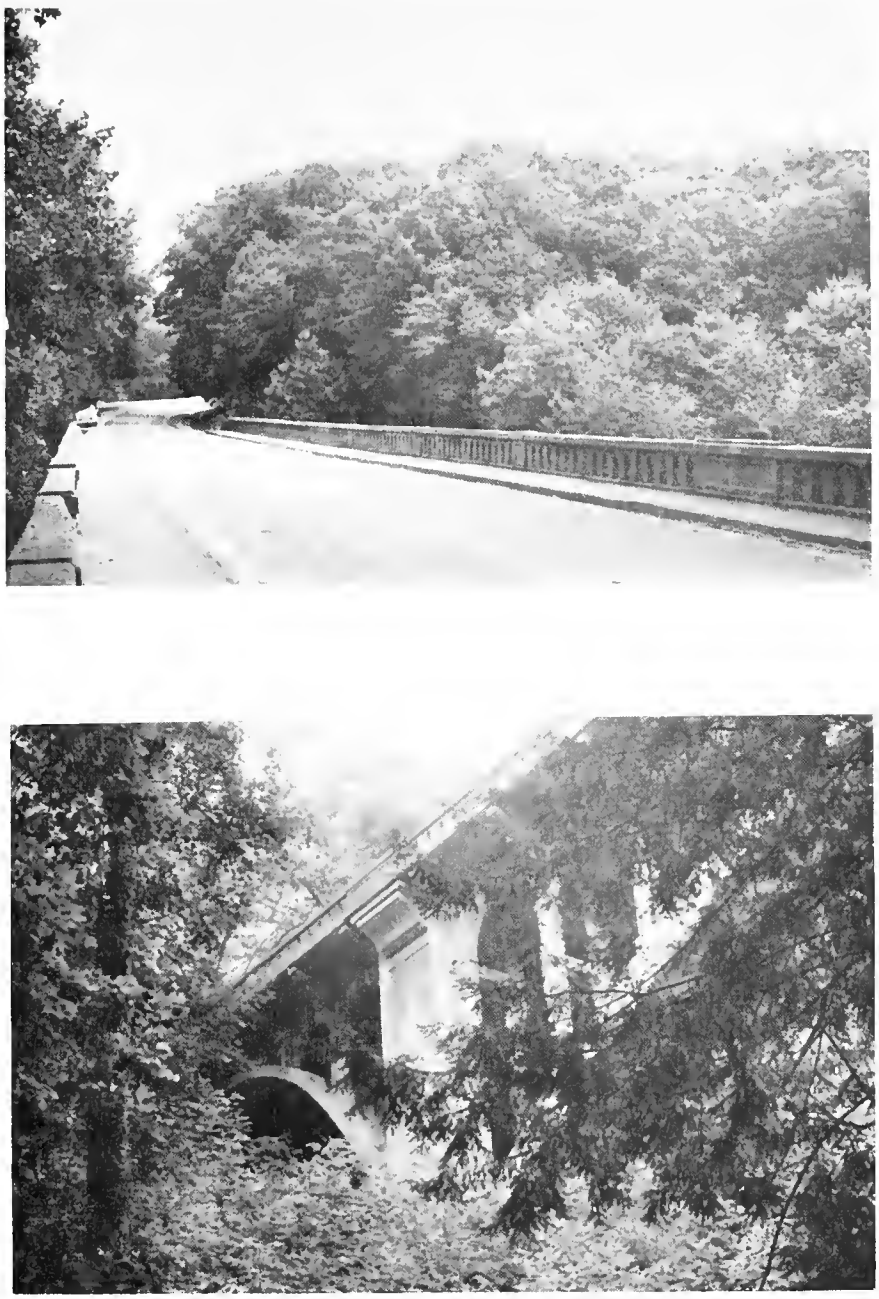

Figure 41. Existing Structure at Turkey Run

5.3 Thermal Effects During Construction

During the cantilevering phase of construction each opposing span behaves as a statically determinate cantilever beam. As a result, the only structural response induced by thermal gradients is geometrical. When a cantilever beam is subjected to a constant linear thermal gradient along its entire length each section deforms with constant curvature. The curvature is a function of the magnitude of the thermal gradient, the thermal properties of the concrete, and the depth of the member. From beam theory we know that constant curvature along a cantilever member causes a tip deflection of $\phi L^2/2$. Since ϕ is a function of the temperature gradient, the magnitude of the tip deflection must vary directly with the temperature gradient. Figure 42 demonstrates the variation of tip deflection resulting from the typical daily gradient variation curve shown earlier. Dimensional parameters used in plotting this curve correspond to the Turkey Run bridge. The maximum gradient of 25° F occurs at 3 p.m. The outcome of the instrumentation will determine whether this gradient is excessive or typical.

As segments are cantilevered from the central pier elevation corrections must be made in order to maintain the design grade. This correction is usually made by wedging a wire mesh at the interface of two segments after the application of epoxy but prior to temporary post-tensioning. The procedure is illustrated in Figure 43. The magnitude of this correction depends on the difference between the design elevation and the actual elevation. If this correction were valid alignment control should be adequate. Figure 43 demonstrates a

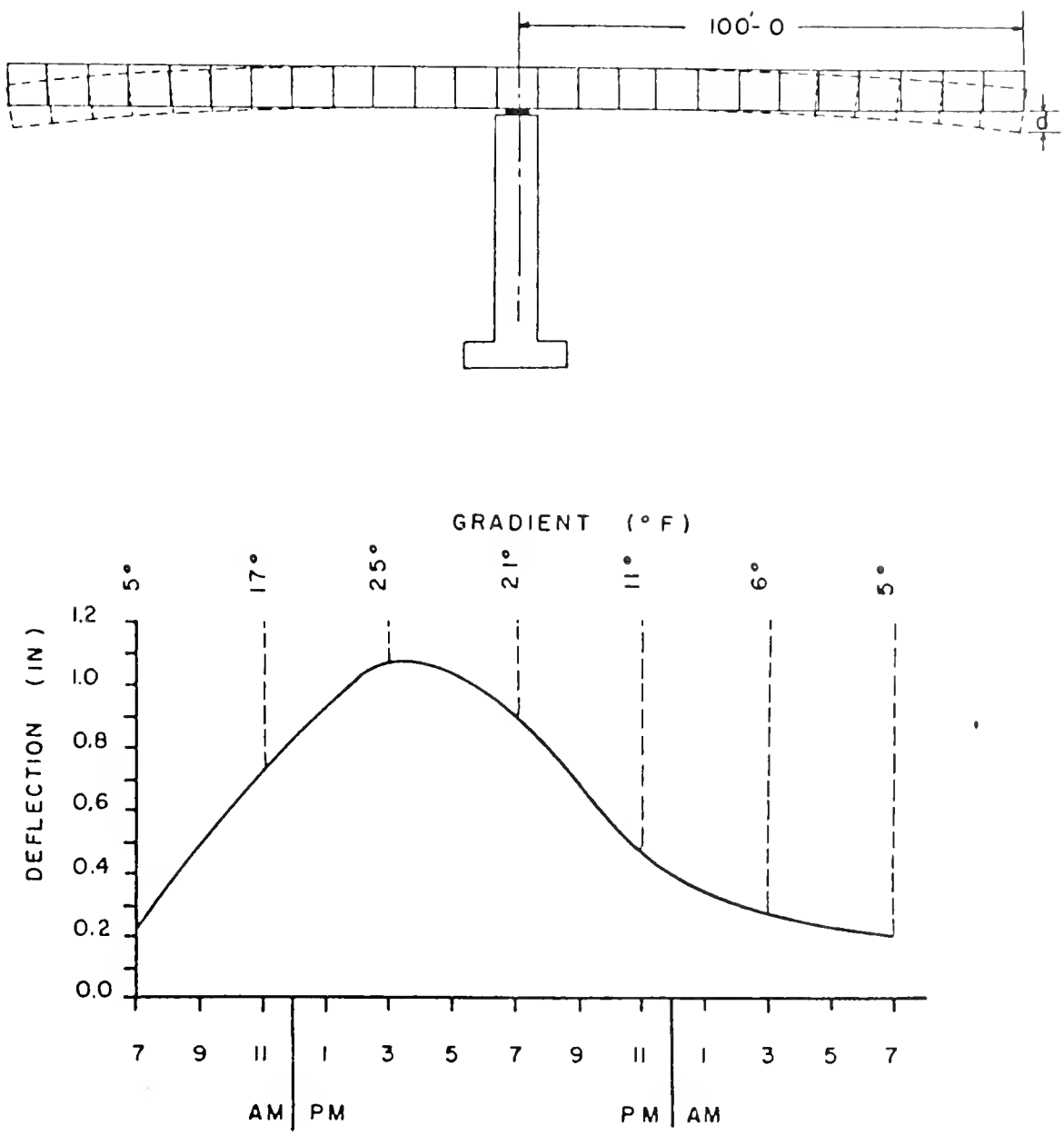

Figure 42. Temperature Induced Deflections of Cantilever

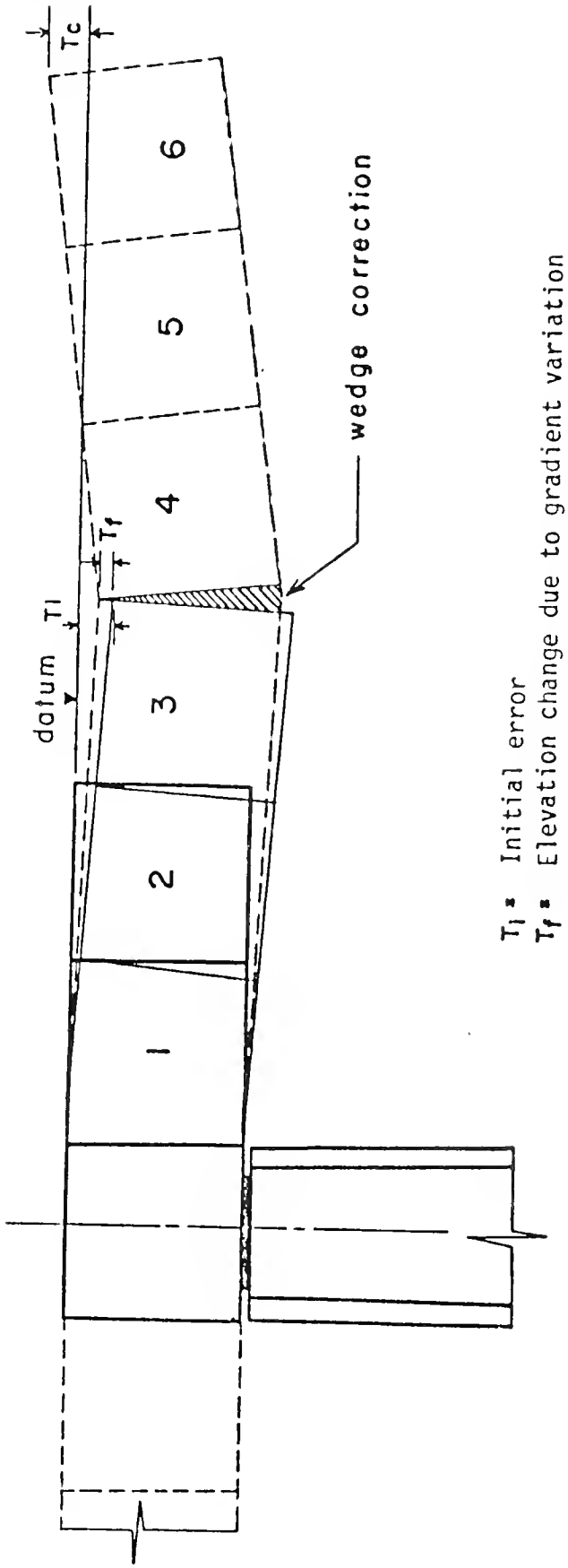

Figure 43. Alignment Error Due to Thermal Effects

sequence of construction events which cause alignment errors even though elevation corrections are made. Suppose segments 1, 2 and 3 are cantilevered under identical thermal conditions. Due to thermal gradients the tip of segment 3 deflects by a magnitude, T_i. T_i is the difference in design and actual elevations at the time of reading. If there are delays between the time of reading and the cantilevering of segment 4, the tip of segment 3 might rise by an amount T_f, depending on the change in gradient magnitude during the time interval. Assuming thermal conditions remain constant during the cantilevering of segments 4, 5 and 6, the total accumulated error at the tip of segment 6 is T_c. This sequence of events is idealized to demonstrate how alignment errors can occur. In actuality the accumulation of errors is erratic and depends on several variables. Nevertheless, one can infer that by minimizing T_i and T_f during each placement and correction sequence the total accumulated error will be smaller. T_i is a minimum when the thermal gradient is a minimum, perhaps during the early morning. T_f will be smaller if the time delay between reading and correction is minimized.

In order to provide data which will indicate times of minimum thermal gradients, gradients should be measured during 24 hour periods at different times of the year. It is recommended that at least four sets of gradient variation data be collected, corresponding to the seasonal variation of climate. As mentioned earlier, the tip deflection variation can be caused by other conditions. The difference between specified and actual post-tensioning forces can cause tip deflections which are different than those predicted by calculations.

Other factors such as unbalanced construction loads or improper fit of segment interfaces may also cause tip deflections. It is desirable to determine the relative magnitude of thermally induced deflections and those caused by other sources. It is recommended that tip elevations be monitored during construction after placement of segments 24 and 25. These segments contain the thermistor installations and are located far enough from the pier to have significant deflections. By monitoring gradients and deflections simultaneously perhaps a correlation can be made which will verify calculations and reveal the significance of thermal deflections relative to deflections caused by other sources. A recommended procedure would be to monitor deflections by setting a level over the pier on the inside of the box cross-section while monitoring temperatures by taking hourly thermistor readings. It should be noted that the data acquisition system will not be available during this stage of construction due to inaccessibility. As a result, thermistor readings will have to be made manually with portable equipment. The thermistor installations are described in detail at the end of this section.

5.4 Thermal Effects in Completed Structure

As mentioned earlier the completed indeterminate structure must respond to thermal gradients by undergoing a change in the statical system. For instance, suppose the two-span continuous Turkey Run bridge was replaced by two simple spans with no continuity over the pier. Thermal gradients would cause constant curvature. If the thermal gradients are constant along both spans it follows that the slope over the pier must be zero. The only way the released structure can have

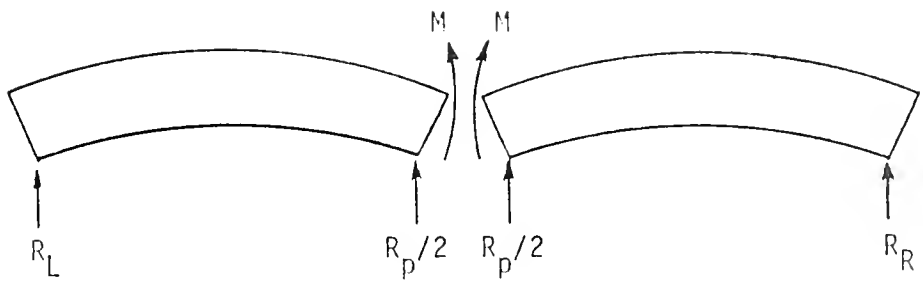

Figure 44. Cutback Structure

zero slope of the pier is for a restoring moment, M, to be applied. The restoring moment causes the reactions R_L and R_R to increase and R_P to decrease. These reaction variations are due to thermal response only. Figure 45 shows reaction variations R_L and R_R due to the typical daily thermal gradient distribution shown earlier. The abutment reactions increase by as much as 54 kips under a thermal gradient of 25° F. The design total reaction for the abutments, considering one box section only, is 550 kips. The thermal reaction variation is 10% when live load is included and 13% when considering dead load only. If the thermal gradients of the Turkey Run bridge are of the same order of magnitude as the typical distribution used above, the reaction variations become fairly significant. Reactions were actually measured on the French project cited earlier and it was found that support reactions varied by 15-25% due to thermal response.

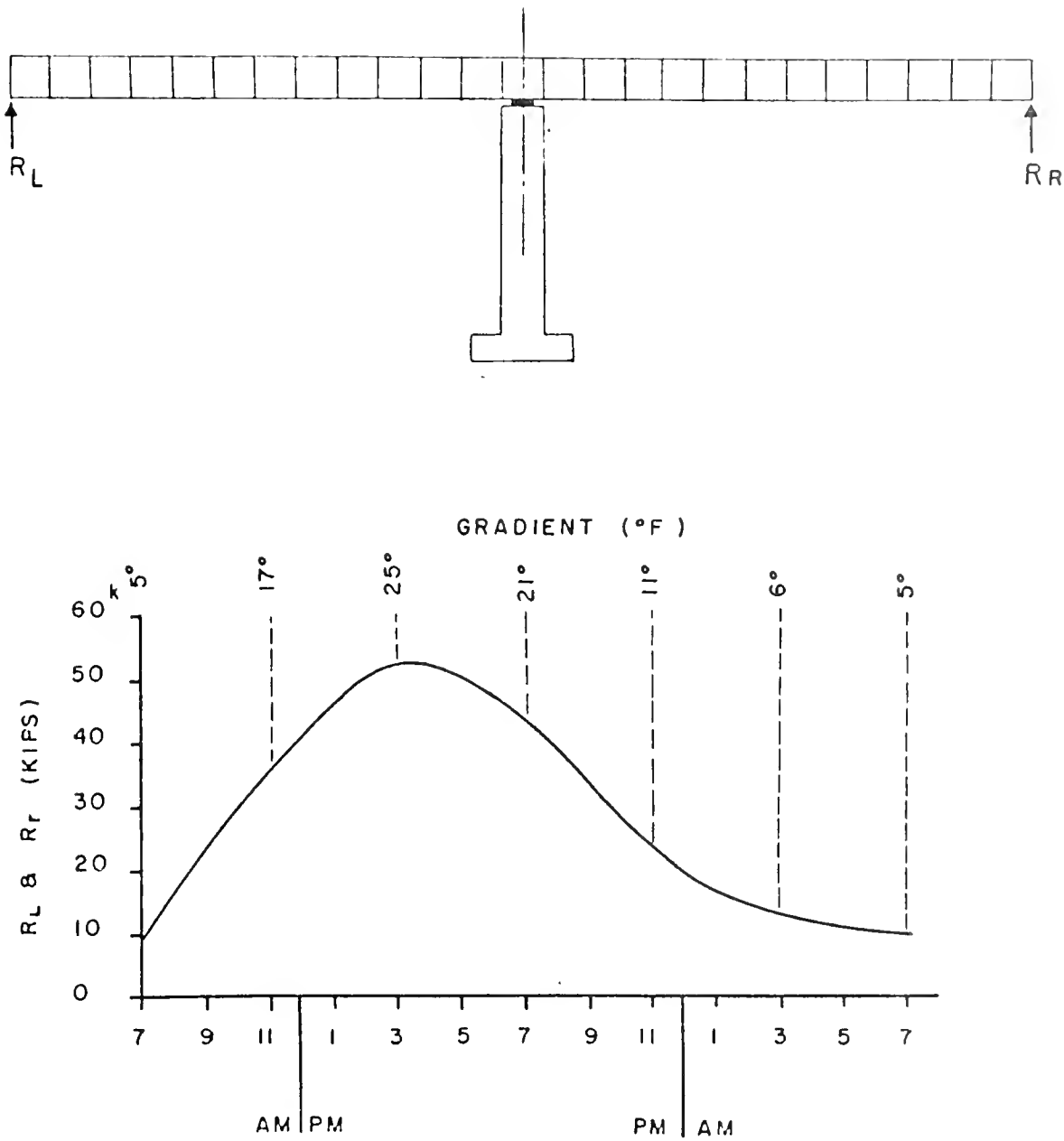

Figure 45. Reaction Variation Due to Thermal Gradients

Reaction variations of the order of magnitude illustrated above should be considered in design. Prestress or post-tensioning levels are based on the combination of stresses from dead load and live load. The post-tensioning forces determine concrete tensile stresses under service conditions. For the stresses to be representative of actual service load behavior, the statical system (tensioning forces, dead load, live load) must be accurately determined. Thermal response causes the abutment reactions to increase and causes some relaxation in the positive moment post-tensioning force. These conditions combine to cause increased tensile stresses in the positive moment region. If thermal reaction variations are predicted and post-tensioning forces increased appropriately, stress levels will be assured of falling within the allowable range. By determining the maximum gradients in the Turkey Run bridge the relevance of this consideration can be evaluated. For example, if the gradients are on the order of 25° F or greater, the variation of actual and predicted stresses becomes significant and should be considered in design.

5.5 Instrumentation Details

The thermistors used to measure thermal gradients consists of probes containing resistors whose resistance varies markedly with temperature. The components are contained in a vinyl coating which guards against abrasion and corrosion when encased in concrete. The variation of temperature versus resistance is non-linear when the thermistor component is used alone. By using additional resistor composites the output can be linearized. The schematic below demonstrates this technique (Figure 46). The components in the box represent the thermistor.

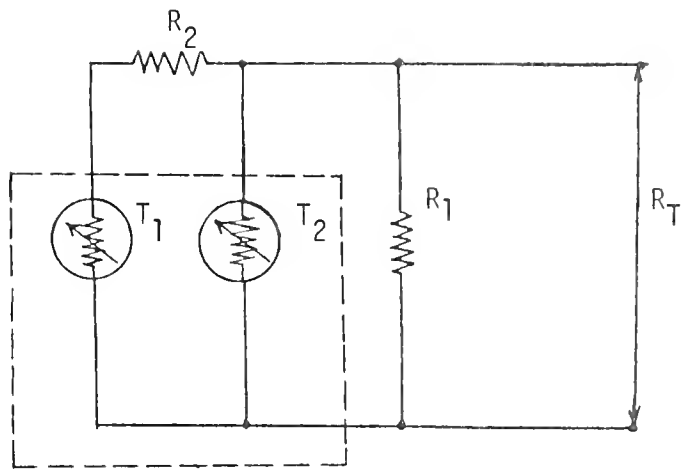

Figure 46. Schematic of Thermistor Circuit

The resistor values R_1 and R_2 are selected to provide a specific temperature range of output. (R_1 = 18,700 Ω, R_2 = 32,250 Ω for temperatures between -30° C to +50° C). When long lead wires are used it would be necessary to correct for resistance of the leads. Readings will be taken near the location of the thermistors thus requiring leads of less than 10 ft. Desensitization error will therefore be negligible, and the equation for temperature versus resistance can be expressed as follows,

$$R_t = (-127.096)T + 12175 \qquad (10)$$

T = temperature °C

R_t = total resistance output

It should be noted that this equation is only applicable when the resistor composites are as specified for the desired temperature range.

Figure 47 shows the locations of the thermistors in segments 24 and 25. Four thermistors are placed at each of the two test sections (24 and 25). The thermistors are located at mid-depth of the segment slabs in order to average local gradients between the inside and outside surfaces of the slabs. The temperature difference between the top and bottom slabs will represent the overall section gradient with local slab gradients being considered negligible in affecting longitudinal flexural response. The adjacent spans are cantilevered independently. Since the thermistors are located in each span, two sets of gradient variation data can be obtained during each cantilevering phase.

Figure 48 shows details of the thermistor installation. The encapsulated thermistor component is wired in place prior to casting. The leadwire is encased in a rigid conduit for protection. After the forms are stripped, the conduit plug is removed giving access to the thermistor leadwire from inside the box section. After erection, temperature measurements at any installation can be made by using a portable battery powered ohm-meter. Since two thermistors are located at each box a two channel switching box will be used for monitoring. Readings will be taken at 1 hour intervals. This will allow a single switching box and ohm-meter to be used for the entire project.

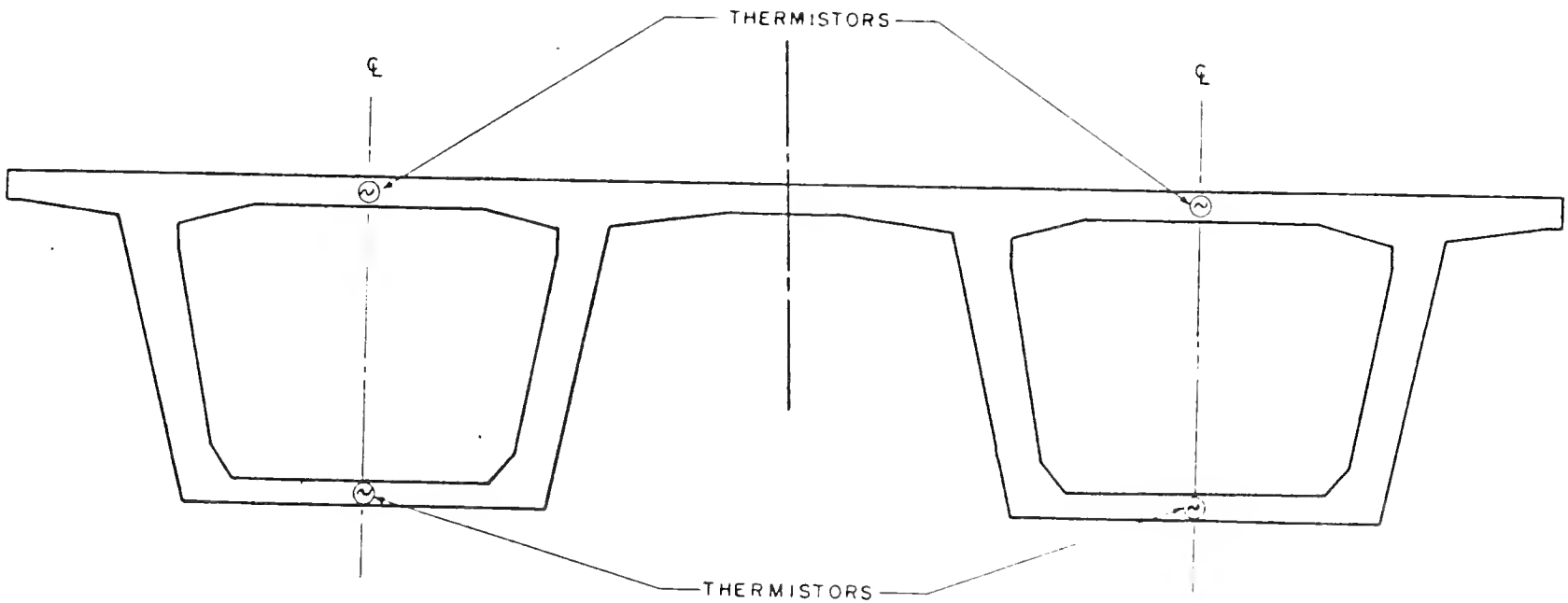

Figure 47. Thermistor Locations Segments 24 & 25

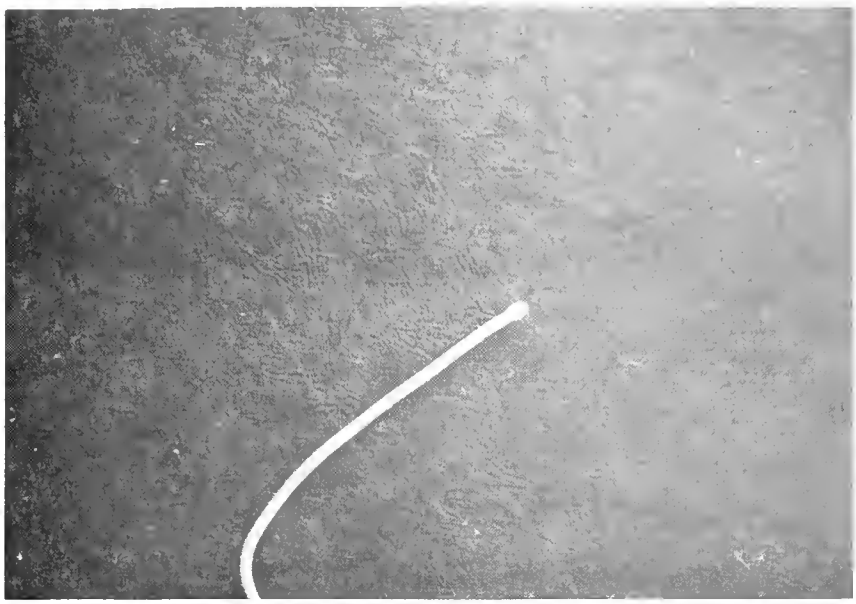

Figure 48. Thermistor and Thermistor Installation

NOTES

1 Diruy, Lau, Leger, "Constations A Long Terme Sur Un Ouvage En Beton Precontraint: Le Pont De Champigny -Sur-Yonne", Association Francaise des Ponts et Charpentes, October 1974, pp. 17-36.

CHAPTER VI

LONG-TERM DEFORMATIONS

Long-term deformations under sustained dead load result from the combined effects of creep and shrinkage. In a two span continuous structure such as the Turkey Run bridge, long-term deformations cause a relative rotation to take place at the central support section. The rotation due to creep and shrinkage is the difference between deformations at the service life of the bridge and those upon initial loading. This net rotation at the support section causes a moment re-distribution within the span and thus causes stresses to be different than those used in design. Since most shrinkage takes place before erection in the case of precast structures it is generally assumed that this effect is minimal. Relative rotations will be measured in the Turkey Run bridge in an attempt to determine the significance of creep rotations.

Mechanical strain gages will be used to measure rotations at the pier support section. A set of gage holes are permanently glued to the bottom of the top slab and top of the bottom slab on both segments over the pier. Each set of holes are located at mid-span of the respective slabs. These holes are drilled in small metal plates which are glued with epoxy to the concrete surface. Relative movement of the holes will be measured by a Whittemore strain gage. A 10 in. gage length will be used. Ideally initial gage readings should be taken in the unstressed state. However, stresses will vary considerably during

construction due to the increasing dead load as segments are cantilevered and due to stresses created by post-tensioning forces. As a result initial measurements cannot be taken until a span is complete.

By knowing long-term strains in the top and bottom slabs one can determine the creep rotation occuring during the specified time period. With this information the re-distribution of dead load moments can be determined.

CHAPTER VII

SUMMARY AND CONCLUSIONS

An instrumentation scheme has been developed to monitor transverse bending tractions, thermal gradients, and creep rotations in the Turkey Run segmental bridge. Instruments and recommended procedures have been specified in an attempt to minimize probable instrumentation errors. Upon review of the analysis data it was found that many of the tractions to be measured are small, thus requiring scrutiny in accounting for errors.

The empirical results found during the instrumentation program are to be compared to the results of the analytic models described in this report. A finite element analysis and an influence surface analysis were used to predict transverse bending tractions. Comparison of the two analyses revealed that the influence surface analysis was conservative relative to the finite element technique. This indicates that the finite element model may provide a better behavioral representation and may correlate better with measured tractions.

Data gathered upon completion of phase II of this project should add to the body of information currently used in segmental design and should provide a good check on the analysis techniques currently used.

BIBLIOGRAPHY

BIBLIOGRAPHY

1. Kashima, S., Construction and Load Tests of a Segmental Precast Box Girder Bridge Model, University of Texas at Austin, 1974.

2. Maisel, B. I., Ph.D., Methods of Analysis and Design of Concrete Boxbeams with Side Cantilevers, Technical Report of the Cement and Concrete Association, Nov. 1974, pp. 1-20.

3. Muller, Jean, "Ten Years of Experience in Precast Segmental Construction", Journal of the Prestressed Concrete Institute, Jan.-Feb, 1975.

4. PCI Bridge Committee, "Tentative Design and Construction Specifications of Precast Segmental Box Girder Bridges", April 1975.

5. PCI Post-Tensioning Committee, "Recommended Practice for Grouting of Post-Tensioned Prestressed Concrete", Nov.-Dec. 1972.

6. PCI Segmental Construction, "Recommended Practice for Segmental Construction in Prestressed Concrete", Journal of the Prestressed Concrete Institute, March-April 1975.

7. PCI Seminar, "Design of Precast Segmental Bridges", Chicago, Sept. 25, 1973.

8. Swann, R. A., "A Feature Survey of Concrete Box Spine-Beam Bridges", Technical Report of the Cement and Concrete Association, June 1972.

9. Technical Bulletin of Association Francaise des Ponts et Charpentes, "Long Term Experiments on a Prestressed Concrete Bridge: The Bridge of Champigny-Sur-Yonne", March 1972, pp. 19-37.

10. Mortlock, J. D., "The Instrumentation of Bridges for the Measurement of Temperature and Movement", Transport and Road Research Report 641, 1974.

11. Lacey, G. C. and Breen, J. E., "Long Span Prestressed Concrete Bridges of Segmental Constructure, State of the Art", Report 121-1, Center for Highway Research, University of Texas at Austin, May 1969.

12. Breen, J. E., Cooper, R. L., and Gallaway, T. M., "Minimizing Construction Problems in Segmentally Precast Box Girder Bridges", Report 121-6F, Center for Highway Research, University of Texas at Austin, August 1975.

13. Libby, James R., "Segmental Box Girder Bridge Superstructure Design", Journal of the American Concrete Institute, May 1976, No. 5, Proceedings V. 73.

14. Homberg, Hellmut, "Decks with Variable Thickness (Fahrbahnplatten mit veraenderlicher Dicke), Springer-Verlag, New York, 1968, Vols. I and II.

15. Batla, F. A., "Finite Element Analysis of Prestressed Concrete Box Girders", Ph.D. Dissertation, Purdue University, December 1976.

16. Belmain, M. and Le Bourdelles, Y., Etude du retrait et des deformations de fluage dans un pont en beton preconstraint construit par encorbelement. (Study of Shrinkage and Creep Deformations in a Prestressed Concrete Bridge Constructed in Cantilever), Annales des Ponts et Chaussees, No. II, 1971.

17. Chu, K. H. and Dudnik, E., "Concrete Box Girder Bridges Analyzed as Folded Plates", Concrete Bridge Design, ACI Publication SP23, 1969.

18. Kropp, P. K., "Use of Precast-Prestressed Concrete for Bridge Decks", Joint Highway Research Project 75-15, Purdue University, July 1975.

APPENDICES

APPENDIX A

Installation Details and Strain Gage Data

Appendix A

Installation Details and Strain Gage Data

A.1 Surface Gage Installations (Type I and II)

Strain gages mounted on an exposed concrete surface must be protected from adverse environmental effects. The effects of moisture from ambient sources as well as the migratory moisture of the concrete are detrimental to the gage installation and produce inaccurate observed strains. Ambient temperature variations also cause strain drift or "apparent strain" due to varying thermal properties of the concrete and gage backing material. This phenomenon should be accounted for when strain measurements are taken over an extended period. In the case of short-term live load strain measurements, the protective precautions outlined below should guard against detrimental effects of moisture and small short-term temperature variations.

The type I surface installation of Figure A1 is for measuring concrete surface strains in regions of low transverse stress at which gage factor corrections for transverse sensitivity is not required. The type II installation of Figure A2 features a gage positioned at 90° from the primary gage in order to measure transverse strains used in gage factor correction calculations for the primary gage. This installation is used in areas of high transverse strain where transverse sensitivity of primary gages can produce significant errors in strain measurements.

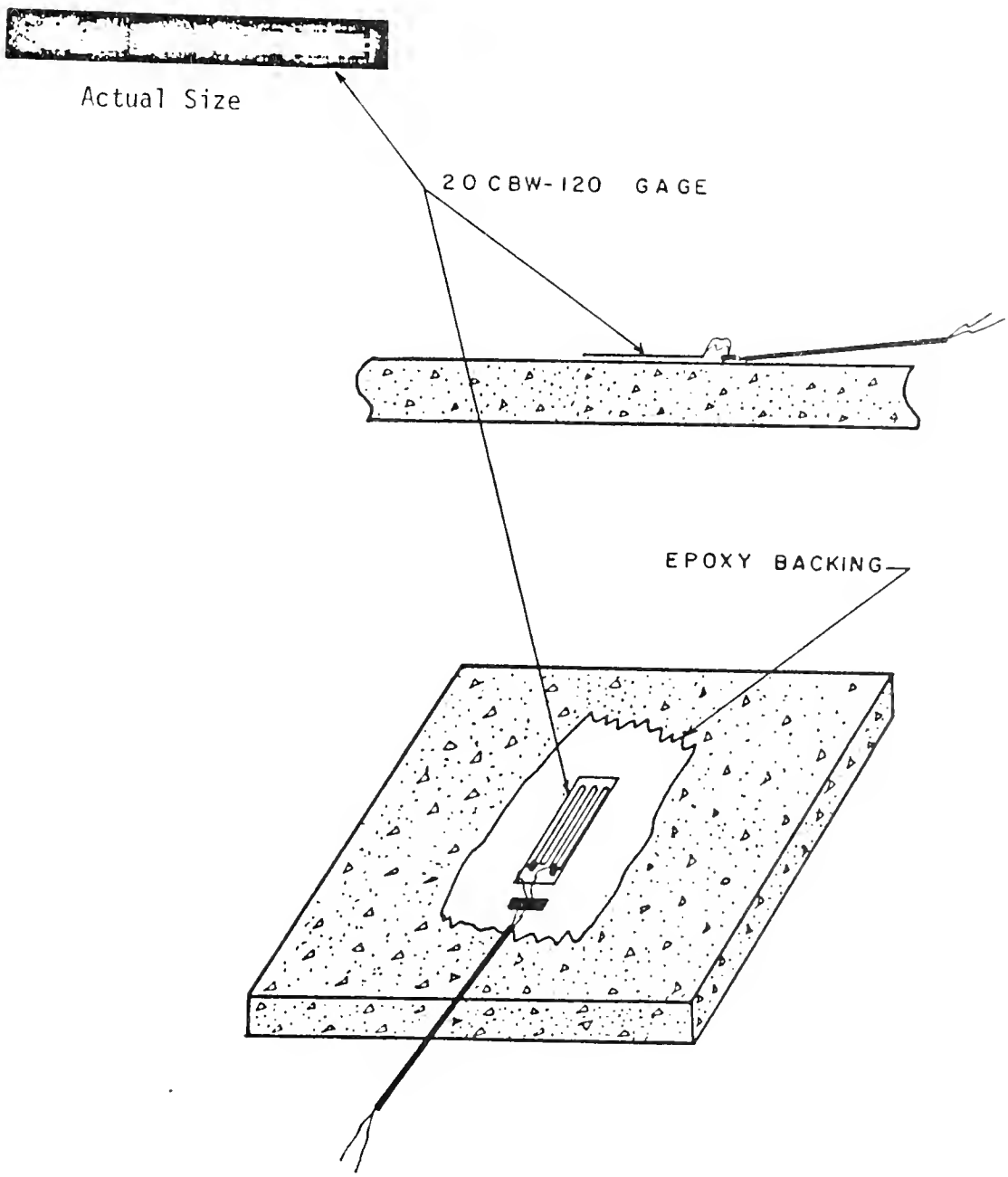

Figure A1. Type I Installation

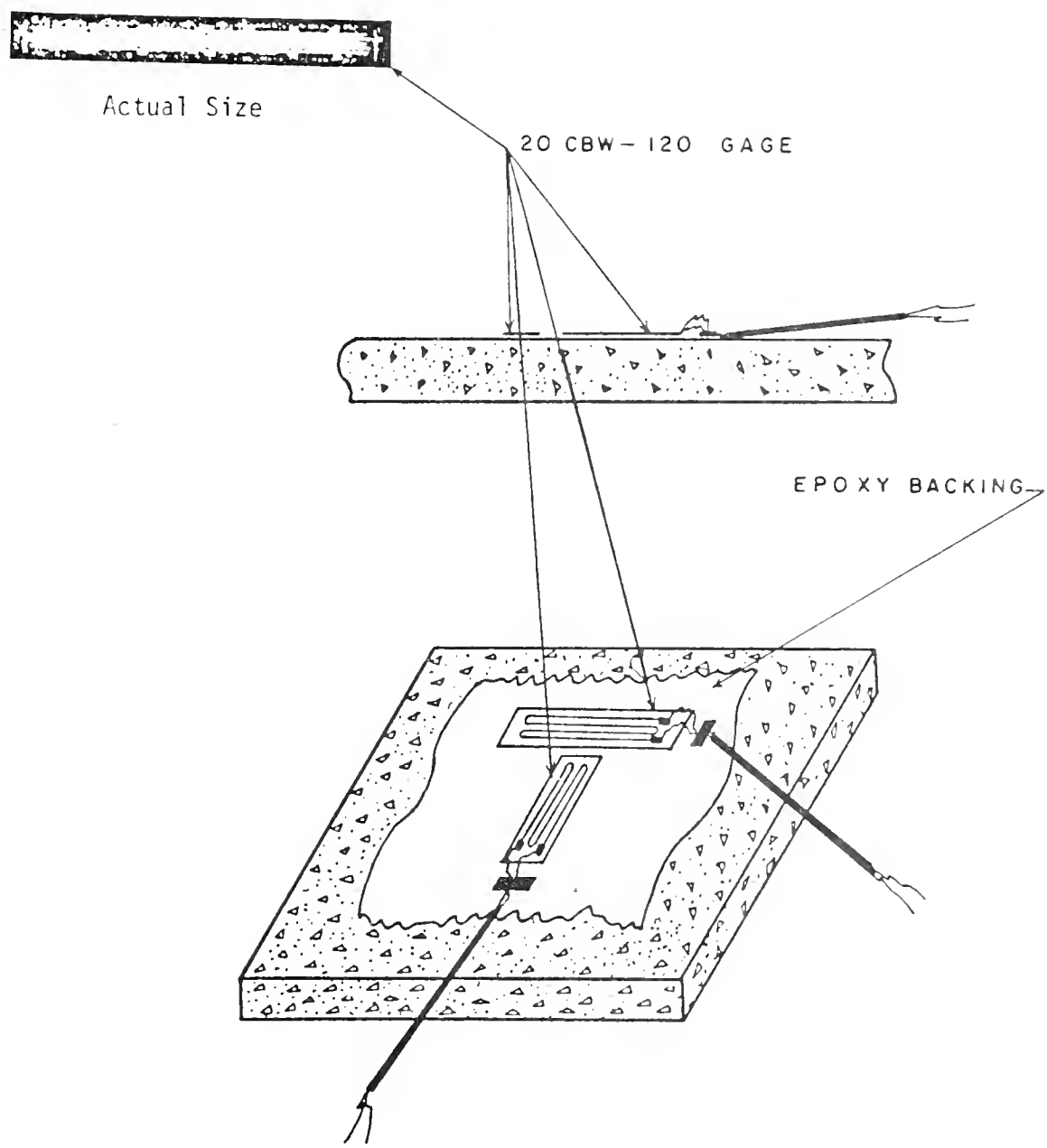

Figure A2. Type II Installation

Details of Installation Procedure

1) Sand surface removing all rough projections.

2) Clean surface with solvent.

3) Apply initial epoxy coating and heat cure for 1-1/2 - 2 hours.

4) Apply epoxy coating for gage bonding.

5) Apply gage with continual clamping force and heat cure for 1-1/2 - 2 hours.

6) Solder leads providing strain relief and apply protective coating.

Data for the surface gages are listed below:

Gage type:	20CBW-120
Resistance:	120 ohms
Gage factor:	2.085 ± 0.5%
Transverse sensitivity:	-0.7%
Gage Length:	2.0 in.

A.2 Reinforcement Bar Installations (Type III)

The same general considerations for ambient effects apply to bar installations as for surface installations. Steps of the application procedure are illustrated in Figure A3. Notice that three different types of protective coating are applied to each gage. These gages are welded to the bars. Weldable gages are more moisture resistant and more durable. A small spot welding unit was used to weld the stainless steel alloy gage backing to the bar. Gages were welded at approximately 10 watt-sec with a probe pressure of about 5 pounds. The gage was then coated with a latex enamel coating, a rubber compound coating, a metal foil coating, and finally sealed with a joint sealer.

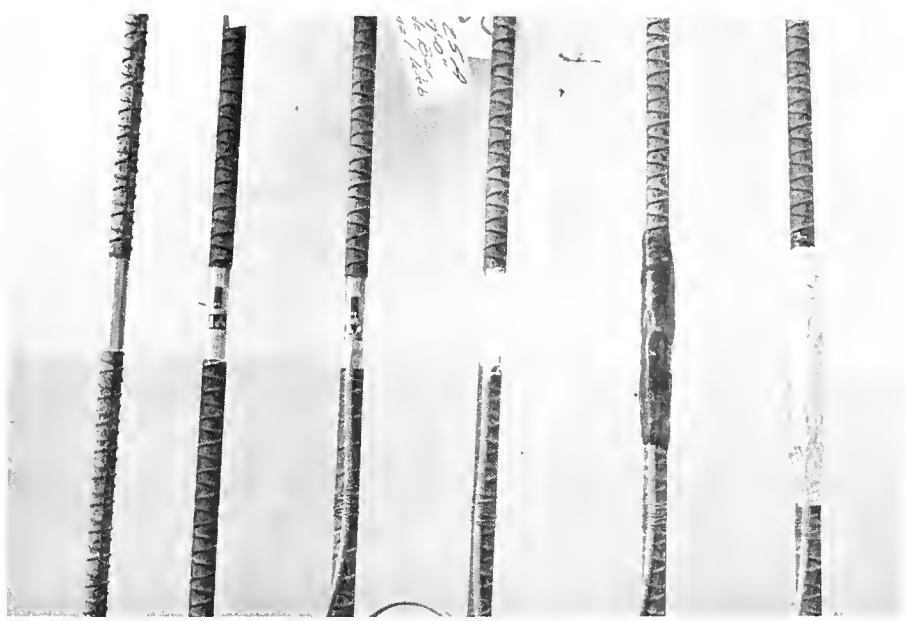

Figure A3. Steps in Application of Bar Gages

Data for the weldable gages are listed below.

Gage type:	CEA-06-W250A-120
Resistance:	120.0 ± 0.4%
Gage factor:	2.04 ± 0.5%
Transverse sensitivity:	+0.2%
Gage length:	.250 in.

APPENDIX B

Material Properties

Appendix B

Material Properties

In order to interpret moment tractions from the strain data gathered it is necessary to know the stress-strain properties of the instrumented bars and the concrete used in the instrumented segments. All instrumented reinforcement bars were taken from the same heat along with ten samples of 24 inch length. Stress-strain curves determined by testing these samples can be used to determine the elastic modulus of the heat. Three or four standard 6" x 12" concrete test cylinders were made for each instrumented segment. A cylinder was made from concrete placed near each installation. Cylinders were steam cured with the segment. Each test cylinder is to be stored with the segment until testing. This will ensure that the cylinders are subjected to the same atmospheric conditions as the segments. Cylinders should be tested to determine stress-strain properties near the time at which the bridge is tested for transverse bending.

APPENDIX C

Average Diameters of Instrumented Reinforcement Bars

Appendix C

Average Diameters of Instrumented Reinforcement Bars

Gage No.	Bar Diameter (in.)
A1	.590
A2	.585
A3	.457
A4	.446
A5	.459
A6	.457
A7	.452
A8	.459
A15	.583
A16	.587
A17	.453
A18	.451
A19	.453
A20	.452
A21	.451
A22	.452
B1	.599
B2	.586
B3	.585
B4	.594

Gage No.	Bar Diameter (in.)
B5	.585
B6	.585
B11	.585
B12	.588
B13	.591
B14	.592
B15	.593
B16	.589
C1	.582
C2	.589
C3	.591
C4	.587
C5	.590
C6	.586
C11	.589
C12	.587
C13	.591
C14	.591
C15	.593
C16	.590
D1	.584
D2	.589
D3	.456
D4	.455

Gage No.	Bar Diameter (in.)
D5	.462
D6	.460
D7	.456
D8	.455
D15	.586
D16	.589
D17	.451
D18	.451
D19	.453
D20	.452
D21	.451
D22	.450

APPENDIX D

Bridge Plans and Details of Instrument Location

SEGMEN
TRANSVI
INSTRUI

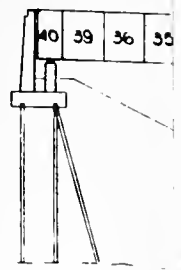

Existing Abut.*1

Abut.*1

Note: Existing substructure
mmimum of 4' cleara
ground line, except e
removed to approx. r

D

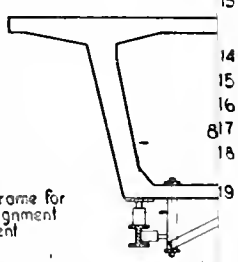

Jacking frame for lateral alignment adjustment

Location of jacking frame in Seg. 26 or 27 to be determined by the Contractor and approved by the Engineer.

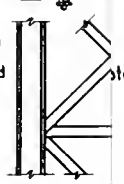

D

TEMPORARY SUPP
No Sc

Note: Temporary support
able to support a 54
lateral stiffness for a
erection procedure s
Each leg of the strut c
400 kip axial load
Each corner of the cr
a 120 kip downward l

* or Founded on existi

ERECTION PROCEDURE

1. Install the cradle on the North pier shaft and place jacks at each corner as shown
2. Place the pier segment (Segment *1) and insert (but do not tighten) the tie-down bolts.
3. Adjust horizontal and vertical alignment using jacks and then tighten tie down bolts.
4. Erect Segment 2 using temporary prestressing, and then erect segment 3 using temporary prestressing.
5. Insert Tendons 101A & 101B and post-tension as required, then remove temporary prestressing.
6. If necessary, loosen tie-down bolts and use jacks to adjust horizontal and vertical alignment. Be sure to retighten tie-down bolts after adjustment.
7. Install and dry-pack permanent pier bearing pads, then transfer load to permanent bearings by removing jacks. Retighten tie-down bolts if necessary.
8. Place struts under segments 2 & 3 as shown. Set struts tight aginst bottom of segments and dry-pack or shim at footing as required.
9. Erect segments 4 thru 27 in numerical order and post-tension tendons 102A thru 113 as required. Periodically check and adjust alignment using wire fabric in joints between segments. See the Special Provisions for more explicit details about checking and adjusting alignment.
10. Place the temporary support structures as shown under segments 26 & 27. Take care to install the bearing assemblies in such a manner as to prevent excessive tipping of the superstructure when the struts and cradle are removed (Step 11) but to still allow adjustment of the horizontal and vertical alignment (Step 12).
11. Remove the tie-down bolts, cradle assembly, and struts from the pier.
12. Check horizontal and vertical alignment and adjust if necessary. These adjustments must use the pier bearings as a pivot point. If one end of the cantilever is raised the other must be free to move downward, if one end is rotated northward the other must be free to move southward. After this point no adjustment to the alignment of the entire superstructure is possible, and all future adjustments must be made as outlined in step 9 and the Special Provisions. After adjustment make sure all temporary support bearings are set tight against segments.
13. Erect segments 28 thru 41 in numerical order and post-tension tendons 201 thru 203 as required. Check alignment and adjust if necessary, as outlined in step 9 and the Special Provisions.
14. Install and dry-pack the permanent bearings at the abutments.
15. Install and post-tension tendons 301 and 302.
16. Remove the temporary support structures.
17. Install and post-tension tendons 303 and 304.
18. Repeat steps 1 thru 17 for the South half of the structure (may be done concurrent with North half if desired)
19. Construct the curbs and center joint. The curbs must be placed prior to or in conjunction with the center joint. All construction loads must be removed from the structure before initial set of the concrete occurs. If it is not possible to pour an entire curb or the center joint before initial set occurs, then the construction will be broken into small enough pours to make this possible. If smaller pours are used, the pouring sequence will be arranged so that the portion over the pier will be poured last.

te: Erection procedure is suggested method. Contractor shall submit erection plan to the Engineer for approval prior to fabrication of the segments. Calculations showing design of members shall be included in order that the Engineer can check the procedure and equipment to be used.

CONSTRUCTION DETAILS

INDIANA STATE HIGHWAY COMMISSION

SCALE:- AS NOTED DATE:-

DRAWING:- C 8 OF 20 SHEET:- OF
PROJECT:- RS-390(2)
CONTRACT NO.
BRIDGE FILE:- 47-61-6570

DESIGNED SJH CKD JRG
DRAWN CKD SJH
TRACED CKD

Figure D1. Construct

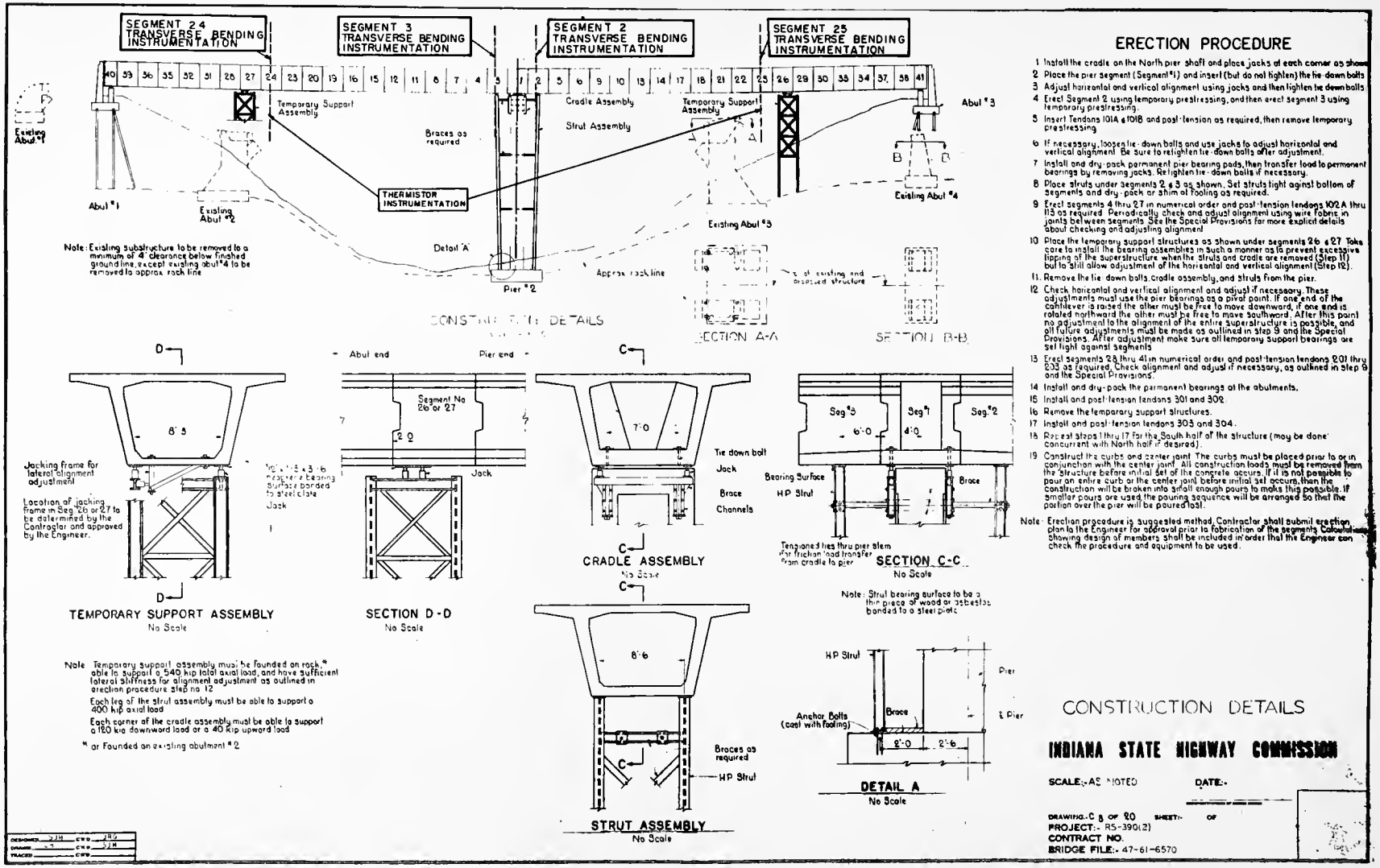

ERECTION PROCEDURE

1. Install the cradle on the North pier shaft and place jacks at each corner as shown
2. Place the pier segment (Segment #1) and insert (but do not tighten) the tie down bolts
3. Adjust horizontal and vertical alignment using jacks and then tighten tie down bolts
4. Erect Segment 2 using temporary prestressing, and then erect segment 3 using temporary prestressing.
5. Insert Tendons 101A & 101B and post-tension as required, then remove temporary prestressing
6. If necessary, loosen tie-down bolts and use jacks to adjust horizontal and vertical alignment. Be sure to retighten tie-down bolts after adjustment.
7. Install and dry-pack permanent pier bearing pads, then transfer load to permanent bearings by removing jacks. Retighten tie-down bolts if necessary.
8. Place struts under segments 2 & 3 as shown. Set struts tight against bottom of segments and dry-pack or shim of fooling as required.
9. Erect segments 4 thru 27 in numerical order and post-tension tendons 102A thru 113 as required. Periodically check and adjust alignment using wire fabric in joints between segments. See the Special Provisions for more explicit details about checking and adjusting alignment
10. Place the temporary support structures as shown under segments 26 & 27. Take care to install the bearing assemblies in such a manner as to prevent excessive tipping of the superstructure when the struts and cradle are removed (Step 11) but to still allow adjustment of the horizontal and vertical alignment (Step 12).
11. Remove the tie down bolts, cradle assembly, and struts from the pier.
12. Check horizontal and vertical alignment and adjust if necessary. These adjustments must use the pier bearings as a pivot point. If one end of the cantilever is raised the other must be free to move downward, if one end is rotated northward the other must be free to move southward. After this point no adjustment to the alignment of the entire superstructure is possible, and all future adjustments must be made as outlined in step 9 and the Special Provisions. After adjustment make sure all temporary support bearings are set tight against segments
13. Erect segments 28 thru 41 in numerical order and post-tension tendons 201 thru 203 as required. Check alignment and adjust if necessary, as outlined in Step 9 and the Special Provisions.
14. Install and dry-pack the permanent bearings at the abutments.
15. Install and post-tension tendons 301 and 302.
16. Remove the temporary support structures.
17. Install and post-tension tendons 303 and 304.
18. Repeat steps 1 thru 17 for the South half of the structure (may be done concurrent with North half if desired).
19. Construct the curbs and center joint. The curbs must be placed prior to or in conjunction with the center joint. All construction loads must be removed from the structure before initial set of the concrete occurs. If it is not possible to pour an entire curb or the center joint before initial set occurs, then the construction will be broken into small enough pours to make this possible. If smaller pours are used, the pouring sequence will be arranged so that the portion over the pier will be poured last.

Note: Erection procedure is suggested method. Contractor shall submit erection plan to the Engineer for approval prior to fabrication of the segments. Calculations showing design of members shall be included in order that the Engineer can check the procedure and equipment to be used.

CONSTRUCTION DETAILS

INDIANA STATE HIGHWAY COMMISSION

SCALE:- AS NOTED DATE:-

DRAWING:- C 8 OF 20 SHEET:- OF

PROJECT:- RS-3901(2)

CONTRACT NO.

BRIDGE FILE:- 47-61-6570

Figure D1. Construction Details

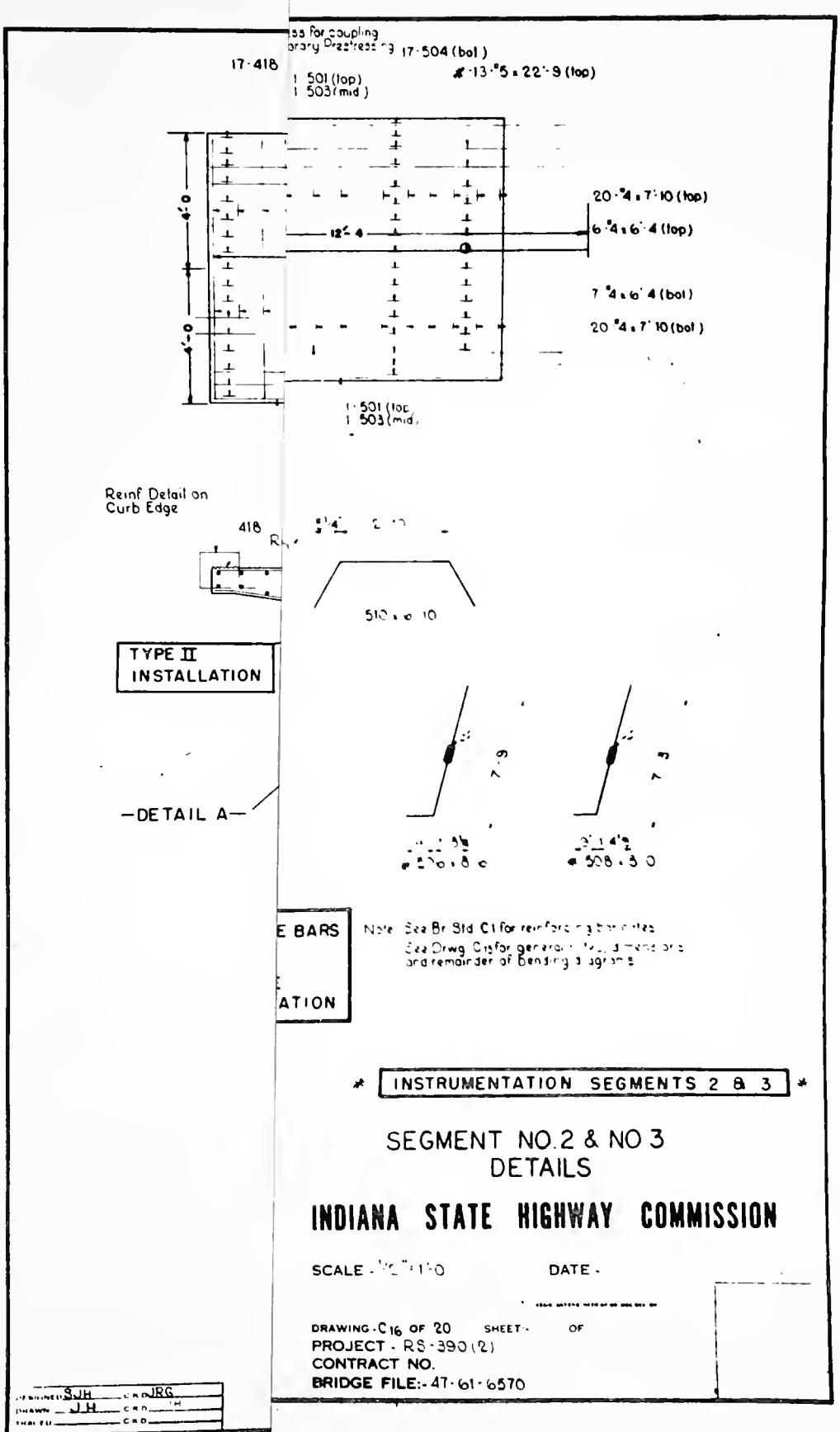

Figure D2. Segment

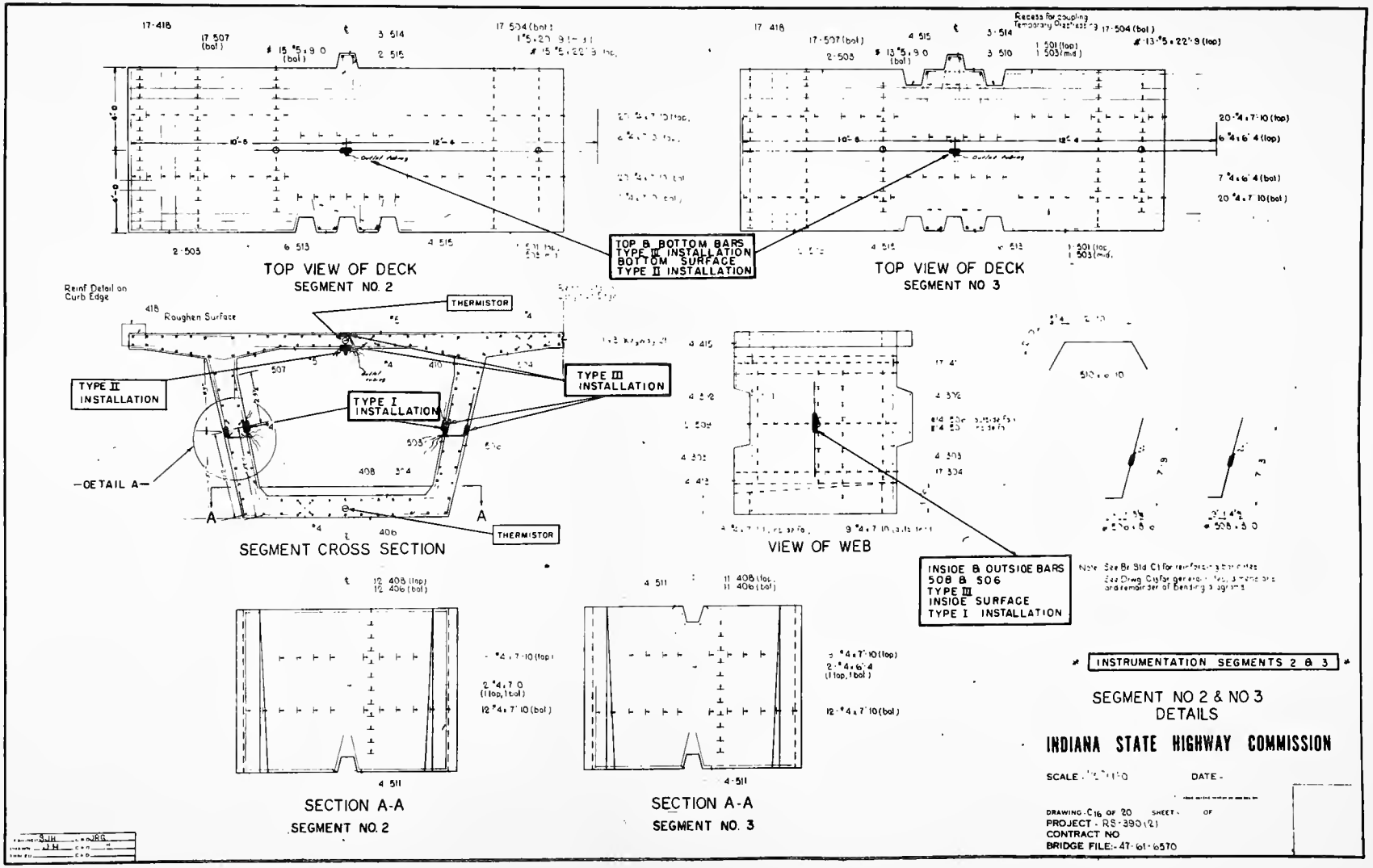

Figure D2. Segment 2 and 3 Details

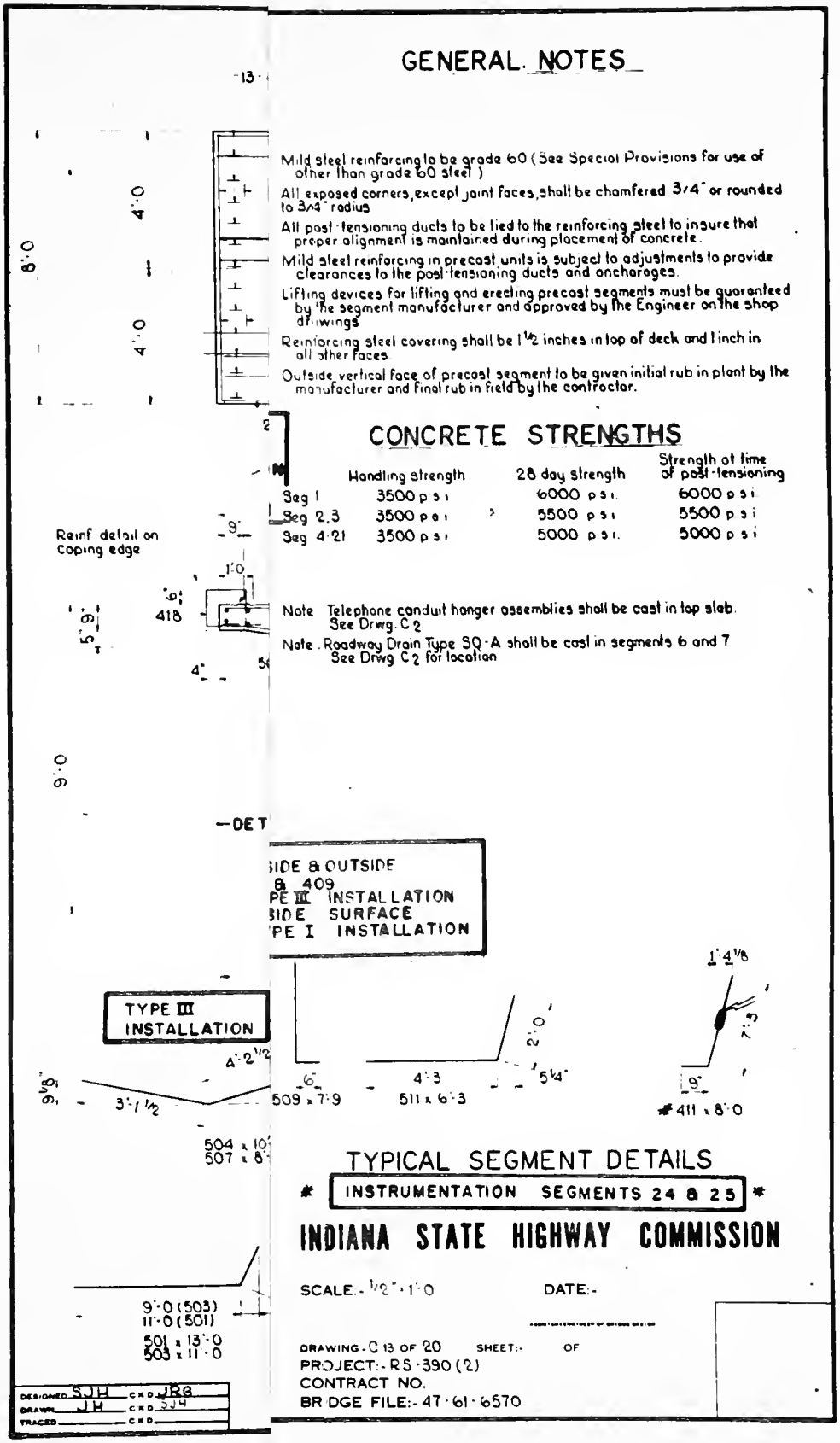

Figure D3. Segment

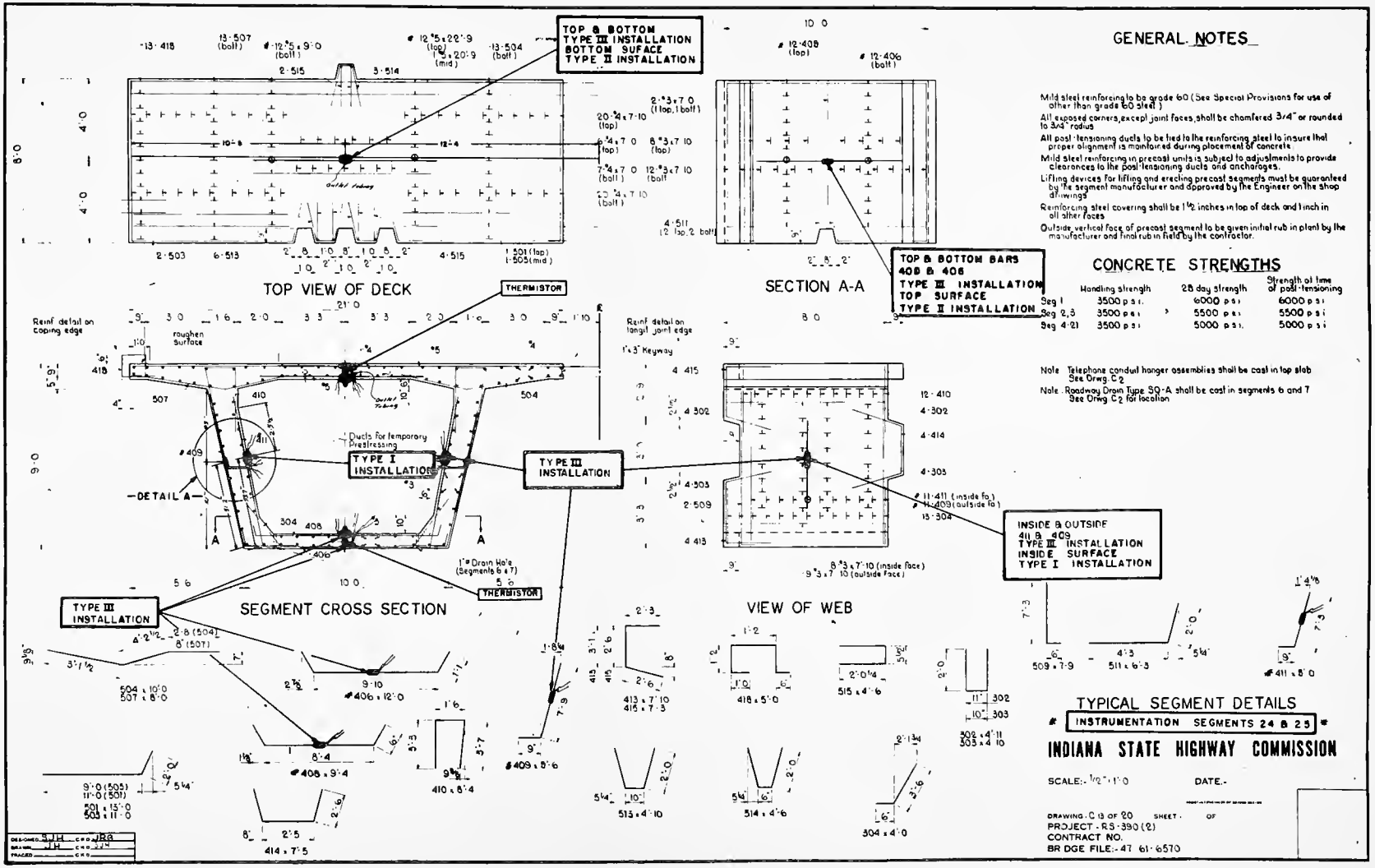

Figure D3. Segments 24 and 25 Details

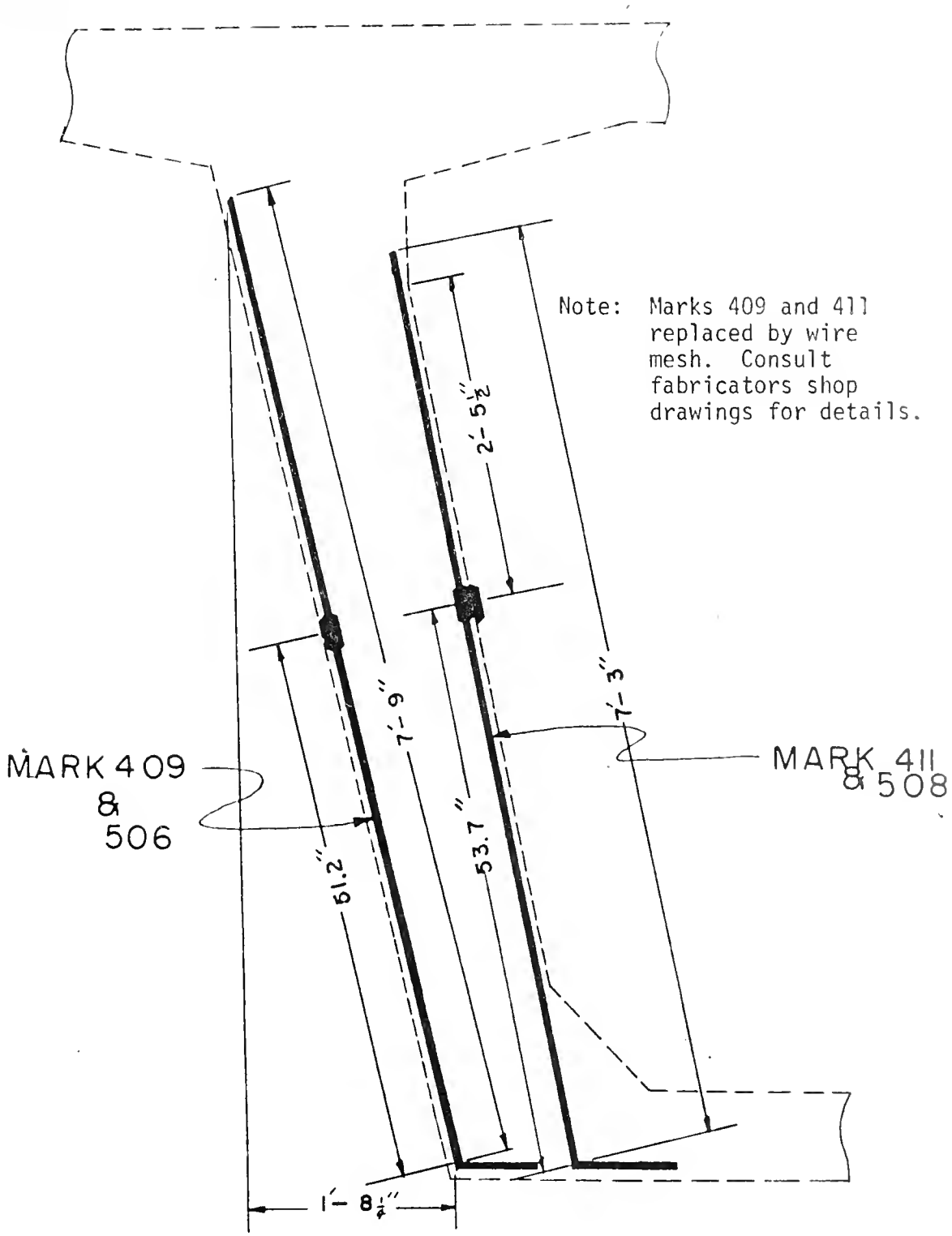

Figure D4. Detail A

COVER DESIGN BY ALDO GIORGINI